

THESIS

RELIABILITY ASSESSMENT OF DETERIORATING REINFORCED CONCRETE BRIDGES
SUBJECTED TO EARTHQUAKE AND FOUNDATION SCOUR

Submitted by

Jingzhe Ren

Department of Civil and Environmental Engineering

In partial fulfillment of the requirements

For the Degree of Master of Science

Colorado State University

Fort Collins, Colorado

Spring 2016

Master's Committee:

Advisor: Bruce Ellingwood

John van de Lindt

Scott Shuler

Copyright by Jingzhe Ren 2016

All Rights Reserved

ABSTRACT

RELIABILITY ASSESSMENT OF DETERIORATING REINFORCED CONCRETE BRIDGES SUBJECTED TO EARTHQUAKE AND FOUNDATION SCOUR

This study assesses the structural reliability of a deteriorating reinforced concrete bridge subjected earthquake and foundation scour during its service life. This study relies on probabilistic models of natural hazards and structural deterioration based on in-service inspection and utilizes methods of time-dependent reliability assessment. The results of the study reveal the potential influences of competing hazards on structural response of bridges over their service lives.

The thesis is structured in five chapters: (1) Introduction, including motivation and objectives of the study; (2) Literature review, addressing the background of natural hazards modelling and time-dependent reliability assessment; (3) Methods for modelling natural hazards and structural deterioration of bridges probabilistically; (4) Performance assessment of deteriorating bridges under competing hazards, providing numerical measures of structural reliability for a three-span reinforced concrete bridge based on a finite element model; (5) Conclusion and recommendations, summarizing the main research findings and discussing a possible direction for further studies.

ACKNOWLEDGEMENTS

I would like to express deep gratitude to my advisor Dr. Bruce Ellingwood for his guidance, encouragement and support throughout this study, for his expertise in this field that motivated me to work in this area.

I would also like to thank my committee members, Dr. John van de Lindt and Dr. Scott Shuler. I am extremely grateful for their assistance and suggestion on my thesis.

I am also thankful to my friends for their moral support.

DEDICATION

I would like to dedicate this work to my present and future family...

TABLE OF CONTENTS

	Page
ABSTRACT.....	ii
ACKNOWLEDGEMENTS.....	iii
DEDICATION.....	iv
LIST OF TABLES.....	viii
LIST OF FIGURES.....	xii
CHAPTER	
1 Introduction.....	1
1.1 Motivation for study.....	1
1.2 Research objectives and scope.....	2
1.3 Organization of thesis.....	3
2 Literature review – state of the art.....	5
2.1 Load and resistance factor design (LRFD) of bridges.....	5
2.2 Reliability basis for bridge design and fundamental gravity load requirements.....	6
2.3 Earthquake-resistant design of bridges.....	8
2.4 Assessment and mitigation of foundation scour effects.....	10
2.5 Structural deterioration –mechanisms, models, and significance to bridge performance.....	11
2.6 Vulnerability of bridges to earthquake and bridge scour.....	13
2.7 Critical appraisal of existing practices.....	14
3 Methods for modeling earthquake and scour hazards and structural response of a deteriorating bridge.....	16

3.1	Time-dependent reliability assessment.....	16
3.2	Analysis of scour.....	19
3.3	Structural deterioration model, data, and comparison between deterioration and corrosion.....	23
3.4	Analysis of competing hazards.....	31
4	Performance assessment of deteriorating bridges under competing scour and earthquake hazards.....	33
4.1	General analysis procedures.....	33
4.2	Analytical models of reinforced concrete bridge.....	34
4.3	Sensitivity analysis.....	37
4.4	Probabilistic seismic demand analysis.....	41
4.5	Seismic fragility analysis for bridge components.....	50
4.6	Combining component seismic fragility curves.....	57
4.7	Service life prediction of bridges under competing hazards.....	62
4.8	Closure.....	66
5	Conclusions and recommendations for further study.....	68
5.1	Summary of major research findings.....	68
5.2	Recommendations for further study.....	69
	References.....	70
	Appendix A – Description of finite element model of bridge.....	70
A.1	Analytical models of major bridge components.....	75
A.2	Seismic response.....	81
	Appendix B – Data of natural hazards.....	83

B.1 Scour.....	83
B.2 Bridge deterioration.....	85
Appendix C – Component PSDMs and fragilities.....	87
C.1 Component PSDMs.....	87
C.2 Bridge component fragilities.....	94
Appendix D – Results of sensitivity analysis.....	97

LIST OF TABLES

	Page
Table 2.2.1 Limit States.....	7
Table 2.2.2 Load Factors for Dead Load.....	8
Table 2.3.1 National Bridge Inventory Condition Ratings.....	12
Table 3.2.1 Mean and coefficients of variation of scour parameters.....	22
Table 3.3.1 Parameter uncertainty in analytical bridge models.....	29
Table 4.1.1 Database of ground motion records.....	34
Table 4.3.1 Ground motion records used in sensitivity analysis.....	38
Table 4.4.1 Probabilistic seismic demand models for eight component responses (GM_{xy} as scaling PGA).....	42
Table 4.4.2 Probabilistic seismic demand models for eight component responses (AM_{xy} as scaling PGA)	43
Table 4.4.3 Probabilistic seismic demand models for eight component responses ($SRSS_{xy}$ as scaling PGA).....	43
Table 4.4.4 Probability seismic demand models for eight component responses (Scour with lower discharge rate).....	47
Table 4.4.5 Probability seismic demand models for eight component responses (Scour with higher discharge rate).....	47
Table 4.4.6 Strength degradation parameters.....	48
Table 4.4.7 Relationship between NBI rating and residual resistance.....	49
Table 4.5.1 Medians and dispersions for bridge component limit states using Bayesian updating.....	50
Table 4.5.2 Parameters for bridge component fragilities (Without scour or deterioration).....	50
Table 4.5.3 Parameters for bridge component fragilities (Scour with lower discharge rate).....	51

Table 4.5.4 Parameters for bridge component fragilities (Scour with higher discharge rate).....	51
Table 4.5.5 Parameters for bridge component fragilities (Without scour or deterioration, when NBI rating =3).....	54
Table 4.5.6 Parameters for bridge component fragilities (Scour with lower discharge rate, when NBI rating =3).....	54
Table 4.5.7 Parameters for bridge component fragilities (Scour with higher discharge rate, when NBI rating =3).....	55
Table 4.6.1 System fragilities for different hazard condition.....	59
Table 4.7.1 Conditional failure rate function (No scour occurs).....	65
Table 4.7.2 Conditional failure rate function (Scour with lower discharge rate).....	65
Table 4.7.3 Conditional failure rate function (Scour with higher discharge).....	65
Table A-1 Model Prosperities of Abutment.....	80
Table B-1 Annual peak discharge rate.....	83
Table B-2 Transition probability for superstructure condition (concrete).....	85
Table B-3 Transition probability for superstructure condition (steel).....	85
Table B-4 Transition probability for substructure condition (concrete).....	85
Table B-5 Transition probability for substructure condition (steel).....	86
Table C-1 Probability seismic demand models for eight component responses (Scour with higher discharge rate, when NBI rating=6).....	87
Table C-2 Probability seismic demand models for eight component responses (Scour with lower discharge rate, when NBI rating=6).....	88
Table C-3 Probability seismic demand models for eight component responses (Without Scour or deterioration, when NBI rating=6).....	88
Table C-4 Probability seismic demand models for eight component responses (Scour with higher discharge rate, when NBI rating=5).....	89

Table C-5 Probability seismic demand models for eight component responses (Scour with lower discharge rate, when NBI rating=5).....	89
Table C-6 Probability seismic demand models for eight component responses (Without Scour or deterioration, when NBI rating=5).....	90
Table C-7 Probability seismic demand models for eight component responses (Scour with higher discharge rate, when NBI rating=4).....	90
Table C-8 Probability seismic demand models for eight component responses (Scour with lower discharge rate, when NBI rating=4).....	91
Table C-9 Probability seismic demand models for eight component responses (Without Scour or deterioration, when NBI rating=4).....	91
Table C-10 Probability seismic demand models for eight component responses (Scour with higher discharge rate, when NBI rating=3).....	92
Table C-11 Probability seismic demand models for eight component responses (Scour with lower discharge rate, when NBI rating=3).....	92
Table C-12 Probability seismic demand models for eight component responses (Without Scour or deterioration, when NBI rating=3).....	93
Table C-13 Parameters for bridge component fragilities (Scour with higher discharge rate, when NBI rating=6).....	94
Table C-14 Parameters for bridge component fragilities (Scour with lower discharge rate, when NBI rating =6).....	94
Table C-15 Parameters for bridge component fragilities (Without scour or deterioration, when NBI rating = 6).....	94
Table C-16 Parameters for bridge component fragilities (Scour with higher discharge rate, when NBI rating = 5).....	95
Table C-17 Parameters for bridge component fragilities (Scour with lower discharge rate, when NBI rating =5).....	95

Table C-18 Parameters for bridge component fragilities (Without scour or deterioration, when NBI rating =5).....	95
Table C-19 Parameters for bridge component fragilities (Scour with higher discharge rate, when NBI rating =4).....	96
Table C-20 Parameters for bridge component fragilities (Scour with lower discharge rate, when NBI rating =4).....	96
Table C-21 Parameters for bridge component fragilities (Without scour or deterioration, when NBI rating =4).....	96
Table D-1 Seismic response of bridge components (Steel strength).....	97
Table D-2 Seismic response of bridge components (Concrete strength).....	97
Table D-3 Seismic response of bridge components (Bearing shear modulus).....	98
Table D-4 Seismic response of bridge components (Passive stiffness of abutment).....	98
Table D-5 Seismic response of bridge components (Active stiffness of abutments).....	98
Table D-6 Seismic response of bridge components (Deck mass).....	99
Table D-7 Seismic response of bridge components (Damping ratio).....	99
Table D-8 Seismic response of bridge components (Steel strength).....	99
Table D-9 Seismic response of bridge components (Concrete strength).....	100
Table D-10 Seismic response of bridge components (Bearing shear modulus).....	100
Table D-11 Seismic response of bridge components (Passive stiffness of abutment).....	100
Table D-12 Seismic response of bridge components (Active stiffness of abutments).....	101
Table D-13 Seismic response of bridge components (Deck mass).....	101
Table D-14 Seismic response of bridge components (Damping ratio mass).....	101

LIST OF FIGURES

	Page
Figure 4.2.1 MSSS concrete girder bridge configuration.....	35
Figure 4.2.2 Concrete member reinforcing layout (a) Column (b) Bent beam.....	36
Figure 4.3.1 Tornado diagrams of column ductility under ground motions (a) GM-1 and (b) GM-2.....	39
Figure 4.3.2 Tornado diagrams of abutment passive response under ground motions (a) GM-1 and (b) GM-2.....	40
Figure 4.4.1 Annual peak flow discharge rate.....	44
Figure 4.4.2 The histograms of the occurrence probability of a range of scour depth.....	45
Figure 4.4.3 Probability of exceedance of scour depth.....	46
Figure 4.5.1 Component fragilities of bridge subjected to seismic hazard.....	52
Figure 4.5.2 Component fragilities of bridge subjected to seismic hazard and scour hazard with lower discharge rate.....	53
Figure 4.5.3 Component fragilities of bridge subjected to seismic and scour hazard with higher discharge rate.....	53
Figure 4.5.4 Component fragilities of bridge subjected to seismic hazard, when NBI rating = 3.....	55
Figure 4.5.5 Component fragilities of bridge subjected to seismic and scour hazard with lower discharge rate, when NBI rating = 3.....	56
Figure 4.5.6 Component fragilities of bridge subjected to seismic and scour hazard with higher discharge rate, when NBI rating = 3.....	56
Figure 4.6.1 System seismic fragility of deteriorating bridge subjected to seismic hazard.....	59
Figure 4.6.2 System seismic fragility of deteriorating bridge subjected to seismic and scour hazard (Lower discharge rate).....	60

Figure 4.6.3 System seismic fragility of deteriorating bridge subjected to seismic and scour hazard (Higher discharge rate).....	60
Figure. 4.6.4 System fragilities of the bridge that under initial condition and NBI rating=4 for slight damage state.....	61
Figure. 4.6.5 System fragilities of the bridge that under initial condition and NBI rating=4 for moderate damage state.....	62
Figure 4.7.1 Time-dependent failure rate of deteriorating bridge (San Francisco).....	63
Figure 4.7.2 Time-dependent failure rate of deteriorating bridge (Charleston).....	64
Figure 4.7.3 Survivor function of bridge service life.....	66
Figure A.1 Typical elastomeric pad for fixed and expansion types elastomeric bearings.....	76
Figure A.2 Analytical model of elastomeric bearing with fixed dowels.....	77
Figure A.3 Analytical model of elastomeric bearing with expansion dowels in longitudinal direction.....	78
Figure A.4 (a) Layout of pile-bent girder seat type abutment (b) Definition of longitudinal abutment behavior.....	79
Figure A.5 Analytical Model of abutment (a) Soil contribution (b) Pile contribution.....	79
Figure A.6 (a) Analytical Model of foundation (b) Configuration of bridge footings.....	81
Figure A.7 Deck displacement time histories.....	82

Chapter 1

Introduction

1.1 Motivation for study

Reinforced concrete (RC) bridges in the United States are susceptible to damage from operating conditions, natural hazards, deterioration due to aging, and other mechanisms of physical attack (Ellingwood 2005). Among these hazards, earthquake and foundation scour are very common for bridges. According to the Federal Highway Administration (2009), and Harrison and Morris (1991), there are hundreds of thousands of existing bridges located in active seismic zones, with nearly 400,000 bridges over waterways, many of which are exposed to erosion of channel beds around their foundations. For bridges that are exposed to both earthquake and foundation scour hazards, it is necessary to consider the effects of both hazards in the design procedure implemented for new bridges as well as the risk assessment and possible rehabilitation of existing bridges.

To ensure safety against multiple hazards, current design procedures in the United States consider the hazard demands individually (Crosti et al. 2011). However, this approach overlooks the correlation between multiple hazards and their structural effects, which generally would lead to an underestimation of the risk induced by these hazards during the service life of the bridge if the structural effects were to be positively correlated. While some studies of the influence of scour effects on seismic response of bridges are available (e.g., Alipour et al. 2013; Wang et al. 2014), the methodologies in these papers did not consider bridge deterioration effects due to structural aging. Deterioration of bridges manifests itself in a number ways - spalling of RC bridge girders due to freeze-thaw action or application of aggressive de-icing chemicals, alkali-silicate reactions in the concrete, and corrosion of steel reinforcement in RC columns, to name just a few (Ellingwood, 2005) - and the losses of these components may have a significant impact on the seismic response of bridges (Ghosh and Padgett 2010). Thus, to predict the

performance of a deteriorating bridge that is exposed to both earthquake and scour hazards, the results might be unconservative if bridge deterioration were not included in the analysis. While one of the most common mechanisms of bridge deterioration is due to corrosion from chloride concentrations in deicing salts (e.g., Enright and Frangopol 1998), this mechanism, by itself, would be insufficient for bridges in which damage due to alkali-silica reactions or freeze-thaw cycling has also occurred. A study in which the correlations among bridge responses to structural deterioration from several mechanisms, earthquake, and foundation scour are taken into account will reveal a more accurate picture of the risks to reinforced concrete bridges so affected during their service lives.

1.2 Research objectives and scope

The main objective of this study is to develop a time-dependent survival function (defined as the probability that the life of the bridge exceeds some period, t) for a deteriorating reinforced concrete bridge structure exposed to earthquake and foundation scour hazards during its service life. This survival function could be adopted to develop a policy on routine inspections and maintenance behaviors for a reinforced concrete bridge. To accomplish this objective, three probability models for reliability analysis are developed, which include: a stochastic model of bridge deterioration and hazard functions of earthquake and foundation scour. Seismic fragilities of bridges used to illustrate the methodology are constructed using finite element analysis. The method of modeling and sources of data are summarized as follows:

- 1) A probabilistic model of bridge deterioration is developed using the theory of Markov chains, and the data adopted in this model are obtained from the FHWA.
- 2) A hazard function defining the likelihood of foundation scour is derived from regression analysis of laboratory test results.
- 3) Hazard functions for earthquake are established for a bridge that has sustained different damage levels of scour and deterioration, utilizing the seismic fragility methodology of previous

works. The earthquake records applied in the analysis are from United States Geological Survey (USGS).

- 4) Utilizing the results of the three previous tasks, survival functions for the bridge are determined, considering combinations of earthquake and scour hazards to assess the safety level of a reinforced concrete bridge structure during its service life.
- 5) Case studies are presented based on finite element models developed in SAP2000, which consider the combined effects of earthquake, deterioration and scour. The uncertainties in bridge modelling parameters are incorporated in the finite element models using a Latin Hypercube sampling approach.

The type of bridge structure analyzed in this study is a two-span reinforced concrete bridge, which is more sensitive to seismic loads compared to long-span bridges, such as suspension bridges and cable-stayed bridges. This study concentrates on reinforced concrete bridges that are located in earthquake-prone regions where there is also a potential risk of bridge deterioration and scour.

1.3 Organization of thesis

This thesis contains five chapters, the last four of which address essential ingredients of time-dependent reliability of deteriorating bridges exposed to scour and/or earthquake. In Chapter 2, a literature review of related standards and previous studies, design requirements of bridge resistance and reliability assessments for gravity loads, earthquake and scour hazards is presented. An evaluation of deterioration and the multi-hazard influences on bridge performance are described briefly, and the state-of-the-art and current practices of bridge design and condition assessment are critically appraised. In Chapter 3, the methodologies for modeling bridge deterioration, hazards functions for earthquake and scour, and a model to assess competing hazards scour are introduced. Chapter 4 presents a series of numerical studies; two of these are intended to benchmark the current study against previous work and to highlight the impact of failing to incorporate structural deterioration due to aging in bridge risk assessment. Finite element models are developed to support the numerical analysis of deteriorating

bridges under competing scour and earthquake hazards. Based on the numerical results, conclusions and suggestion for future study are given in Chapter 5. References are provided in the final section.

Appendix A contains a description of the finite element bridge model that is analyzed in this study;

Appendix B contains natural hazard data needed in the analysis; Appendix C contains the numerical results of seismic response, and the results of sensitivity analysis are presented in Appendix D.

Chapter 2

Literature review – state of the art

2.1 Load and resistance factor design (LRFD) of bridges

Until about twenty years ago, the design of bridge structures and substructures in the United States, was performed using allowable stress design (ASD), in which the uncertainties in material resistance and applied loads were covered by safety factors. In 1989, work began on an entirely new specification in which the uncertainties in load(s) and material resistance(s) are represented by load factor(s) and resistance factor(s) respectively. This new specification is the *AASHTO Load and Resistance Factor Design (LRFD) Bridge Specification*, which was first approved for use in 1994. The latest edition is the 2012 edition (AASHTO 2012).

To satisfy structural safety requirements, the primary principle in structural design is that the resistance of the structure must exceed the effect of the applied loads, so that,

$$\text{Resistance} \geq \text{Effect of loads} \quad (2.1.1)$$

In the LRFD method, the effect of the loads on the right hand side of eqn. (2.1.1) are multiplied by their load factors, γ_i , which reflect uncertainties in the load intensities. For a specific strength design limit state (flexure, shear, compression), the effect of loads may include a combination of different load types Q_i . The required strength is given by $\sum \gamma_i Q_i$, which must not exceed the design strength, defined as the product of the nominal strength, R_n , and a resistance factor, ϕ : (AASHTO, 2012),

$$\phi R_n \geq \sum \eta_i \gamma_i Q_i \quad (2.1.2)$$

The load factors, γ_i and resistance factor ϕ are based on principles of structural reliability analysis (Nowak et al. 2000), and reflect the uncertainties in the determination of the loads (and load

combinations) and strengths. The load modifier, η_i accounts for the effects of ductility, redundancy and operational importance.

For a satisfactory design, the factored nominal resistance (design strength) should equal or exceed the required strength, calculated from the combination of the factored load effects for a particular limit state. Load and resistance factors are chosen from structural reliability analysis so that there is a reasonably high probability that the actual resistance of the structure will be enough to support the loads (AASHTO 2012).

The *AASHTO LRFD Specification* offers some advantages over the ASD Bridge Design Specification, in that it (FWHA Manual 2001):

- 1) Accounts for variability in both resistance and load;
- 2) Achieves relatively uniform levels of safety based on the strength of the steel and reinforced concrete in the superstructure, substructure and foundation for different limit states and foundation types.
- 3) Provides more consistent levels of safety in the bridge superstructure and substructure, as both are designed using the same loads for predicted or target probabilities of failure.

The limitations of the LRFD method include (FWHA Manual 2001):

- 1) The development of load and resistance factors to meet individual situations requires the availability of statistical data and probabilistic algorithms.
- 2) Resistance factors vary with design methods and are not constant.

2.2 Reliability basis for bridge design and fundamental gravity load requirements

The performance of bridges is measured in terms of the reliability index, β , or probability of failure, P_F . In previous work (Nowak 1995), a reliability-based calibration procedure for the load and resistance factor design (LRFD) bridge code was presented, in which uncertainties were taken into account by modelling loads and resistances as random variables. Detailed reliability requirements and limit states for bridge are defined in the *AASHTO LRFD Bridge Design Specifications* (AASHTO 2012).

According to the AASHTO (2012), bridges shall be designed for specific limit states to achieve the requirements of constructability, safety, and serviceability. There are several limit states defined in the standard to ensure structural safety under different loads or hazards and the values of target reliability index for these limit states depend on the specific design requirements. The limit states and the corresponded descriptions are shown in Table 2.2.1. Components and connections of the bridge structure must satisfy the factored load combinations for gravity loads at each limit state (See Table 2.2.1). The target values of reliability index for the limit states depend on the bridge of interest; for strength limit states under gravity loads due to traffic, $\beta = 3.5$.

Table 2.2.1 Limit States (AASHTO 2012)

Limit State	Description
Service Limit State	Restrictions on stress, deformation, and crack width under regular service conditions
Fatigue Limit State	Restrictions on stress range as a result of a single design truck occurring at the number of expected stress range cycles.
Fracture Limit State	A set of material toughness requirements of the AASHTO Materials Specifications
Strength Limit State	Ensure that strength and stability, both local and global, are provided to resist the specified statistically significant load combinations that a bridge is expected to experience in its design life
Extreme Event Limit States	Ensure the structural survival of a bridge during a major earthquake or flood, or when collided by a vessel, vehicle, or ice flow, possibly under scoured conditions.

Gravity loads used in the design of bridges include dead load, vehicular live load (LL) and pedestrian live load (PL). Dead load includes weight of structural components and nonstructural attachments (DC), weight of wearing surfaces and utilities (DW), and vertical pressure from dead load of earth fill (EV) (AASHTO 2012). For each type of dead load, the maximum and minimum load factors in each load combinations are shown in Table 2.2.2.

Table 2.2.2 Load Factors for Dead Load (AASHTO 2012)

Load Type	Load Factor	
	Maximum	Minimum
DC ^a : Component and Attachments	1.25	0.9
DW: Wearing Surfaces and Utilities	1.50	0.65
EV: Vertical Earth Pressure		
• Overall Stability	1.00	N/A
• Retaining Walls and Abutments	1.35	1.00
• Rigid Buried Structure	1.30	0.90
• Rigid Frames	1.35	0.90
• Flexible Buried Structures		
○ Metal Box Culverts and Structural Plate Culverts with Deep Corrugations	1.5	0.9
○ Thermoplastic culverts	1.3	0.9
○ All others	1.95	0.9

^a When load combination relating to very high ratios of dead load to live load forces, the maximum and minimum load factors of DC equal to 1.50, 0.9 respectively.

Vehicular live loading on the roadways of bridges or incidental structures is designated as HL-93, and consist of a combination of the: design truck or design tandem, and design lane load (AASHTO 2012). A pedestrian load of 0.075 ksf is applied to all walkways wider than 2.0 ft and is considered simultaneously with the vehicular design live load in the vehicle lane. Where vehicles can mount the walkway, the pedestrian load need not be considered concurrently (AASHTO 2012).

2.3 Earthquake-resistant design of bridges

Bridges must be designed to satisfy the extreme limit state under major earthquakes or other load combinations that include seismic load effects. The design earthquake motions and forces specified in the AASHTO Specification (2012) are based on a 7% probability of their being exceeded in 75 yr (equivalent

to an earthquake with a return period of approximately 1,034 years). The general principles used for the development of earthquake-resistant design in the AASHTO Specification (2012) are (Baker et. al 2013),

- 1) Small to moderate earthquakes should be resisted within the elastic range of the structural components without significant damage;
- 2) Realistic seismic ground motion intensities and forces should be used in the design procedures;
- 3) Exposure to shaking from large earthquakes should not cause collapse of all or part of the bridge. Where possible, damage that does occur should be readily detectable and accessible for inspection and repair.

For earthquake-resistant design, displacement-based procedures are thought to be more reliable than strength-based procedures to identify the limit states that cause damage leading to collapse; besides, displacement-based procedures produce more efficient designs against collapse in some cases (AASHTO 2012). The design forces for earthquake depend on bridge location, type of bridge and operational category of bridge, etc. For example, based on the uniform load method, the formula of the equivalent static earthquake loading P_e can be expressed as (AASHTO 2012),

$$P_e = \frac{C_{sm}W}{L} \quad (2.3.1)$$

in which, P_e = equivalent uniform static seismic loading per unit length of bridge applied to represent the primary mode of vibration (kip/ft); C_{sm} = the dimensionless elastic seismic response coefficient; W = total weight of bridge (kips); and L = total length of the bridge (ft).

For bridges in which coupling occurs in more than one of the three coordinate directions within each mode of vibration, the multimode spectral analysis method shall be applied. As a minimum, a linear dynamic analysis using a three-dimensional model shall be used. The member forces and displacements may be estimated by combining the respective response quantities (e.g. moment, force, displacement, etc.) from the individual modes; commonly used methods for assessing these combinations are the

Complete Quadratic Combination (CQC) method and the square root of the sum of the squares method (SRSS) (AASHTO 2012).

2.4 Assessment and mitigation of foundation scour effects

Scour is the water-induced erosion of soil around the foundation of a structure, and is classified mainly in three forms: long-term aggradation and degradation, contraction scour, and local scour (Wang, et al 2014). Local scour can be one of most structural damaging forms of scour (Alipour, et al 2013), and can cause considerable loss to the lateral resistance of a bridge, which could be perilous for bridges subjected to seismic loads. Foundation local scour refers to the erosion due to the obstruction of the bridge foundation and the formation of strong eddy currents around the foundation. About 84 percent of the bridges in the United States are over waterways (Landers et al. 1996); for most of these bridges, there is some risk of local scour. According to Shirole and Holt (1991), a survey of U.S. bridge failures since 1950 showed that 60 percent of 823 failures surveyed were associated with hydraulics, which includes channel bed scour around bridge foundations and channel instability. Furthermore, because of the effects of scour on structural system response characteristics (Alipour, et al 2013), e.g., loss of support, decreasing lateral stiffness and lengthening of the natural period of the bridge system, the performance of a bridge may be influenced significantly by scour, especially under seismic loads. Thus, it is important to deal with scour properly in design.

To ensure the safety of a scoured bridge, the effects of scour should be evaluated and minimized during the bridge service life. In the *AASHTO LRFD Bridge Design Specifications* (AASHTO 2012), several extreme event limit states must be considered to ensure the structural survival of a bridge during events, such as earthquake under scour conditions. Some countermeasures, such as armor, flow- altering devices and channel realignment (Johnson and Niezgoda 2004), can reduce the effects of scour. However, a better evaluation of the scour process will improve the design and bridge performance against foundation scour. According to current research (Melville 1983; Johnson 1995; Alipour, et al 2013), the most common approach to evaluate the effects of pier scour is simply to estimate scour depth around

bridge pier, which is based on pier scour equations and data from laboratory and records of river flow.

The added cost of making a bridge less vulnerable to scour is small when compared to the total cost of a bridge failure, which can easily exceed the original cost of the bridge itself.

2.5 Structural deterioration –mechanisms, models, and significance to bridge performance

Structural deterioration causes a loss in strength over time. Since the factors that govern deterioration are uncertain in their intensity and structural effect, the structural resistance must be modeled as a time-dependent stochastic process. Numerous degradation mechanisms are possible in a RC bridge: chloride attack leading to reinforcement corrosion, alkali silica reactions in the concrete and freeze-thaw cycle attack are among the most important. Among these degradation mechanisms, strength loss due to corrosion of the steel reinforcement has been most commonly considered in deterioration modeling of RC bridges (Enright and Frangopol 1998). During the service life of a bridge, structural deterioration may cause its resistance to fall below its design level for gravity loads (dead load and traffic live loads), and many bridges in the United States have been posted as a result. According to the American Society of Civil Engineers, more than half of the 599,766 bridges in the country are approaching the end of their design lives, and nearly a quarter of them require significant maintenance or replacement to ensure acceptable continued performance (ASCE 2009). In addition, bridge deterioration may increase the likelihood of failure due to environmental effects, including extreme winds and earthquakes. According to Ghosh and Padgett (2010), bridge deterioration may decrease the seismic vulnerability of some components, but will increase the vulnerability of most critical components. Because of the uncertainties generated by deterioration in prediction of bridge performance under seismic loads or others service loads, it is important to estimate strength losses due to deterioration stochastically.

Two groups of methods have been used in previous studies to model the time-dependent behavior of bridges. The first group is based (primarily) on models of the reinforcement corrosion mechanism that allows the decrease in capacity of a reinforced concrete structure to be determined as a function of corrosion loss (Mori and Ellingwood 1993b; Enright and Frangopol 1998). These corrosion loss models

have various levels of sophistication, ranging from simple reaction-controlled empirical models developed by scaling material deterioration experiments conducted under accelerated aging conditions in a laboratory to physics-based models based on Fick's second law of diffusion and Faraday's equation to determine the period required to initiate corrosion and propagate it to a failure state (Mori and Ellingwood 1993b). The second group is based on non-mechanics-based models that are based on condition rating data from the National Bridge Inventory (NBI) or other similar resources. NBI ratings are determined by the rating of every individual component in the bridge on a scale of 0 to 9. As part of the national bridge inspection program, states are required to inspect bridges in their states every two years using the guidelines established by the Federal Highway Administration (FHWA) and to report the results to the FHWA (Estes and Frangopol 2001). The ratings and corresponding descriptions of bridge conditions are listed in Table 2.3.1. The bridge ratings are developed primarily through visual inspections of the major bridge components. Different components might very well have different numerical ratings. In contrast to the physics-based models above, the NBI ratings do not reflect any single deterioration mechanism and present an overall picture of the condition of the bridge.

Table 2.3.1 National Bridge Inventory Condition Ratings (FHWA 1988)

NBI rating	Description	Repair action
9	Excellent condition	None
8	Very good condition	None
7	Good condition	Minor maintenance
6	Satisfactory condition	Major maintenance
5	Fair condition	Minor repair
4	Poor condition	Major repair
3	Serious condition	Rehabilitate
2	Critical condition	Replace
1	Imminent failure condition	Close bridge and evacuate
0	Failed condition	Beyond corrective action

The NBI ratings represent the bridge condition (and deterioration) over time as an integer stochastic process. This stochastic condition model is developed through a statistical analysis, which provides sample functions of bridge deteriorated states as a function of elapsed time (Bolukbasi et al.

2004) or a series of probabilities that bridge components remain in a specific state or transition to a lower state every two years (Cesare et al. 1992). The advantage of the NBI-based group of methods is that the bridge deterioration model can incorporate a variety of deterioration mechanisms, which all are reflected in the condition number assigned to the bridge following inspection. However, the bridge condition rating data is not related specifically to a bridge resistance variable, which is needed in time-dependent reliability assessment. Thus, to determine the time-dependent reliability, this integer process must be transformed into a measure of bridge resistance that can be used in a structural reliability analysis. In previous work (Wang et al. 2011), the transformation was developed by combining the condition rating function of elapsed time (Bolukbasi et al. 2004) and the results of parametric studies of reinforced concrete beams subjected to corrosion attack (Enright and Frangopol 1998). For example, if the deterioration of reinforced concrete beams is dominated by corrosion, the effects of deterioration (in terms of NBI) can be assumed to equal to that resulting from corrosion, providing a calibration point for coupling the two methods. This approach of transformation can be expanded to other bridge components, as will be described subsequently.

2.6 Vulnerability of bridges to earthquake and bridge scour

The vulnerability of bridges to earthquake and scour have been presented in previous works (Alipour, et al 2013; Wang, et al. 2014) by seismic fragility curves.

In the study by Alipour et al. (2013), nine two-span RC bridges with various designs and configurations were analyzed and five fragility curves for a range of scour depths ranging from one meter to five meters were defined in terms of earthquake intensity measured by peak ground acceleration (PGA). The study showed that for a given value of PGA, the probability of bridge failure increased with an increase in scour depth,

In the study of Wang et al. (2014), three types of RC bridges (e.g., a continuous box-girder bridge, a multi-span simply supported (MSSS) concrete girder bridge, and a multi-span continuous (MSC) concrete girder bridge) were analyzed to reveal the effects of scour on the seismic response of a

bridge; in that study, the intensity measure (IM) was spectral acceleration at the fundamental period of the bridge. Wang, et al, (2014) provided fragility curves at the component rather than at the system level and the fragility analysis showed that scour has a significant effects on capacities of the key components. However, the results also showed that for the columns of MSSS and MSC concrete girder bridges, scour has a positive effect on bridge seismic response. One possible reason for this non-intuitive result is that scour leads to a longer vibration period and spectral acceleration decreases with period lengthening for this particular bridge. An earlier study (Padgett et al 2008) also found that the spectral acceleration is not the optimal IM for seismic response analysis of bridge portfolios with a range of fundamental periods (Padgett et al. 2008).

These two studies show that it is better to assess the vulnerability of bridges subjected to earthquake and scour by considering earthquake and scour as multi-hazards rather than individually.

2.7 Critical appraisal of existing practices

Numerous previous studies (e.g. Mori and Ellingwood. 1993b; Enright et al. 1998) have assessed the reliability of deteriorating RC structures based on corrosion. However, the effects of corrosion or, more generally structural deterioration, are seldom considered in an analysis of structures under seismic or others extreme loads (e.g. Alipour et al. 2013; Wang et al. 2014), which limits the application of these previous studies.

Wang et al. (2011) related the NBI ratings to structural resistance by adopting the NBI rating model of Bolukbasi et al. (2004). In this approach, NBI ratings are modeled as a polynomial function of elapsed time, which means the NBI ratings are deterministic in each single year rather than a random variable, and the uncertainties in NBI ratings model are neglected, which would lead to inaccuracies in the transition process. Alipour et al. (2011) presented the joint probabilities of failure of bridges subjected to earthquake and scour. However, Alipour's analysis was based on a scenario event, and time-dependent information (including deterioration) was not presented, which is essential information for developing strategies for bridge design, maintenance and repair. According to the requirements of reliability in

AASHTO (2012), such strategies would be better derived from a survival function or reliability function of bridge service life.

Accordingly, in this study, a more comprehensive model for bridge deterioration will be presented, and an approach to time-dependent reliability assessment will be developed to predict the performance of bridge during its service life. The methodologies employed in this comprehensive model are presented in the following chapter.

Chapter 3

Methods for modeling earthquake and scour hazards and structural response of a deteriorating bridge

In this chapter, the methodologies used in this study, including the probabilistic models for seismic, bridge scour and deterioration hazards, and the structural fragility models needed to assess the influences of the hazards on a bridge, are presented.

3.1 Time-dependent reliability assessment

3.1.1 Earthquake analysis

The seismic hazard at any site may be described in terms of the probability distribution of the IM, X , defined most commonly by either effective peak ground acceleration (PGA) or spectral acceleration (SA) at the fundamental period of the structure. The probability that acceleration, X , is less than some specified value x is given, in approximation, by a Type II distribution of largest values, defined as (O'Connor and Ellingwood 1987):

$$F_S(x) = P(X \leq x) = \exp \left[- \left(\frac{x}{u} \right)^{-k} \right] \quad (3.1.1)$$

Thus, the probability density function $f_S(x)$ is,

$$f_S(x) = \frac{k}{u} \left(\frac{x}{u} \right)^{-k-1} \exp \left(- \left(\frac{x}{u} \right)^{-k} \right) \quad (3.1.2)$$

where the characteristic extreme, u , and shape, k , are parameters of the distribution.

The parameters u and k can be derived from a regression analysis of site-dependent earthquake hazard data provided by the US Geological Survey (USGS) at a specific site

(<http://geohazards.usgs.gov/hazardtool/application.php>). Alternatively, the mean seismic hazard curve from the USGS website can be used in its non-parametric form in reliability assessment.

3.1.2 Structural response

Structural response analysis and system resistance are represented in this study by bridge fragility curves. Bridge fragility curves, which express the probability that the bridge reaches a damage state under a given ground motion intensity, $IM = x$, play an important role in seismic risk assessment of bridges (Nielson and DesRoches 2006). The different components of bridges, such as bridge deck, supporting girders, pier caps, piers (columns), abutments and foundation, may perform differently under seismic loads, and the failure of each component may affect the performance of the bridge system in different ways. Previous research (Nielson 2005; Tavares et al. 2012) has identified the abutments, columns and bearings as being critical in bridge performance; hence, this study focuses on the role of these three components. Thus, analyses of the bridge without considering the different seismic responses of the bridge components may not capture the real seismic response of bridge. In this study, a component-level approach is adopted in bridge fragility analysis, and the bridge is considered as a system of components failing in series. The seismic fragility is simply defined as the probability that the seismic demand (D) on structure causes a response, R , that exceeds a pre-determined performance limit associated with a state of damage ranging from loss of functionality to incipient collapse under a given level of seismic loading. Previous research (Padgett et al. 2008) has indicated that the PGA, X , is an appropriate measure of seismic intensity for bridge performance assessment. Thus, the seismic fragility is given by the following conditional probability:

$$Fragility = P[D \geq R | X = x] \quad (3.1.3)$$

in which x = specific peak ground motion intensity. Eqn. (3.1.3) is easily evaluated by developing a probability distribution for the demand conditioned on a given PGA, a process sometimes referred to as probabilistic seismic demand model (PSDM). The seismic demand on the structure often is quantified

using metrics, such as deformation and ductility. According to Cornell et al. (2002), the estimate for the median demand (m_D) can be represented by a power law model as,

$$m_D = ax^b \quad (3.1.4)$$

in which, a and b are regression coefficients. The scatter in demand tends to increase linearly with an increase in X , implying that the coefficient of variation (COV) in demand is constant (Cornell et al 2002). The probability distribution of demand X . is often assumed to be a lognormal distribution.

Under the assumption that the capacity can be described by a lognormal distribution as well, the seismic fragility of each bridge component can be described by the lognormal distribution,

$$P(F_i) = P[D > R | X = x] = \Phi \left(\frac{\ln(m_D / m_R)}{\sqrt{\zeta_D^2 + \zeta_R^2}} \right) \quad (3.1.5)$$

in which m_D is determined as a function of x from Eqn. (3.1.3), m_R is median value of resistance; ζ_R and ζ_D are logarithmic standard deviation of resistance and demand respectively; $P(F_i)$ is the probability of component i . reaching a certain limit state, given demand x .

The generation of PSDMs for bridges follows the general procedure of Nielson and DesRoches (2006):

- 1) Assemble N ground motions which represent a broad range of values for PGA . The ground motions can be selected from previous earthquake records, such as those in the PEER Strong Motion Database (<http://peer.berkeley.edu>).
- 2) Generate N statistical samples of the bridge using importance sampling. The samples must include statistical parameters that are significant for modeling uncertainties in seismic response of the bridge.
- 3) Input the ground motions and modelling parameters, and perform a non-linear time history analysis.

- 4) For each analysis, record the peak responses and values of PGA , and plot them in a log-log space. Estimate parameters in Eqn. (3.1.4) by a regression analysis and the residual, which defines the parameter ξ_D in Eqn. (3.1.5).

The limit states of damage for the various bridge components are assessed using a physics-based approach or engineering judgement. In this study the specific limit states of damage are adopted from the study of Nielson (2005), which are obtained using Bayesian updating of capacity curves.

The fragility of the system is assumed to follow a lognormal distribution. The probability of failure of the bridge P_f^E under seismic demand can be estimated by,

$$P_f^E = \int_0^{\infty} F_R(x) f_S(x) dx \quad (3.1.6)$$

3.2 Analysis of scour

3.2.1 Scour hazard

The probabilistic model of scour hazard begins with the model to calculate scour depth, based on the equation recommended by the FHWA (2001):

$$D_s = 2.0yK_1K_2K_3K_4 \left(\frac{b}{y} \right)^{0.65} F_r^{0.43} \quad (3.2.1)$$

in which, D_s is the scour depth measured from the average channel bed elevation to the bottom of the scour hole; y is the flow depth just upstream of the pier; b = the pier width; σ is sediment gradation ; and F_r is the upstream Froude number, defined as $F_r = V/(gy)^{1/2}$, where V is approach flow velocity;

the K_1 is correction factor that accounts for the nose shape of the pier; K_2 is coefficient that accounts for the angle between the direction of flow and the direction of the pier; K_3 is coefficient that accounts for streambed conditions, and K_4 is coefficient that accounts for the bed material size.

Eqn. (3.2.1) is recommended for both live-bed and clear-water condition (Alipour, et al. 2012).

The relationship between the flow discharge rate and flow depth, y just upstream of the pier for a channel with a rectangular cross-section is assumed to be given by Manning's equation:

$$Q = \frac{by}{n} \left(\frac{by}{b+2y} \right)^{2/3} S^{1/2} \quad (3.2.2)$$

where Q is the discharge rate ; n is the Gauckler–Manning coefficient (non-dimensional); and S is the slope of the hydraulic grade line or the linear hydraulic head loss, which is the same as the channel bed slope when the water depth is constant.

In previous work, Chee (1982) and Chiew (1984) conducted experiments to test variation of scour depth. In contrast, Johnson (1992) started from a deterministic model known as the CSU equation ("Highways" 1988) to develop a best-fit equation for scour depth. Uncertainties in flow depth and sediment gradation were considered in this model. The form of the model, developed from a nonlinear least-squares algorithm, is described as (Johnson 1992),

$$D_s = \lambda(2.02)(y) \left(\frac{b}{y} \right)^{0.98} F_r^{0.21} \sigma^{-0.24} \quad (3.2.3)$$

in which, λ is the model correction factor, which is intended to incorporate uncertainty due to the model structure (Ang and Tang 1984).

According to Eqn. (3.2.2), Eqn. (3.2.3) is much less sensitive to the discharge rate of flow than Eqn. (3.2.1), which would lead to an unreasonable result in practice. As a result, Eqn. (3.2.1) is adopted in the study.

The Manning equation is the most commonly used formula for calculating flow velocity in open channels. However, the Manning equation is far less accurate when deviations from ideal conditions, such

as small slopes, constant and regular section, etc., become large. Its lack of accuracy is mainly due to the following limitations (Garcia Diza 2005):

- 1) The hypothesis underlying the Manning equation is that the flow resistance effect exists between the contact surface of the wet perimeter and upper soil layer. This is only a correct hypothesis when the stream bed is relatively smooth and the depth is large.
- 2) The Gauckler–Manning coefficient is not constant; it depends on depth and slope, and decreases as the flow depth increases.

The first limitation limits the flows to which the Manning equation can be applied; the accuracy of the results calculated by the Manning equation depends on the flow. The second limitation implies that the value of velocity that is calculated by the Manning's equation may be inaccurate. Johnson (1995, 1996) found that for a selected range of flow depth to pier width ratios, the average of observed scour depth is lower than the scour depth that calculated by Eqn. (3.2.1). The limitations could be a reason for this discrepancy. To overcome these limitations, a model factor λ_s is introduced to Eqn. (3.2.1), which is assumed to have a normal distribution with mean value 0.57 and coefficient of variation (COV) of 0.6 (Johnson and Dock 1998).

Three probability distributions have been suggested to model discharge rate, Q , in Eqn. (3.2.2): the log-Pearson Type III distribution, lognormal distribution and Extreme Type I distribution (Ghosn et al. 2003). In this study, we use the Extreme Type I distribution. The flow depth y then can be derived from Eqn. (3.2.2). Thus, by defining a limit state in terms of scour depth D_p , the probability of exceedance is described by,

$$P_{\text{exceedance}} = P \left[D_s < 2.0 \lambda_s y K_1 K_2 K_3 K_4 \left(\frac{b}{y} \right)^{0.65} F_r^{0.43} \right] \quad (3.2.4)$$

This probability is calculated by Monte-Carlo simulation. The probability distribution parameters means and coefficients of variation (COV) defining the parameters in Eqn. (3.2.4) are summarized in Table 3.2.1. The specific values depend on the flow of interest.

Table 3.2.1 Mean and coefficients of variation of scour parameters

Variable	Distribution	Mean	COV
λ_s (model factor)	Normal (Johnson and Dock 1998)	0.57	0.60
y (flow depth)	Normal (Johnson 1992)	site-dependent	site-dependent
n (Gauckler–Manning coefficient)	Lognormal (FHWA 2001)	0.025	0.275
β (slope)	Normal(Johnson 1992)	site-dependent	0.2
K_3 (condition coefficient)	Normal(Johnson 1995)	1.10	0.05

3.2.2 The influence of scour on bridge performance

As stated in Chapter 2.4, bridge local scour decreases the embedded length of the pile and reduces the lateral support of the bridge. However, scour is unlikely to cause buckling of a bridge column because of the typically massive size of the column. In this study, therefore, the influence of scour is assumed to reduce the stiffness of the pile foundation. The static stiffnesses of a single pile are given by Makris et al. (1994):

$$K_H^{[1]} \approx E_s d \left(\frac{E_p}{E_s} \right)^{0.21} \quad (3.2.5a)$$

$$K_Z^{[1]} \approx 1.9 G_s d \left(\frac{L}{d} \right)^{2/3} \quad (3.2.5b)$$

in which, $K_H^{[1]}$ and $K_Z^{[1]}$ are horizontal and vertical stiffness of a single pile; d and L are diameter and embedded length of the pile; E_p is the Young's modulus of the pile; E_s is the Young's modulus of soil, and G_s is the shear modulus of soil.

The horizontal stiffness for the single pile in Eqn. (3.2.5a) is independent of pile length. In practice, a pile does not deform over its entire length. Instead, pile deformations and stresses reduce to negligible proportions within a distance l_a from the ground surface. The distance l_a is denoted the active pile length, and is on the order of 10 to 15 pile diameters. Eqn. (3.2.5a) is applicable for the piles that have a length L greater than l_a , and for these piles, the exact pile length L is an irrelevant parameter (Gazetas 1984). The local scour only affects the rotational stiffness of the pile. Compared to the rotational stiffness of the pile group, the rotational stiffness of an individual pile is negligible (Makris et al. 1994; Nielson 2005), so the rotational stiffness of each single pile is not incorporated in this study. The composite pile behavior is calculated from the basic geometry of the pile group. The equations for horizontal and rotational stiffness of pile group are presented in Eqn. (3.2.6a) and Eqn. (3.2.6b) respectively (Ma and Deng 2000):

$$K_H \approx \sum_{i=1}^N K_{H,i}^{[1]} \quad (3.2.6a)$$

$$K_R \approx \sum_{i=1}^N K_{Z,i}^{[1]} \cdot x_i^2 \quad (3.2.6b)$$

in which, K_H and K_R are the stiffnesses of a pile group in the horizontal and rotational directions, and x_i is the distance from the centroid of the pile group measured in the direction perpendicular to the axis of rotation.

3.3 Structural deterioration model, data, and comparison between deterioration and corrosion

3.3.1 Deterioration model and conditional failure rate due to deterioration

As noted previously, the condition of a bridge over time can be evaluated qualitatively from the National Bridge Inventory (NBI) condition ratings, which are based on observations of the condition of a large number of bridges (Estes and Frangopol 2001).

As a continuous process, bridge deterioration starts at the beginning of its service life (or following a period of initiation of deterioration), and the subsequent deterioration condition at a given time is highly related to the previous condition. This process can be modeled by a Markov chain, in which the probability distribution of condition at the next state depends only on the current state and not on the sequence of events that preceded it. Thus, in this study, a probabilistic deterioration model for a bridge is developed from the NBE condition ratings using a Markov chain. It is important to note that a Markov chain is a discrete-time process. Eqn. (3.3.1) shows the Markovian transition matrices (MTM) for bridge components (Cesare et al. 1992),

$$T = \begin{bmatrix} T_{99} & T_{98} & T_{97} & T_{96} & T_{95} & T_{94} & T_{93} & T_{92} & T_{91} & T_{90} \\ 0 & T_{88} & T_{87} & T_{86} & T_{85} & T_{84} & T_{83} & T_{82} & T_{81} & T_{80} \\ 0 & 0 & T_{77} & T_{76} & T_{75} & T_{74} & T_{73} & T_{72} & T_{71} & T_{70} \\ 0 & 0 & 0 & T_{66} & T_{65} & T_{64} & T_{63} & T_{62} & T_{61} & T_{60} \\ 0 & 0 & 0 & 0 & T_{55} & T_{54} & T_{53} & T_{52} & T_{51} & T_{50} \\ 0 & 0 & 0 & 0 & 0 & T_{44} & T_{43} & T_{42} & T_{41} & T_{40} \\ 0 & 0 & 0 & 0 & 0 & 0 & T_{33} & T_{32} & T_{31} & T_{30} \\ 0 & 0 & 0 & 0 & 0 & 0 & 0 & T_{22} & T_{21} & T_{20} \\ 0 & 0 & 0 & 0 & 0 & 0 & 0 & 0 & T_{11} & T_{10} \\ 0 & 0 & 0 & 0 & 0 & 0 & 0 & 0 & 0 & T_{00} \end{bmatrix} \quad (3.3.1)$$

where T_{ij} is the probability of a bridge component deteriorating from state i to state j in one year. Although bridges are inspected every two years, the data are also available at odd-year ages of bridges, due to the abundant data from the large numbers of bridges that are inspected each year. According to the analysis of bridge deterioration data for New Jersey bridges, the probability of a bridge component deteriorating by more than one state in two years is negligible (McCalmont 1990). Since this matrix is based on one-year transition probabilities, the probability that the condition of a bridge changes by two or more states in year is also negligible. Thus, all probabilities in Eqn. (3.3.1) that represent changes of two or more states are set equal to zero. Second, each row in MTM must sum to one. Thus, the MTM becomes (Cesare et. al 1992):

$$T = \begin{bmatrix} T_{99} & 1-T_{99} & 0 & 0 & 0 & 0 & 0 & 0 & 0 & 0 \\ 0 & T_{88} & 1-T_{88} & 0 & 0 & 0 & 0 & 0 & 0 & 0 \\ 0 & 0 & T_{77} & 1-T_{77} & 0 & 0 & 0 & 0 & 0 & 0 \\ 0 & 0 & 0 & T_{66} & 1-T_{66} & 0 & 0 & 0 & 0 & 0 \\ 0 & 0 & 0 & 0 & T_{55} & 1-T_{55} & 0 & 0 & 0 & 0 \\ 0 & 0 & 0 & 0 & 0 & T_{44} & 1-T_{44} & 0 & 0 & 0 \\ 0 & 0 & 0 & 0 & 0 & 0 & T_{33} & 1-T_{33} & 0 & 0 \\ 0 & 0 & 0 & 0 & 0 & 0 & 0 & T_{22} & 1-T_{22} & 0 \\ 0 & 0 & 0 & 0 & 0 & 0 & 0 & 0 & T_{11} & 1-T_{11} \\ 0 & 0 & 0 & 0 & 0 & 0 & 0 & 0 & 0 & 1 \end{bmatrix} \quad (3.3.2)$$

Finally, the last term $T_{00}=1$ (representing the absorbing state of the chain), because an NBI rating equal to 0 represents the failed condition, and the bridge cannot deteriorate further.

The bridge deterioration process is assumed to have stationary increments in the study by Cesare et.al (1990). However, a time-dependent MTM would be more accurate for the mechanism of bridge deterioration. For example, the deterioration rate of concrete reinforcement will increase in time under sulfate attack, and will be approximately constant under corrosion (Mori and Ellingwood 1993). In this study, then, bridge deterioration is assumed to have stationary increments only over relatively short intervals, n , rather than over the entire service life of the bridge. Thus, the distribution of NBI ratings for a bridge in year t is:

$$q_n = q_0 T_1^t \quad \text{when } t \leq n \quad (3.3.3a)$$

$$q_n = q_0 T_1^n \dots T_m^{t-n} \quad \text{when } t > n \quad (3.3.3b)$$

The probability vector q_0 defines the initial distribution of damage (1,0,0,0,0,0,0,0,0,0); it is assumed that a new bridge has NBI rating 9. Subsequent values T_i define the MTM in the m^{th} time interval.

The MTM is a time-dependent matrix and the terms in MTM can be calculated for each time interval n independently. The approach used to determine the terms in the MTM from experimental data, which have been obtained from bridge inspection programs (FHWA), is based on the common concept that frequency will approximately equal probability for very large samples. Through minimizing the squared difference between the relative frequency and the probability found by Eqn. (3.3.3a) or Eqn. (3.3.3b), the terms $T_{99} - T_{22}$ can be determined by the method of least-squares (Cesare et. al 1992):

$$\min \sum_1^{nm} \left[f_{i,nm} - (q_0 T_1^n \dots T_m^n) i \right]^2 C(nm) \quad \text{for } i=9,8,\dots,1 \quad (3.3.4)$$

where $f_{i,nm}$ = relative frequency of bridges in state i at age nm ; nm = number of years of data available;

$C(nm)$ = number of bridges of age nm .

To get a deterioration model that is related to the resistance of the bridge and can be used in structural reliability analysis, a relationship between NBI ratings and structural deterioration is needed. Such a relationship is described in the following paragraphs.

In previous studies, the *NBI* rating model was deterministic at a given time, and was described by a polynomial function of elapsed time (Jiang and Sinha 1989; Bolukbasi et al. 2004). In this study, the *NBI* rating model for a given bridge is a stochastic process, written as,

$$NBI(t) = NBI_0 C(t) \quad (3.3.5)$$

in which NBI_0 is the initial *NBI* rating, normally equal to 9 (see Eqn. (3.3.3b) and $C(t)$ is a deterioration function which is derived from the *NBI* rating history for the bridge of interest. Because of randomness in service and environmental loads and in time-dependent bridge strength and condition, $NBI(t)$ is a discrete random process.

As noted previously, Cesare, et al (1992) modeled the bridge rating, $NBI(t)$, as a Markov process, and provided the transition probabilities necessary to define the distribution of the bridge rating at any time, t . The mean value and coefficient of variation (COV) of this random process can be described as,

$$E[C(t)] = f_1(t) \quad (3.3.6a)$$

$$COV[C(t)] = f_2(t) \quad (3.3.6b)$$

in which $f_1(t)$ and $f_2(t)$ are functions of time t , and can be derived by regression analysis of *in situ* bridge inspection data.

To define the time-dependent bridge resistance necessary to determine the time-dependent failure probabilities, survival functions and conditional failure rates, it is necessary to convert the bridge rating process, $NBI(t)$, to a process defining the time-dependent resistance, $R(t)$. Adopting the method of Mori and Ellingwood (1993b), the time-dependent structural resistance is described by a random process, which can be written as,

$$R(t) = R_0 G(t) \quad (3.3.7a)$$

$$E[G(t)] = f_3(t) \quad (3.3.7b)$$

$$COV[G(t)] = f_4(t) \quad (3.3.7c)$$

in which R_0 is the initial resistance of bridge components or of the bridge structural system and $G(t)$ is the structural deterioration function that describes the resistance of the bridge structure at any time, t . In contrast to $C(t)$, $G(t)$ is a continuous random process.

It is clear that the discrete process $C(t)$ and the continuous process $G(t)$ are related, since they provide alternative descriptions of the capacity of the bridge in time. However, developing the relation between the two processes is not straightforward. The process $C(t)$ is determined primarily by visual inspection, and may reflect one or more simultaneously occurring mechanisms of deterioration. In contrast, determination of $G(t)$ generally starts with time-dependent material testing for a specific deterioration mechanism – corrosion, spalling, freeze-thaw damage, fatigue. If several of these mechanisms occur simultaneously, they must be combined to obtain an overall $G(t)$ for the bridge

structure. This combination is difficult, especially if there are synergistic effects from the different mechanisms. The following section presents a simple approach to overcome this difficulty.

Before developing the relationship between the processes $G(t)$ and $C(t)$, four assumptions are made. According to Sobanjo et al. (2010), the lognormal distribution is suitable for modeling many failure degradation processes, such as corrosion, crack growth and failures resulting from chemical reactions or processes. Based on this idea, the first assumption is that in any given year, $G(t)$ and $C(t)$ can be modeled as random variables, and both follow the lognormal distribution. At the same time, we assume that the deterioration of the bridge structure is dominated by corrosion, and that $G(t)$ can be considered as the structural deterioration function for corrosion. Although the NBI ratings are based on visual inspection and judgment of the inspector, the mechanisms of deterioration, such as spalling, cracking, etc, affect the capacity of the bridge. Thus, the NBI ratings are assumed to have a directly relationship with capacities of bridge components. Since both of $G(t)$ and $C(t)$ follow the lognormal distribution in any given year, and the two process are not independent, $G(t)$ and $C(t)$ are assumed as have a linear relationship. As a result, the question is how to define the relationship between these two random processes.

Combining Eqn. (3.3.6a), Eqn. (3.37b) and Eqn. (3.3.6b), Eqn. (3.3.7c), the relationship between $C(t)$ and $G(t)$ can be inferred:

$$G(t) = f[C(t)] \quad (3.3.8)$$

in which $f[C(t)]$ is a linear function of $C(t)$. It is important to note that the relationship is not age dependent, and this result is consistent with the essence of the NBI rating system. For each bridge component, $C(t)$ is known, and $G(t)$ can be computed by substituting $C(t)$ in Eqn. (3.3.8). Thus, after the transition of NBI ratings, the time-dependent resistances of bridge component, i , can be described as,

$$R(t) = R_0 G(t) \quad (3.3.9)$$

3.3.2 The influence of deterioration on bridge performance

Structural deterioration influences the performance of a bridge. This study focuses on the seismic response of a bridge susceptible to bridge deterioration and local scour. The modelling parameters, summarized in Table 3.3.1, cover most factors that would affect the seismic response. However, the effects of deterioration can be limited to a subset of the parameters in Table 3.3.1. Parameters that are related only to the material strength and stiffness, such as elastic modulus and shear modulus, generally are not affected by deterioration. Besides, even if some cross-section losses occur due to spalling and cracking of the concrete, the stiffness and mass of each bridge element will not decrease significantly provided that the reinforcement remains intact. Thus, the effects of deterioration will be modeled by its effects on steel and concrete strength.

Table 3.3.1. Parameter uncertainty in analytical bridge models (Nielson and DesRoches 2006)

Modelling parameter	Probability distribution	Distribution parameters ^a		Units
		1	2	
Steel strength	Lognormal	$\lambda = 459.4$	$\zeta = 0.08$	MPa
Concrete strength	Normal	$\mu = 33.8$	$\sigma = 4.3$	MPa
Bearing shear modulus	Uniform	$l = 0.66$	$u = 2.07$	MPa
Bearing coefficient of friction	Lognormal	$\lambda = \ln(\text{med})$	$\zeta = 0.1$	
Passive stiffness of abutment	Uniform	$l = 11.5$	$u = 28.8$	KN/mm/n
Active stiffness of abutments	Uniform	$l = 2.2$	$u = 6.6$	KN/mm/n
Deck mass	Uniform	$l = 0.9$	$u = 1.1$	
Damping ratio	Normal	$\mu = 0.045$	$\sigma = 0.0125$	

^aParameters for the normal distribution: (μ , σ) = mean and standard deviation; for the lognormal distribution, (λ , ζ) = median, coefficient of variation; for the uniform distribution, (l , u) = minimum and maximum value. Dimensions are given in mm; strengths in MPa.

Time-dependent resistances for bridge components are obtained by converting the NBI ratings to structural resistance, as described previously. However, resistance must be specified in a way that can be utilized in a finite element model. To this end, we assume that all capacities of reinforced concrete members, such as shear and moment capacities, will deteriorate at a rate defined by $G_i(t)$. Strictly speaking, the impact of deterioration would depend on the limit state considered; however (as will be

shown subsequently), the flexural capacity is the most important limit state considered. Thus, in first approximation, the capacities can be written as;

$$M_n(t) = M_{n,0}G_i(t) \quad (3.3.10a)$$

$$V_n(t) = V_{n,0}G_i(t) \quad (3.3.10b)$$

The moment capacity of a lightly reinforced concrete flexural member can be described as (ACI 318-14),

$$M_n = A_s f_y (d - a/2) \quad (3.3.11)$$

where A_s is area of non-prestressed longitudinal tension reinforcement; f_y is specified yield strength of reinforcement; d and a are geometrical parameters. According to Eqn. (3.3.11), the moment capacity degrades in same rate with steel strength degradation. In the study by Enright and Frangopol (1999), the same degradation rate is derived. Similarly, the shear strength for the members that subject to shear and flexure only can be described as (ACI 318-14),

$$V_n = 2\lambda\sqrt{f'_c}b_wd + \frac{A_v f_{yt}d}{s} \quad (3.3.12)$$

where λ is a modification factor accounting for concrete strength; $\sqrt{f'_c}$ is square root of specified compressive strength of concrete; A_v is area of shear reinforcement within spacing s ; f_{yt} is specified yield strength f_y of transverse reinforcement; and b_w is geometrical parameter.

For shear capacities of reinforced members, Angelakos et al. (2001) investigated the effect of concrete strength on shear strength of large beam members. They conducted an experimental program of twelve 1000 mm deep beams with concrete strength varying from 21 to 80 N/mm². They concluded that changing the concrete strength by a factor of 4 had almost no influence on the shear strength of these large beams. The beam components of the bridge that are modeled in this study can be considered as large beams. Besides, according to Eqn. (3.3.12), the shear capacity that provided by reinforce steel is much

larger than the provided by concrete. For columns subject to axial compression, the shear strength can be described as (ACI 318-14),

$$V_n = 2 \left(1 + \frac{N_u}{2000A_g} \right) \lambda \sqrt{f'_c} b_w d + \frac{A_v f_{yt} d}{s} \quad (3.3.13)$$

where N_u is factored axial force normal to the cross section and A_g is gross area of concrete section.

Thus, for beam components and column components subjected to shear, the degradation rates of shear capacity are assumed as same value with that of steel strength.

As a result, the time-dependent strengths of steel and concrete can be written as,

$$f_y(t) = f_{y,0} G(t) \quad (3.3.14a)$$

$$f'_c(t) = f'_{c,0} [G(t)]^2 \quad (3.3.14b)$$

where $f_{y,0}, f'_{c,0}$ are the initial strength of steel and concrete.

3.4 Analysis of competing hazards

A review of the literature (Stewart et al. 2003) has suggested that it is unusual for bridge deterioration to cause failure of a bridge without some external cause. Therefore, bridge deterioration is treated as a supplemental influence factor that will be taken into account in reliability assessment of the bridge under earthquake and scour hazard. In addition, bridge scour is modeled as a stationary process in this study. A scenario analysis is conducted to assess the reliability of the bridge under competing hazards. According to Sobanjo et al. (2010), the time-dependent failure probability can be modeled as a Weibull distribution. The Weibull distribution is mathematically defined as,

$$f(t) = \frac{\beta}{\alpha} \left(\frac{t}{\alpha} \right)^{\beta-1} \exp \left[- \left(\frac{t}{\alpha} \right)^\beta \right] \quad (3.4.1)$$

where α is scale parameter; β is shape parameter; and t is the time to failure.

The Weibull distribution is a form of probability distribution, which can approximate other known probability distributions. If $\beta=1$, it becomes an exponential distribution; if $\beta=2$ it becomes a Raleigh distribution; if $\beta \approx 3.6$, it approximates a normal distribution. When the Weibull distribution is applied to model failure of a structure, the values of β have distinct physical meanings, as discussed below. In particular, $\beta=1$ indicates a constant failure rate; $\beta > 1$ indicates a wear-out period (Aberbethy 1996). A larger value of β implies a higher conditional failure rate for structure. If the time-dependent failure probability follows a Weibull distribution, the survival function $S(t)$ can be described as,

$$S(t) = \exp\left[\left(-\frac{t}{\alpha}\right)^\beta\right] \quad (3.4.2)$$

By definition, $S(t)$ is the probability that the bridge life exceeds time t . Thus, the conditional failure rate $h(t)$ is defined as,

$$h(t)dt = \frac{S(t) - S(t + dt)}{S(t)} \quad (3.4.3)$$

According to Eqn. (3.4.2), and Eqn. (3.4.3), the conditional failure rate can be written as,

$$h(t) = \frac{\beta}{\alpha} \left(\frac{t}{\alpha}\right)^{\beta-1} \quad (3.4.4)$$

Thus, the survival function can be rewrote as,

$$S(t) = \exp[-H(t)] \quad (3.4.5)$$

in which, $H(t) = \int_0^t h(t)dt$ is the accumulation of failure rate over a specific time.

In this chapter, the mathematically models for this study are presented. In the following chapter, an analytical of typical reinforced concrete bridge model is built by SAP 2000, to give numerical results for the reliability assessment of a bridge subjected to single hazard and competing hazards.

Chapter 4

Performance assessment of deteriorating bridges under competing scour and earthquake hazards

4.1 General analysis procedures

The objective of this chapter is to examine the impacts of coupled bridge foundation scour and deterioration on bridge seismic response. An analytical model of a reinforced concrete bridge is introduced in Section 4.2. A sensitivity analysis is conducted in Section 4.3 to test the contribution of each bridge modelling parameter to the seismic response. In Sections 4.4 and 4.5, the method that was introduced in Chapter 3.1.2 is adopted to define the seismic fragility for each bridge component. For this purpose, a suite of 24 natural earthquake records was taken from the Pacific Earthquake Engineering Research Center (PEER) ground motion database and was used for seismic response analyses of the bridge. The detailed information of the earthquake records is shown in Table 4.1.1; with one exception, the epicentral distances associated with these records all are less than 20 km, making them near-field records. Using the SAP2000 structural analysis program, non-linear 3-D models are created for three situations: a bridge with a constant, random resistance; a bridge that is subjected to scour only, and; a bridge that is subjected to both scour and deterioration. In Section 4.6, the fragility curve of for the entire bridge is derived from the component fragility curves. Treating earthquake, scour and deterioration as three stochastically independent events, a survival function for the bridge is developed in Section 4.7 to predict its service life. Suggestions for reliability-based bridge design also are provided in Section 4.7.

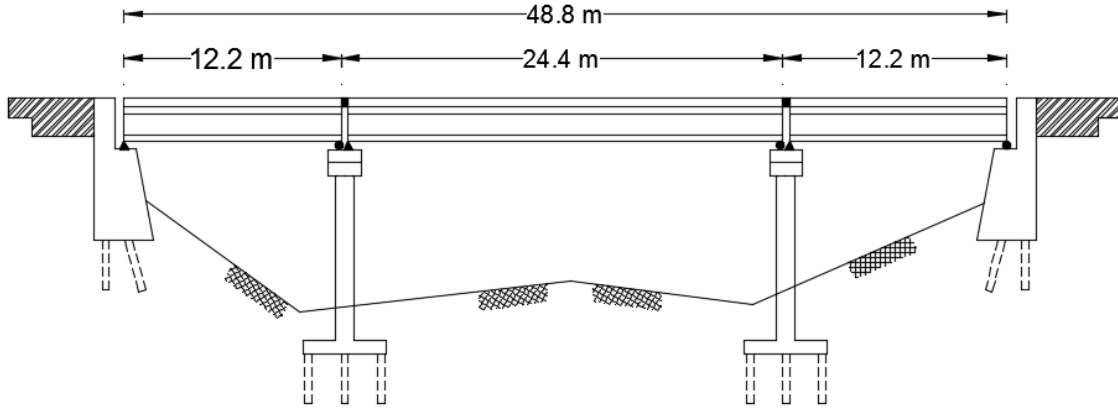
Table 4.1.1. Database of ground motion records (<http://peer.berkeley.edu>)

Earthquake	Location	Year	Magnitude	Epicentral Distance (km)
Gilroy	CA	2001	3.1	6
Northridge	CA	1994	6.7	28.9
Helena	MT	1935	6.2	6-20
Whittier	CA	1987	6.1	9
Loma Prieta	CA	1989	7.1	18
Gulf of California	Mexico	2001	5.7	10
Livermore Aftershock	CA	1980	5.4	10
Sierra Madre	CA	1991	5.8	11.97
Ancona	Italy	1972	4.4	4
Kocaeli	Turkey	1999	7.6	15
Chalfant Valley	CA	1986	6.4	12
Palm Springs	CA	1986	5.9	12
Stone Canyon	CA	1972	4.7	5
Westmorland	CA	1981	5.7	4
Petrolia	CA	1991	6	10
Petrolia Aftershock	CA	1992	7	15
Parkfield earthquake	CA	2004	6	8
Morgan Hill	CA	1984	6.2	9
Superstition Hills	CA	1987	6.6	2
Alum Rock	CA	2007	5.4	9.2
Bishop	CA	1984	3.7	6
Manjil–Rudbar	Iran	1990	7.4	15
Kobe	Japan	1995	6.8	16
Nahanni	Canada	1985	6.9	Less than 20

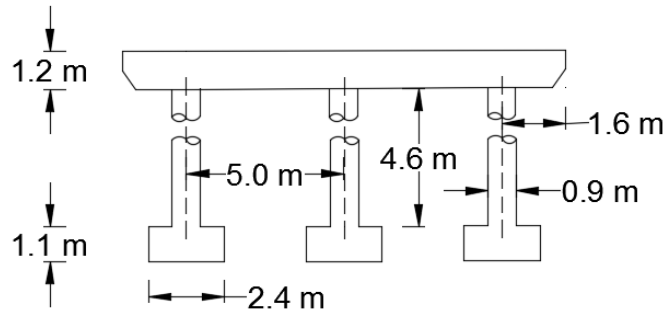
4.2 Analytical models of reinforced concrete bridge

The bridge model used in this study is a typical Multi-Span Simply Supported (MSSS) reinforced concrete bridge, which is adopted from the study by Nielson (2005). The configuration of this (MSSS) reinforced concrete bridge is shown in Figure 4.1. This bridge has three spans, which are 12.2, 24.4 and 12.2 m long, respectively, and the total length of the bridge is 48.8 m. Each span is constructed of eight AASHTO prestressed girders supporting a deck with width 15.01 m (see Figure 4.1c). The girders for the end spans are AASHTO Type I girders which bear on a pile type abutment at one end and a multi-column bent at the other end. The girders for the center span are AASHTO Type III girders. There are

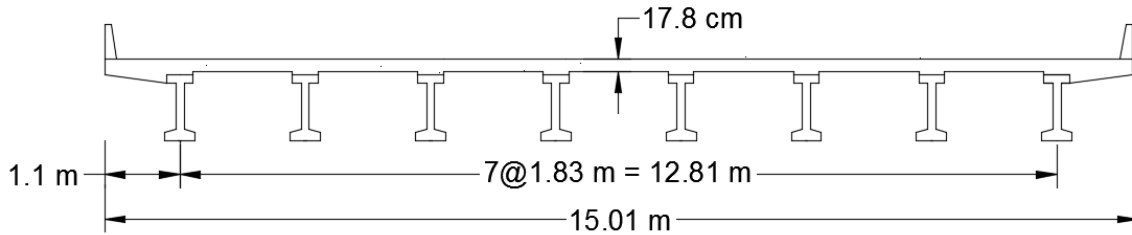
two types of bearings for this bridge: elastomeric bearing with fixed dowels and elastomeric bearing with expansion dowels. <ore detailed information on the bearings is discussed in the following section.



General Elevation



Pier



Deck

Figure 4.2.1 MSSS concrete girder bridge configuration

The reinforcing layout in the bent beam and column for this bridge are shown in Figure 4.2.

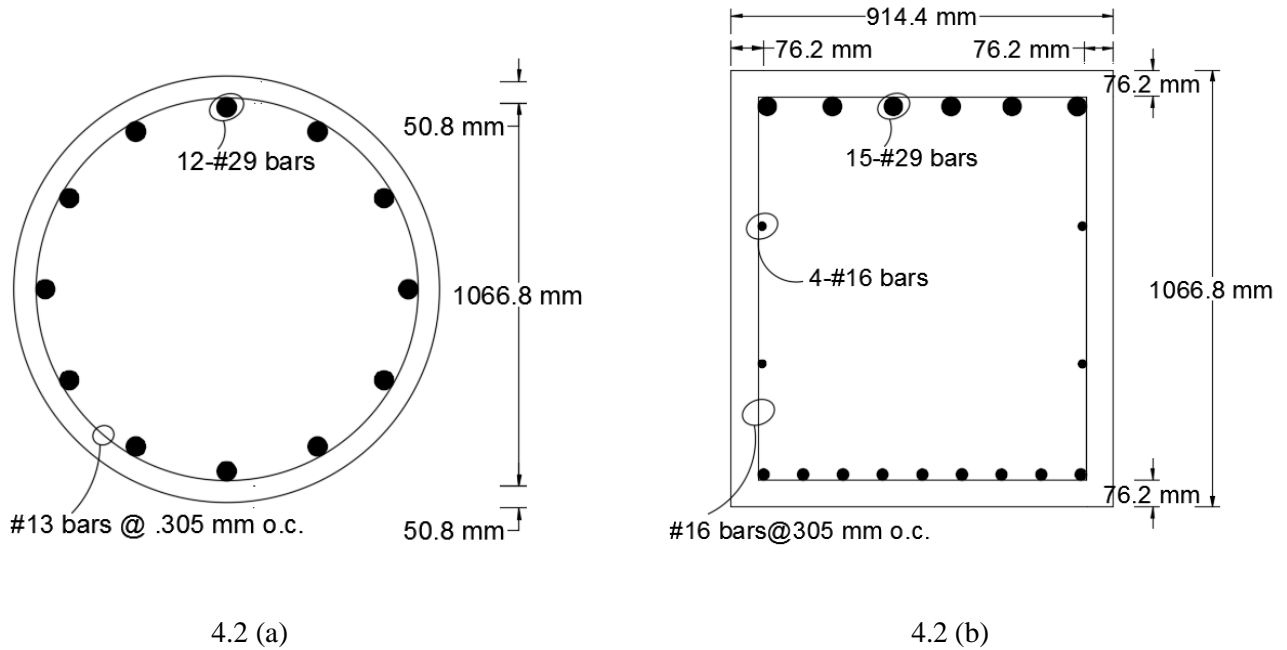


Figure 4.2.2 Concrete member reinforcing layout (a) Column (b) Bent beam

The abutments for this bridge are the pile-bent girder seat type abutment (See Appendix Section A.2.4), and the abutments for this bridge utilize a 2.4 m high back wall in conjunction with ten driven piles. The model of the pile foundation for this bridge is shown in Figure A.6. The pile cap are 2348 mm square and 1092 mm thick reinforced concrete footings. The embedment length of the eight piles from the bottom of the footing is assumed to be 8 m, and there is no positive connection between any two piles.

Uncertainties associated with various analysis parameters have been modeled as random variables in previous studies (Nielson and DesRoches 2006; Padgett et al. 2007) to consider possible variations in key input parameters. In this study, the uncertainties in material properties, stiffness of abutment and deck mass are considered to estimate the variability of seismic response of the bridge; in addition, uncertainties in deterioration are reflected, and a different foundation model is employed to examine stiffness prior to

and following scour. A dynamic analysis of the bridge (see Appendix A) revealed that the periods of vibration in the longitudinal and transverse directions were 0.58, 0.53 seconds, respectively. Damping is taken into account in the model using Rayleigh damping, but it is also treated as a random variable (Nielson and DesRoches 2006). The statistical descriptions of key parameters in the bridge reliability assessment are shown in Table 3.3.1.

The superstructure, which includes the deck and girders, is assumed to remain linear during seismic load. Pounding between segments of the deck is modeled by an impact element. Non-linear behavior is expected for the bridge columns subjected to earthquake forces. A P-M₂-M₃ plastic hinge element is used in SAP2000 to describe this type of column behavior. The bearing models are incorporated in SAP2000 by two parallel link elements, which account for the contribution of elastomeric pads in addition to the effect of the steel dowels. The abutment is modeled by two parallel multilinear elastic link elements to simulate the behaviors of the abutment in the longitudinal and transverse directions. The foundation is modeled by translational and rotational springs. The stiffness of the springs is calculated by the equations in Section 3.2.2.

Detailed information of the analytical bridge model is discussed in Appendix A.

4.3 Sensitivity analysis

According to the study of Nielson (2005), the bridge fragility is estimated by combining the fragilities of the major components. Rather than concentrate the research on the most fragile component, the component level approach can reveal the responses of the major bridge components at the same time, thereby avoiding a misrepresentation of bridge overall fragility (Nielson and DesRoches 2006). Adopting the same approach in this study, the major components of the bridge are selected as the column, bearing, and abutment, and the seismic responses of these components are obtained in terms of ductility demand, deformation or other key response parameters; these responses are used to develop the fragilities of bridge components.

After the determination of modelling parameters and bridge components, a sensitivity analysis is conducted to relate the modelling parameters to the seismic responses of bridge components. The sensitivity of major bridge components is depicted by a tornado diagram, which is a useful tool to show the sensitivity of a response with respect to the variation of input parameters. At first, an “original” FE model of the bridge analyzed is built up for comparison, in which the modelling parameters in Table 4.2.1 are assumed as the commonly used values. This represents the “benchmark” case. Following this, the response values are estimated when each modelling parameter is varied one at a time between its lower and upper values, and the same process is repeated for the other seven modelling parameters. The lower and upper values of each modelling parameter are taken at its 2th and 98th percentile values respectively. Note that all the response values of the eight bridge components are obtained from nonlinear time-history analyses without considering bridge scour or deterioration, which implies that these factors would not change the conclusions drawn from the sensitivity analysis of the bridge.

Two ground motion records are adopted for this analysis, in which the two records represent a lower and a higher earthquake magnitude. The information on these ground motion records is presented in Table 4.3.1.

Table 4.3.1 Ground motion records used in sensitivity analysis

Ground motion	GM-1	GM-2
Earthquake	Gulf of California (2001)	Parkfield (2004)
PGA of horizontal component 1 (g)	0.125	0.469
PGA of horizontal component 2 (g)	0.067	0.368

The sensitivities of the column ductility and abutment passive response which are the most fragile and least fragile components of the bridge, respectively, are shown in Figure 4.3.1 and Figure 4.3.2. The vertical line represents the “benchmark” case. In the tornado diagrams, the modelling parameters are depicted in descending order of absolute difference between the response values with respect to the lower and upper input modelling parameter values; red and blue represent the lower and upper values of the corresponded modelling parameters.

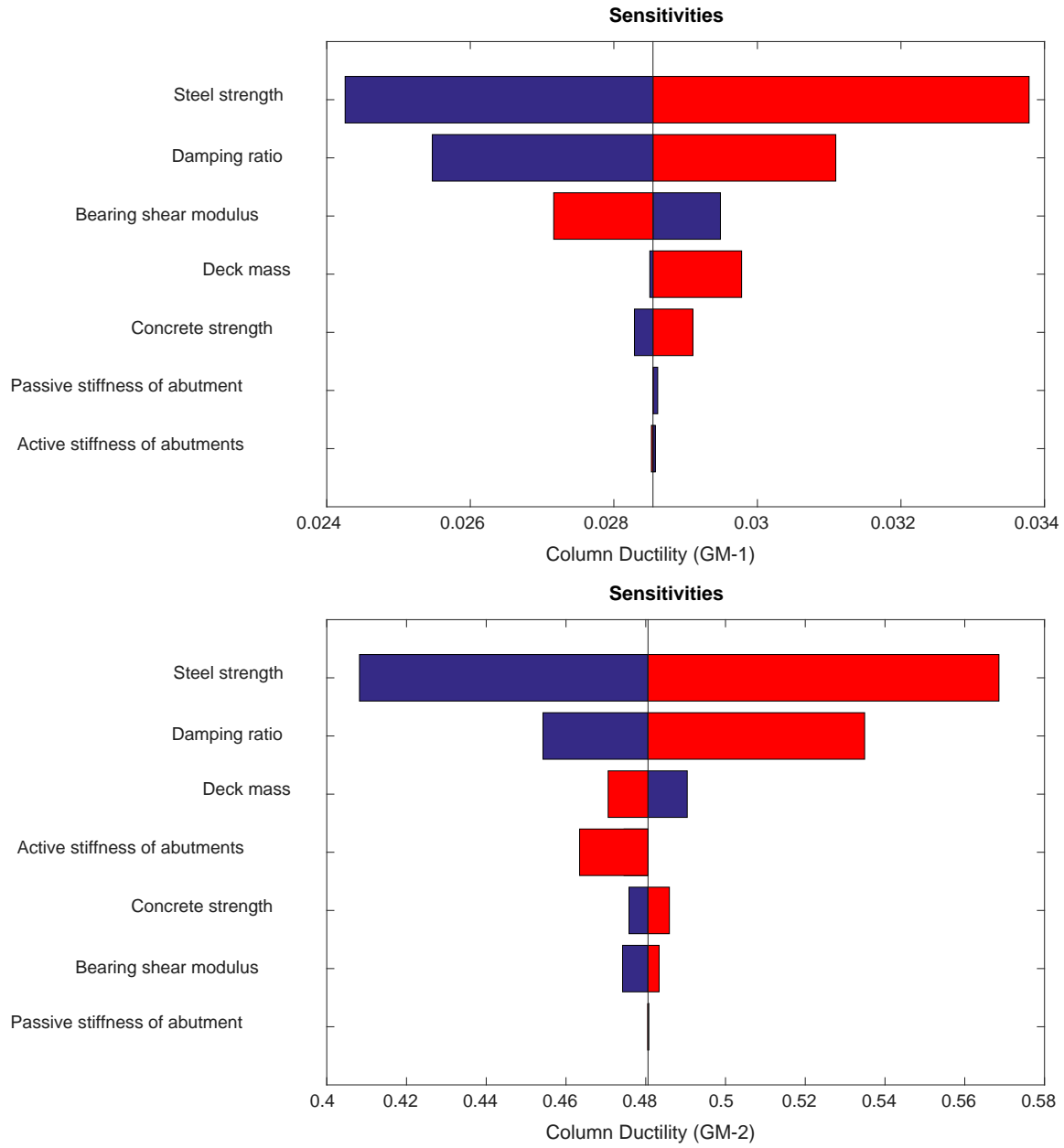


Figure 4.3.1 Tornado diagrams of column ductility under ground motions (a) GM-1 and (b) GM-2

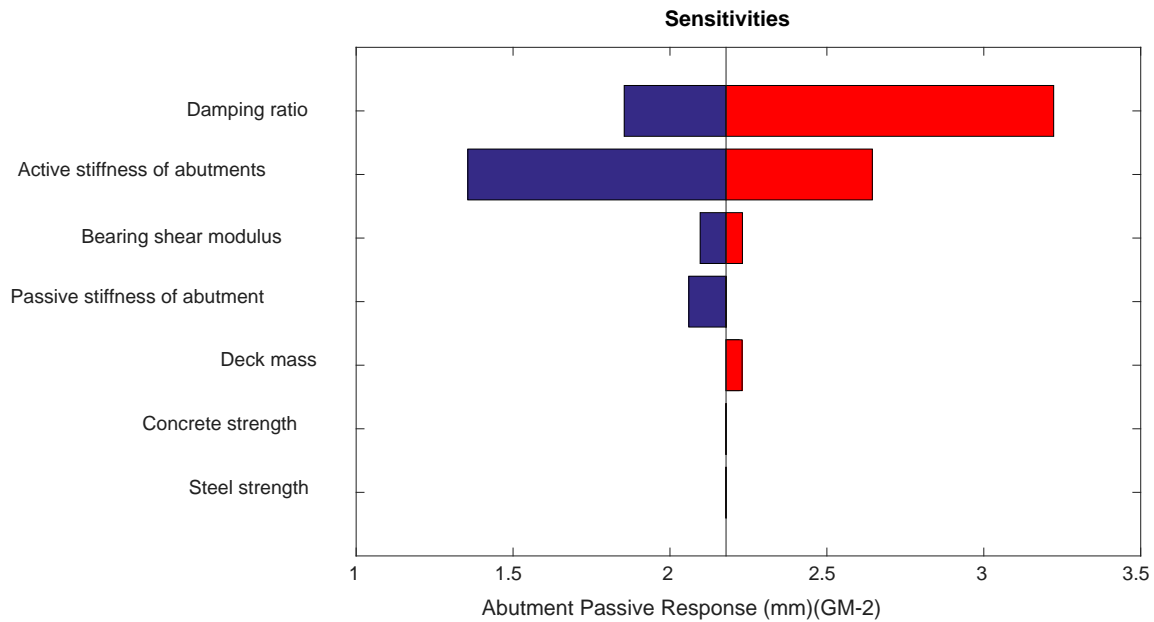
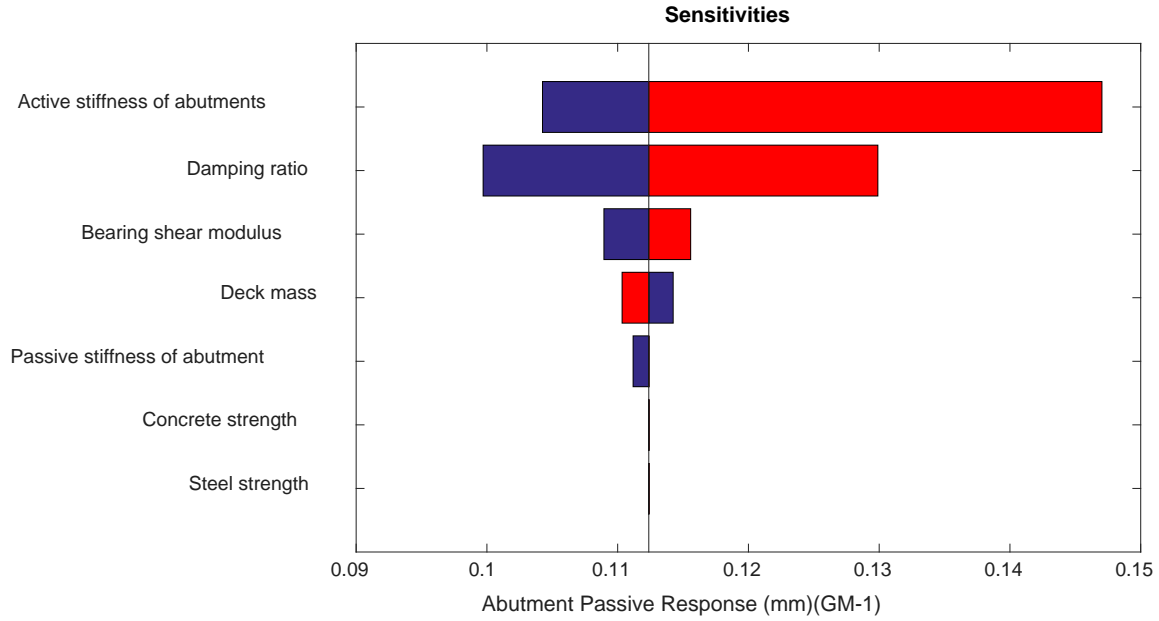


Figure 4.3.2 Tornado diagrams of abutment passive response under ground motions (a) GM-1 and (b) GM-2

The tornado diagram of column ductility shows that steel strength and damping ratio are the two modelling parameters for which the response is most sensitive. Steel strength has a significant impact on

the moment capacity of the column, a higher value of steel strength leading to a lower level of column ductility under the same ground motion. At the same time, damping ratio effects column ductility by reducing the seismic response of bridge; in other word, the response of the bridge is reduced by damping. The two modelling parameters affect the column ductility under earthquake in different ways, but both have a positive influence on the seismic response of the column. For abutment passive response, except for damping ratio which reduces the response of the whole bridge, abutment passive stiffness is the most important modelling parameter.

4.4 Probabilistic seismic demand analysis

4.4.1 PSDM analysis of bridge with stationary resistance

Uncertainties are considered in the bridge model, as noted previously. Thus, prior to generating the PSDMs, statistical samples of the bridge must be created. A Latin-hypercube sampling method (Ayyub and Lai 1989) is adopted to generate 24 statistical samples of the bridge. The samples are paired randomly with the 24 ground motion records and are analyzed using non-linear time history analyses to obtain the PSDMs.

Each earthquake record consists of three components: two perpendicular horizontal components and one vertical component. Vertical ground motions are not considered in this study, since previous studies have shown that they are not necessary for bridge fragility analysis (Nielson and DesRoches 2006; Zakeri et al. 2013). Each set of orthogonal horizontal components of ground motions are randomly paired with a bridge sample, producing a total of 24 nonlinear dynamic analyses for the bridge samples (Zakeri et al. 2013).

Because two components of ground motion records are used in the finite element model, scaling of the PGA is required. The most common of these scaling methods are listed in Beyer and Bommer (2007). The following alternative measures of ground motion intensity (all in terms of PGA) were considered:

- GM_{xy} : The geometric mean of the recorded components x and y is,

$$PGA_{GM_{xy}} = \sqrt{PGA_x \cdot PGA_y} \quad (4.4.1)$$

- AM_{xy} : The arithmetic mean of the recorded components x and y is,

$$PGA_{AM_{xy}} = \frac{PGA_x + PGA_y}{2} \quad (4.4.2)$$

- $SRSS_{xy}$: The square root of the sum of squares of the recorded components x and y is,

$$PGA_{SRSS_{xy}} = \sqrt{PGA_x^2 + PGA_y^2} \quad (4.4.3)$$

Median seismic demands, expressed in terms of scaled PGAs for the different scaling methods are shown in Tables 4.4.1, 4.4.2 and 4.4.3.

Table 4.4.1. Probabilistic seismic demand models for eight component responses (GM_{xy} as scaling PGA)

Response	PSDM	R^2	$\beta_{D PGA}$
$\ln(\mu_\phi)$	$\ln(2.96) + 1.596 \ln(\text{PGA})$	0.7376	0.65
$\ln(fx_L)$	$\ln(21.71) + 1.344 \ln(\text{PGA})$	0.6909	0.62
$\ln(fx_T)$	$\ln(15.23) + 1.164 \ln(\text{PGA})$	0.6240	0.75
$\ln(ex_L)$	$\ln(44.30) + 1.614 \ln(\text{PGA})$	0.7112	0.70
$\ln(ex_T)$	$\ln(23.81) + 1.468 \ln(\text{PGA})$	0.6313	0.77
$\ln(ab_p)$	$\ln(18.95) + 1.833 \ln(\text{PGA})$	0.7506	0.72
$\ln(ab_A)$	$\ln(21.82) + 1.893 \ln(\text{PGA})$	0.7698	0.71
$\ln(ab_T)$	$\ln(16.83) + 1.628 \ln(\text{PGA})$	0.6726	0.78

Table 4.4.2. Probabilistic seismic demand models for eight component responses (AMxy as scaling PGA)

Response	PSDM	R ²	$\beta_{D PGA}$
$\ln(\mu_\phi)$	$\ln(3.01) + 1.630 \ln(\text{PGA})$	0.7539	0.63
$\ln(fx_L)$	$\ln(22.02) + 1.374 \ln(\text{PGA})$	0.7070	0.60
$\ln(fx_T)$	$\ln(15.21) + 1.165 \ln(\text{PGA})$	0.6279	0.75
$\ln(ex_L)$	$\ln(44.79) + 1.645 \ln(\text{PGA})$	0.7243	0.69
$\ln(ex_T)$	$\ln(24.02) + 1.497 \ln(\text{PGA})$	0.6428	0.76
$\ln(ab_p)$	$\ln(18.82) + 1.857 \ln(\text{PGA})$	0.7552	0.72
$\ln(ab_A)$	$\ln(21.65) + 1.918 \ln(\text{PGA})$	0.7742	0.70
$\ln(ab_T)$	$\ln(16.86) + 1.655 \ln(\text{PGA})$	0.6807	0.77

Table 4.4.3. Probabilistic seismic demand models for eight component responses (SRSS_{xy} as scaling PGA)

Response	PSDM	R ²	$\beta_{D PGA}$
$\ln(\mu_\phi)$	$\ln(1.68) + 1.643 \ln(\text{PGA})$	0.7617	0.62
$\ln(fx_L)$	$\ln(13.50) + 1.386 \ln(\text{PGA})$	0.7167	0.59
$\ln(fx_T)$	$\ln(10.14) + 1.166 \ln(\text{PGA})$	0.6271	0.75
$\ln(ex_L)$	$\ln(24.80) + 1.657 \ln(\text{PGA})$	0.7311	0.68
$\ln(ex_T)$	$\ln(14.00) + 1.505 \ln(\text{PGA})$	0.6469	0.75
$\ln(ab_p)$	$\ln(9.54) + 1.861 \ln(\text{PGA})$	0.7545	0.72
$\ln(ab_A)$	$\ln(10.73) + 1.922 \ln(\text{PGA})$	0.7734	0.70
$\ln(ab_T)$	$\ln(9.22) + 1.659 \ln(\text{PGA})$	0.6808	0.77

According to the results in the three tables, when the SRSS_{xy} is chosen to scale the records, the probabilistic seismic demands on the eight bridge components are much lower, leading to a less

conservative estimation of seismic response. Therefore, in this study, the geometric mean of the PGA values of the two horizontal ground motions is chosen for scaling the peak ground acceleration; further justification for this choice is given in Beyer et al. (2007).

4.4.2 PSDM analysis of bridge subjected to bridge scour

For the analysis of bridge scour, historical records on discharge rate in two rivers in the State of Colorado are adopted for the analysis. The records are achieved from the USGS website (<http://nwis.waterdata.usgs.gov/usa/nwis/peak>). For the analysis, Colorado River and Rio Grande are selected as rivers with higher and low lower discharge, respectively. The annual peak flow discharge rate that recorded from 1951 to 2014 of the two rivers are plotted in Figure 4.4.1

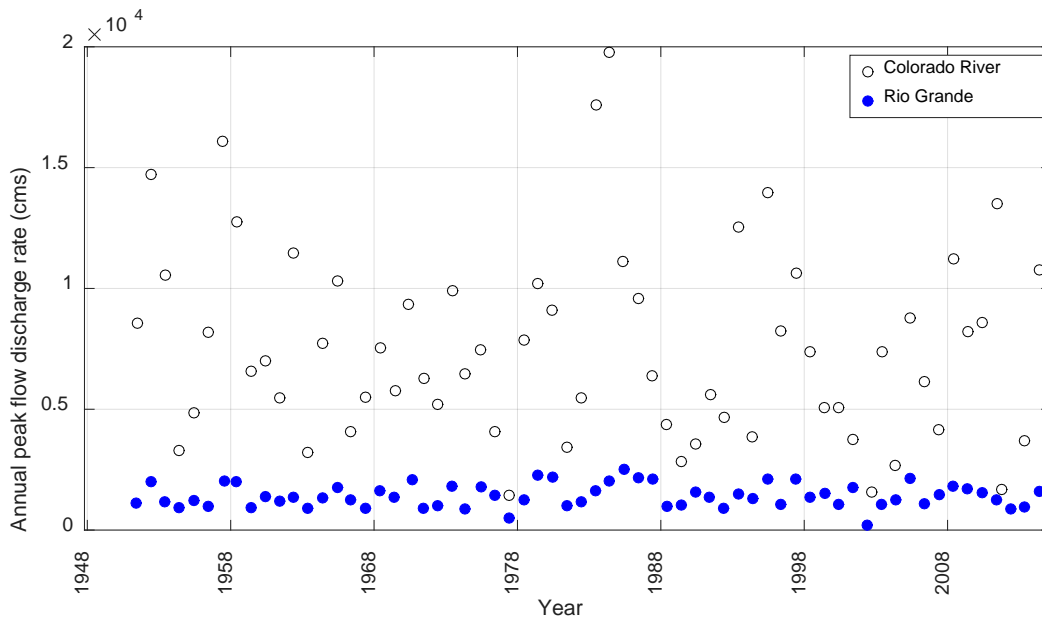


Figure 4.4.1 Annual peak flow discharge rate

The mean value of discharge of the Rio Grande is much less than that of the Colorado River, equaling approximately 20% of that of the higher discharge river; thus, using this discharge data, it is possible to make a comparison to reveal how scour level might affect bridge seismic response.

The scour depth for the two rivers can be calculated according to Eqn. (3.2.1) and Eqn. (3.2.2). The histograms of the occurrence probability of a range of scour depth are shown in Figure 4.4.2

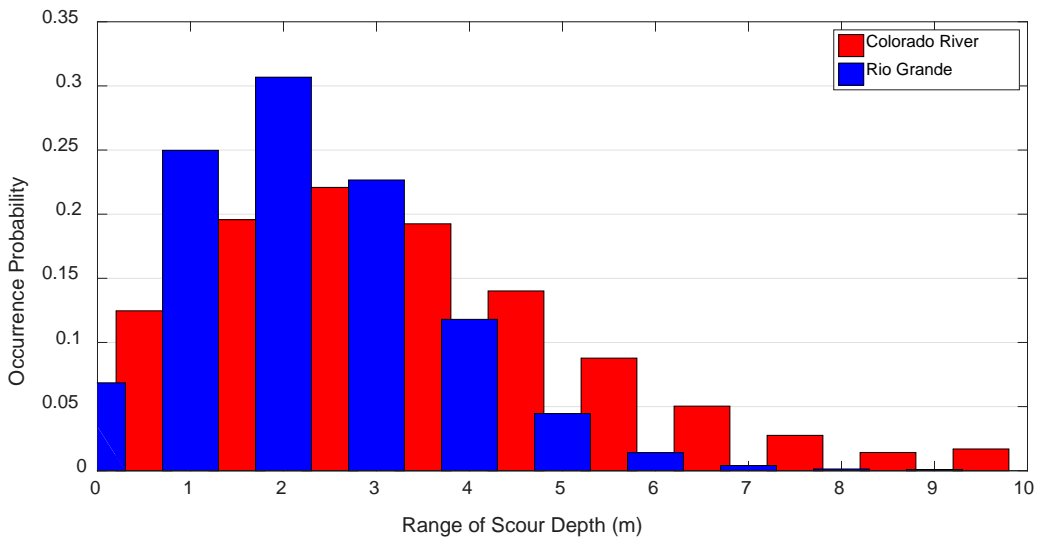


Figure 4.4.2. The histograms of the occurrence probability of a range of scour depth

Figure 4.4.2 indicates that the scour depths are skew-positive for the two rivers considered. However, this observation is based on a sample of scour data for only two rivers. Thus, consistent with the assumptions made in other studies (e.g., Johnson and Ayyub 1991), the scour depth in this study is assumed to follow a normal distribution (Johnson and Ayyub 1991). Based on this assumption, the probability of exceedance of various levels of scour depth is shown in Figure 4.4.3.

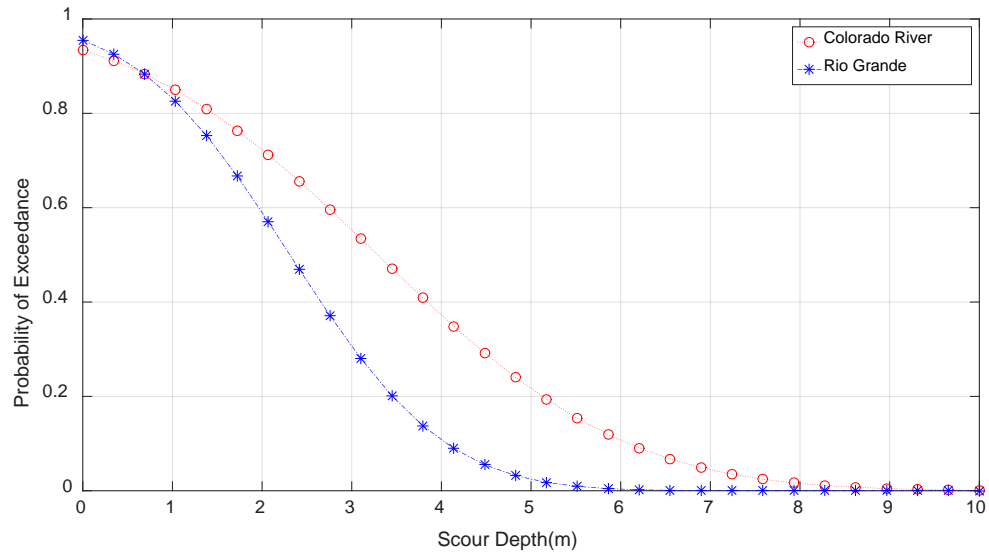


Figure 4.4.3 Probability of exceedance of scour depth

These scour effects are incorporated in the SAP 2000 bridge model using the methodology introduced in Section 3.2.2. Adopting the Latin-hypercube sampling method (Ayyub and Lai 1989), 24 scour depth values are generated for each river and are randomly paired with the 24 finite element bridge samples discussed in Chapter 4.4.1. The PSDMs under the two scour conditions are shown in Table 4.4.4 and Table 4.4.5.

Table 4.4.4. Probability seismic demand models for eight component responses (Scour with lower discharge rate)

Response	PSDM	R ²	$\beta_{D PGA}$
$\ln(\mu_\phi)$	$\ln(2.85) + 1.521 \ln(\text{PGA})$	0.7107	0.72
$\ln(fx_L)$	$\ln(28.13) + 1.484 \ln(\text{PGA})$	0.7174	0.64
$\ln(fx_T)$	$\ln(19.28) + 1.394 \ln(\text{PGA})$	0.6574	0.73
$\ln(ex_L)$	$\ln(54.49) + 1.700 \ln(\text{PGA})$	0.6798	0.80
$\ln(ex_T)$	$\ln(22.49) + 1.480 \ln(\text{PGA})$	0.6771	0.70
$\ln(ab_p)$	$\ln(17.48) + 1.800 \ln(\text{PGA})$	0.7198	0.77
$\ln(ab_A)$	$\ln(21.33) + 1.882 \ln(\text{PGA})$	0.7437	0.76
$\ln(ab_T)$	$\ln(19.22) + 1.720 \ln(\text{PGA})$	0.7187	0.74

Table 4.4.5. Probability seismic demand models for eight component responses (Scour with higher discharge rate)

Response	PSDM	R ²	$\beta_{D PGA}$
$\ln(\mu_\phi)$	$\ln(2.83) + 1.655 \ln(\text{PGA})$	0.7197	0.75
$\ln(fx_L)$	$\ln(29.55) + 1.533 \ln(\text{PGA})$	0.7045	0.68
$\ln(fx_T)$	$\ln(21.89) + 1.451 \ln(\text{PGA})$	0.6709	0.69
$\ln(ex_L)$	$\ln(61.07) + 1.785 \ln(\text{PGA})$	0.6884	0.82
$\ln(ex_T)$	$\ln(22.15) + 1.458 \ln(\text{PGA})$	0.6733	0.70
$\ln(ab_p)$	$\ln(17.51) + 1.8121 \ln(\text{PGA})$	0.7279	0.76
$\ln(ab_A)$	$\ln(21.65) + 1.903 \ln(\text{PGA})$	0.7647	0.72
$\ln(ab_T)$	$\ln(18.60) + 1.709 \ln(\text{PGA})$	0.7152	0.74

4.4.3 PSDM analysis of deteriorating bridge under bridge scour

Bridge deterioration is modeled by a Markov process, which was developed using data from the National Bridge Inventory (NBI) Condition Ratings. The time-dependent Markov transition matrices (MTM) for bridge components are shown in Appendix B. Because there is a lack of data for bridges that

are in a serious condition, the lowest rating number considered in this study is 3, corresponding to the state where the bridge deterioration is serious and major rehabilitation is necessary. Consequently, there are only six terms in every MTM. The value of each term in the MTM is derived from the average of condition ratings (Yi 1990). It should be noted that this approach would be inaccurate when applied to bridges that are in a condition of extreme deterioration where replacement is likely to be necessary.

Adopting the method introduced in Chapter 3.3, NBI ratings are related to residual resistance by regression analysis which based on time-dependent degradation rates of bridge beam that derived from NBI ratings and corrosion of reinforcement. For a reinforced concrete beam in flexure, resistance degradation rate $G(t)$ is defined as (Enright and Frangopol 1998),

$$G(t) = 1 - k_1 t + k_2 t^2 \quad (4.4.4)$$

in which, t is elapsed time; k_1, k_2 are degradation constants. The values for the corrosion initial time T_I and degradation constants k_1, k_2 are shown in Table 4.4.6. In this study, the data for “medium degradation rate” will be used to build up the relationship between NBI ratings and residual resistance.

Table 4.4.6 Strength degradation parameters (Enright and Frangopol 1999)

Degradation rate	$E[T_I]$ (year)	$E[k_1]$	$E[k_2]$	$E[g(75)]$
Medium	4.0	0.0075	0	0.4675
High	2.25	0.015	0.000075	0.3057

For the bridges in which NBI ratings equal 8 or higher, which corresponds to very good condition in Table 2.3.1, no repair action is required. It is reasonable to assume that the resistance of the bridge begins to decrease when the NBI rating equals 7, which is associated with repair action involving minor maintenance. Besides, according to the probability distribution of NBI ratings for bridge beams, the mean value of the NBI rating begins to decrease from 7 beyond an age of about six years (Yi 1990); in other words, bridge deterioration initiates after six years of its service life. As a result, the regression analysis

is based on the data obtained after sixth year. The deterioration function is shown in Eqn. (4.4.5), and the regression coefficient is 0.83. The equation is described as,

$$E[G(t)] = 1.027E[C(t)] + 0.2006 \quad (4.4.5)$$

The relationship between NBI rating and residual resistance has not been discussed in previous studies. Because of the limitation of data, in this study, this relationship is assumed to be linear, and it can be written as,

$$R^* = 1.027N + 0.2006 \quad (4.4.6)$$

in which, R^* is residual resistance and N is NBI rating. NBI ratings and the corresponding residual resistances are shown in Table 4.4.7.

Table 4.4.7. Relationship between NBI rating and residual resistance

NBI rating	Description	Repair action	Residual resistance (%)
9	Excellent condition	None	1
8	Very good condition	None	1
7	Good condition	Minor maintenance	0.99
6	Satisfactory condition	Major maintenance	0.89
5	Fair condition	Minor repair	0.77
4	Poor condition	Major repair	0.66
3	Serious condition	Rehabilitate	0.54
2	Critical condition	Replace	0.43
1	Imminent failure condition	Close bridge and evacuate	0.31
0	Failed condition	Beyond corrective action	0.20

By multiplying the residual resistance factor by the concrete and steel strength in the SAP 2000 model, the PSDMs can be obtained. The PSDMs for each deterioration condition are presented in Appendix C.

4.5 Seismic fragility analysis for bridge components

In this section, according to the PSDMs, the seismic fragilities are calculated based on Eqn. (3.1.5). The component seismic fragilities for slight and moderate damage states are presented. The limit state for each damage state is assessed either by a physics-based approach and/ or a judgmental approach (Nielson and DesRoches 2007). In this study, we adopt the results of Nielson and DesRoches (2007); the limit states of slight and moderate damage state are summarized in Table 4.5.1.

Table 4.5.1. Medians and dispersions for bridge component limit states using Bayesian updating (Nielson and DesRoches 2007)

Component	Slight		Moderate	
	med	disp	med	disp
Concrete Column μ_ϕ	1.29	0.59	2.10	0.51
Elastomeric Bearing Fixed-Long(mm)	28.9	0.60	104.2	0.55
Elastomeric Bearing Fixed-Tran(mm)	28.8	0.79	90.9	0.68
Elastomeric Bearing Expan-Long(mm)	28.9	0.60	104.2	0.55
Elastomeric Bearing Expan-Tran(mm)	28.8	0.79	90.9	0.68
Abutment-Passive(mm)	37.0	0.46	146.0	0.46
Abutment-Active(mm)	9.8	0.70	37.9	0.90
Abutment-Tran(mm)	9.8	0.70	37.9	0.90

The parameters of the lognormal fragilities for bridges that are subjected to only seismic hazard, and both scour and seismic hazard are shown in Table 4.5.2, Table 4.5.3, and Table 4.5.4.

Table 4.5.2. Parameters for bridge component fragilities (Without scour or deterioration)

Component	Slight		Moderate	
	Median (g)	Dispersion	Median (g)	Dispersion
Column	0.59	0.55	0.81	0.52
Fxd Bearing-long	1.24	0.64	3.21	0.62
Fxd Bearing-trans	1.73	0.94	4.64	0.87
Exp Bearing-long	0.77	0.57	1.70	0.55
Exp Bearing-trans	1.14	0.75	2.49	0.70
Abut-passive	1.44	0.47	3.05	0.47
Abut-active	0.66	0.53	1.34	0.61
Abut-trans	0.72	0.64	1.65	0.73

Table 4.5.3. Parameters for bridge component fragilities (Scour with lower discharge rate)

Component	Slight		Moderate	
	Median (g)	Dispersion	Median (g)	Dispersion
Column	0.59	0.61	0.82	0.58
Fxd Bearing-long	1.02	0.59	2.42	0.57
Fxd Bearing-trans	1.33	0.77	3.04	0.72
Exp Bearing-long	0.69	0.59	1.46	0.57
Exp Bearing-trans	1.18	0.71	2.57	0.66
Abut-passive	1.52	0.50	3.25	0.50
Abut-active	0.66	0.55	1.36	0.63
Abut-trans	0.68	0.59	1.48	0.68

Table 4.5.4. Parameters for bridge component fragilities (Scour with higher discharge rate)

Component	Slight		Moderate	
	Median (g)	Dispersion	Median (g)	Dispersion
Column	0.62	0.58	0.84	0.55
Fxd Bearing-long	0.99	0.59	2.28	0.57
Fxd Bearing-trans	1.21	0.72	2.67	0.67
Exp Bearing-long	0.66	0.57	1.35	0.55
Exp Bearing-trans	1.20	0.72	2.63	0.67
Abut-passive	1.51	0.49	3.22	0.49
Abut-active	0.66	0.53	1.34	0.61
Abut-trans	0.69	0.60	1.52	0.68

The fragilities parameterized in Tables 4.5.2 – 4.5.4 are plotted in Figures 4.5.1 through Figure 4.5.3.

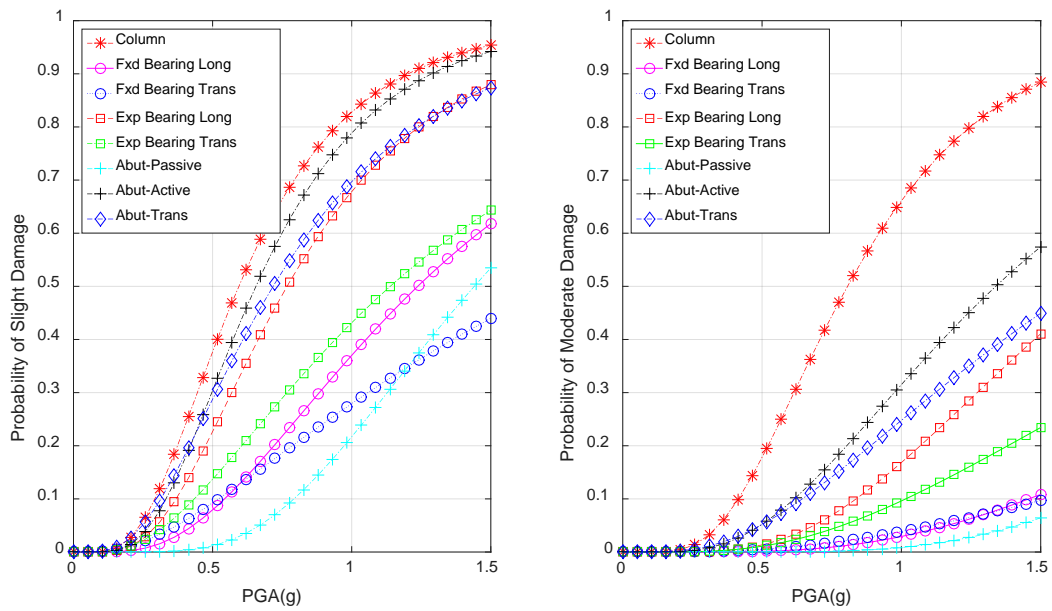


Figure 4.5.1 Component fragilities of bridge subjected to seismic hazard

According to Figure 4.5.1, the bridge column is the most fragile component, while the elastomeric bearing with fixed dowels is the least fragile component of the bridge analyzed. For the abutment fragility in the active direction (discussed in detail in Appendix A), due to the gap of limit state of slight and moderate damage state, the difference between column and abutment active direction fragility increased in the moderate damage state.

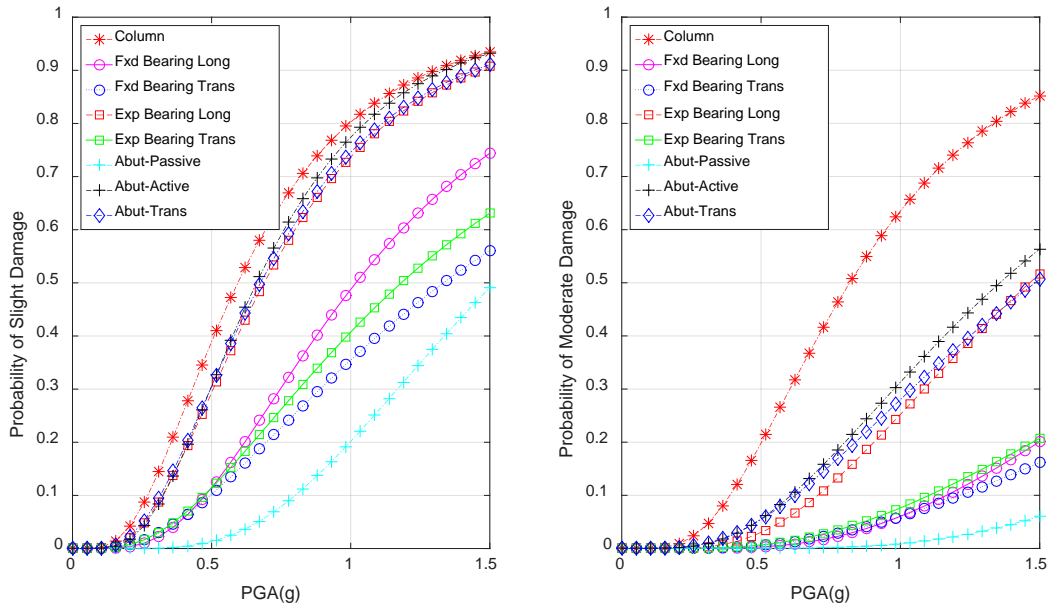


Figure 4.5.2 Component fragilities of bridge subjected to seismic hazard and scour hazard with lower discharge rate

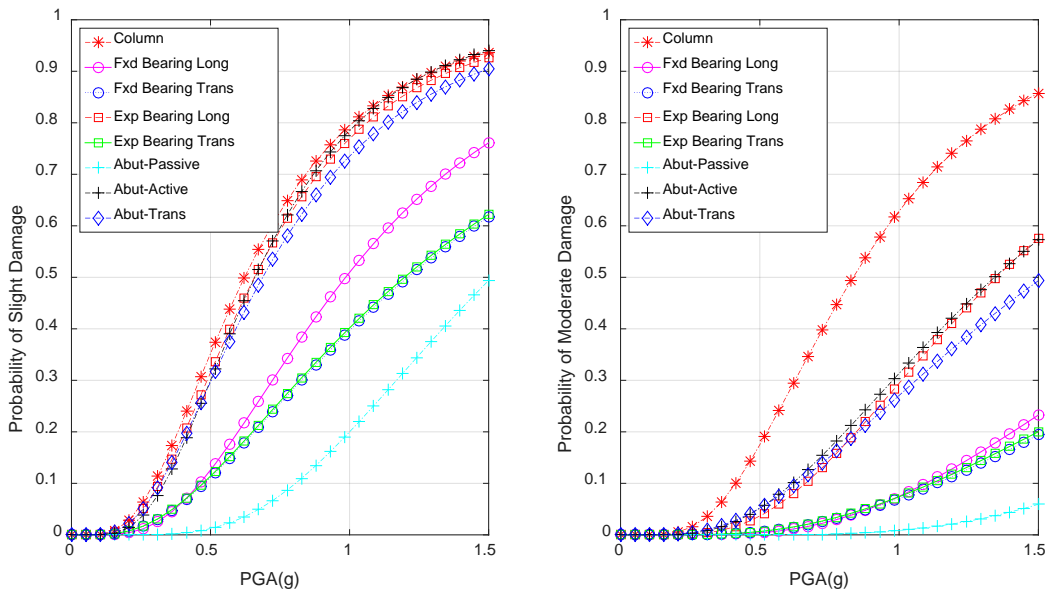


Figure 4.5.3 Component fragilities of bridge subjected to seismic and scour hazard with higher discharge rate

Table 4.5.2 to Table 4.5.4 and the corresponding figures show that the scour hazard has a significant effect on the fragility of key bridge components. For the particular bridge column considered, scour appears to have a beneficial impact on its seismic response, because scour lengthens the period of

vibration of the bridge. However, for other bridge components, scour has a negative influence on their seismic fragility; the elastomeric bearing with expansion dowels is the most negative influenced component.

We consider in this section a bridge in the most serious deterioration condition, one in which the bridge has NBI rating equal to 3. The parameters of lognormal fragilities for such a bridge that is subjected to only seismic hazard, and to both scour and seismic hazard are shown in Table 4.5.5, Table 4.5.6, and Table 4.5.7.

Table 4.5.5. Parameters for bridge component fragilities (Without scour or deterioration, when NBI rating =3)

Component	Slight		Moderate	
	Median (g)	Dispersion	Median (g)	Dispersion
Column	0.40	0.60	0.55	0.57
Fxd Bearing-long	1.25	0.65	3.26	0.63
Fxd Bearing-trans	1.48	0.92	3.80	0.86
Exp Bearing-long	0.82	0.60	1.85	0.58
Exp Bearing-trans	0.90	0.69	1.83	0.64
Abut-passive	1.46	0.48	3.10	0.48
Abut-active	0.69	0.55	1.42	0.63
Abut-trans	0.61	0.58	1.30	0.66

Table 4.5.6. Parameters for bridge component fragilities (Scour with lower discharge rate, when NBI rating =3)

Component	Slight		Moderate	
	Median (g)	Dispersion	Median (g)	Dispersion
Column	0.40	0.65	0.55	0.62
Fxd Bearing-long	1.13	0.63	2.78	0.60
Fxd Bearing-trans	1.22	0.74	2.68	0.69
Exp Bearing-long	0.78	0.62	1.72	0.60
Exp Bearing-trans	1.22	0.74	2.66	0.68
Abut-passive	1.70	0.53	3.75	0.53
Abut-active	0.71	0.57	1.48	0.65
Abut-trans	0.79	0.64	1.83	0.73

Table 4.5.7. Parameters for bridge component fragilities (Scour with higher discharge rate, when NBI rating =3)

Component	Slight		Moderate	
	Median (g)	Dispersion	Median (g)	Dispersion
Column	0.38	0.60	0.50	0.57
Fxd Bearing-long	1.02	0.61	2.37	0.59
Fxd Bearing-trans	1.17	0.73	2.57	0.68
Exp Bearing-long	0.67	0.59	1.38	0.57
Exp Bearing-trans	1.17	0.73	2.56	0.68
Abut-passive	1.55	0.51	3.32	0.51
Abut-active	0.67	0.54	1.38	0.62
Abut-trans	0.78	0.63	1.80	0.72

The fragilities corresponding to the parameterized fragilities tabulated in Figures 4.5.5 – 4.5.7 are plotted through Figure 4.5.4 to Figure 4.5.6. Comparing component fragilities in Table 4.5.4 to those in Table 4.5.1, bridge deterioration increases column fragility significantly, while for bearing and abutment components, the influence is negligible, which is consistent with the results of the previous sensitivity analysis. In this study, the impact of deterioration is limited to the effect of the strength of steel and concrete.

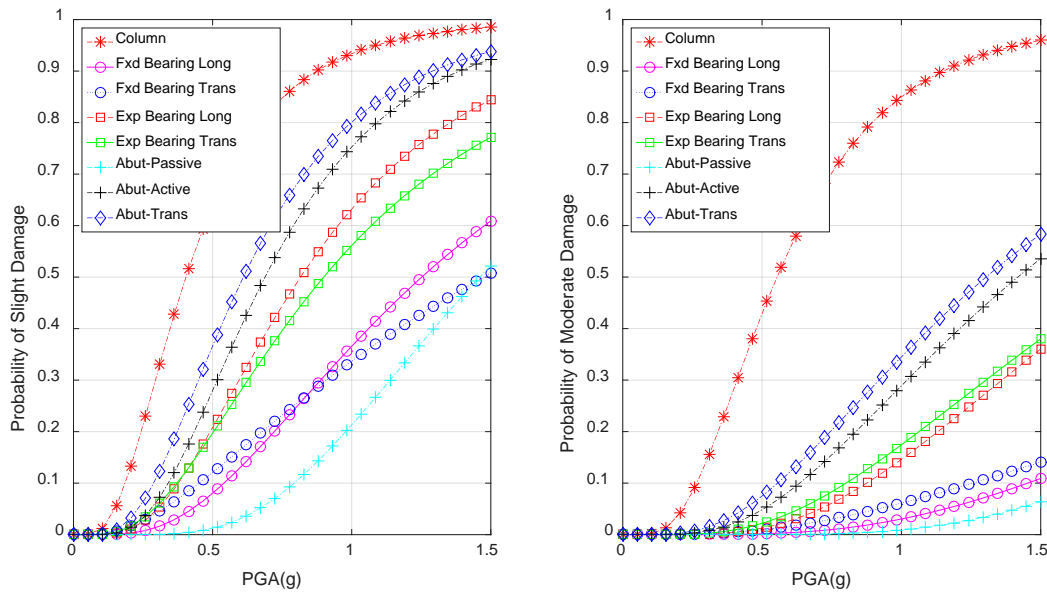


Figure 4.5.4 Component fragilities of bridge subjected to seismic hazard, when NBI rating = 3

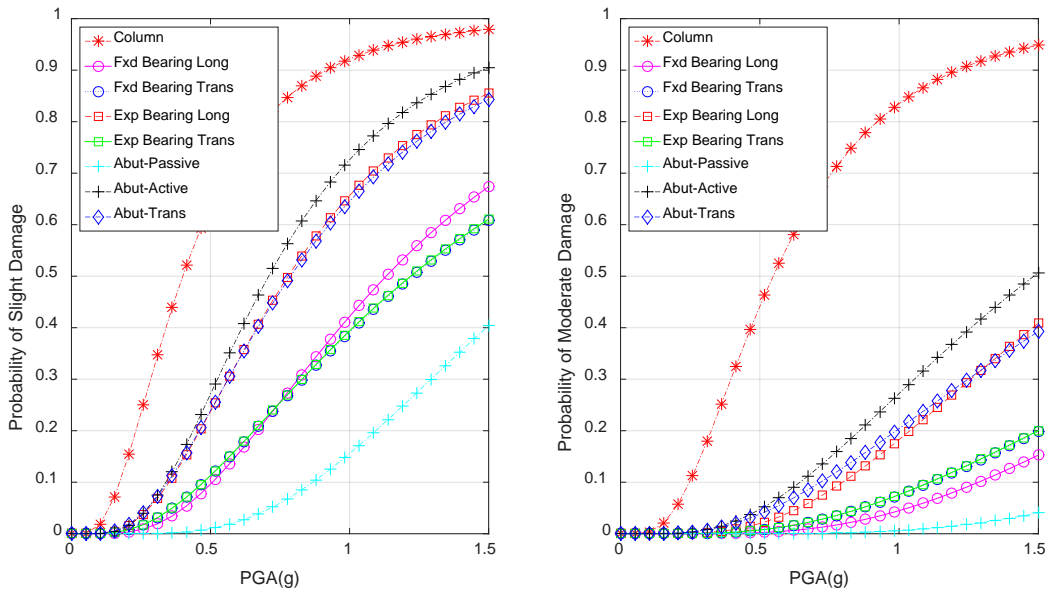


Figure 4.5.5 Component fragilities of bridge subjected to seismic and scour hazard with lower discharge rate, when NBI rating = 3

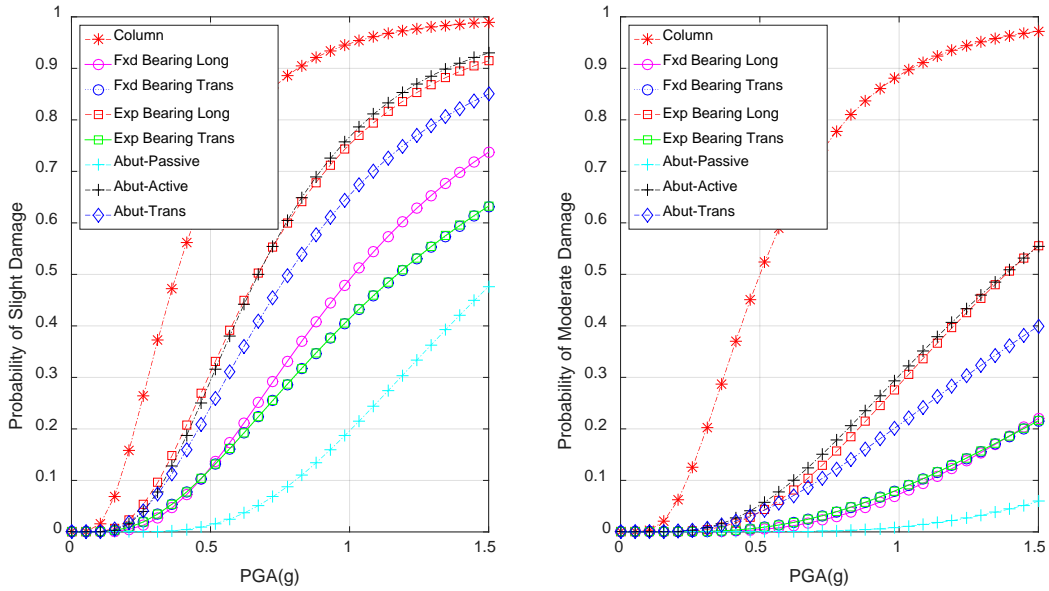


Figure 4.5.6 Component fragilities of bridge subjected to seismic and scour hazard with higher discharge rate, when NBI rating = 3

Figure 4.5.4, Figure 4.5.6 and previous findings reported above for a bridge with deterioration associated with an NBI rating of 3 reveal that the seismic response of the column does not benefit from

scour, which is different from the conclusion drawn for the same bridge in a non-deteriorated condition. It should be noted that in Figure 4.4.1, the river with the higher discharge rate also had a greater standard derivation in discharge rate, which leads to a greater standard derivation of scour depth. As a result, the maximum moment in column has a greater standard derivation under a higher scour level (the more detailed data of discharge rates are shown in Appendix B). As shown in the sensitivity analysis, the seismic response of the column does not change significantly when deterioration occurs, which means the maximum moment in the column will remain the same during a given earthquake for a given scour level. However, deterioration is accompanied by a decrease in the moment-curvature diagram; thus the impact of the upper value of maximum moment will be amplified. In addition, the median PSDMs are obtained from linear regression. , If some amplified data show up in the dataset of the regression analysis, the final result would be enlarged. In other word, scour has the potential to cause P-Delta effects in bridge columns. The same conclusion can be drawn from Figure 4.5.5: when deterioration does not occur, the column will benefit from scour, but P-Delta effect of bridge column will neutralize the beneficial impact of scour once the bridge has deteriorated. Consequently, Figure 4.5.5 shows almost same column fragility as that in Figure 4.5.4, under non-scour conditions.

4.6 Combining component seismic fragility curves

To enable the derivation of the survival function of the bridge during its service life, the overall bridge fragility must be determined. The bridge is assumed to be a series system of the eight monitored components identified in Table 4.5.1, implying that if any of these components fail, the bridge system fails. The lower and upper bounds of system fragility are described as,

$$\max_{i=1}^n P(F_i) \leq P(F_{system}) \leq 1 - \prod_{i=1}^n [1 - P(F_i)] \quad (4.6.1)$$

where $P(F_{system})$ is the probability that the bridge, as a system, reaches a certain limit state. Furthermore, the system fragility function $F_R(x)$ is represented by a conditional probability model, in which the conditioning is on ground motion intensity, $X = x$. The lower bound in Eqn.(4.6.1) represents the

probability of failure for a system whose components are stochastically dependent, while the upper bound is based on the assumption that all component failures are stochastically independent (Choi et al. 2004).

It is easier to combine the eight fragility curves into a system fragility curve if the fragilities of bearing and abutment in different directions are combined first. For bridge bearing, the probability of failure can be written as,

$$P(F_{bearing}) = P(\bar{A}B) + P(A\bar{B}) + P(\bar{A}\bar{B}) \quad (4.6.2)$$

in which, A is the failure of bearing in the longitudinal direction and B is the failure of bearing in the transverse direction. Eqn. (4.6.2) also can be written as,

$$P(F_{bearing}) = P(\bar{A})P(B|\bar{A}) + P(\bar{B})P(A|\bar{B}) + P(\bar{A})P(\bar{B}|\bar{A}) \quad (4.6.3)$$

In this study, the stiffnesses of bearings in the longitudinal and transverse directions is provided by the elastomeric pad and steel dowel. It is unlikely that a bearing fails in the transverse direction but survives in the longitudinal direction. As a result, the terms $P(B|\bar{A})$ and $P(A|\bar{B})$ in Eqn. (4.6.3) are assumed to equal 0, and $P(\bar{B}|\bar{A})$ is assumed as 1. Thus, for both fixed bearings and expansion bearings, the responses in the two directions are stochastically dependent, and the fragilities correspond to the lower bound in Eqn. (4.6.1).

For abutments, the transverse and active responses are dominated by abutment piles, so in the same way, the fragilities in these directions can be combined. On the other hand, the response in the passive direction depends on both abutment piles and abutment soil. It is assumed that the response in the passive direction is independent of that in the active and transverse direction to give a more conservative estimation of abutment fragility.

After combining the fragilities of bearing, abutment and column in different directions, which are based on the physical relationship, Monte-Carlo simulation is adopted to derive the system fragility. The

system fragility parameters for all cases considered are shown in Table 4.6.1; the seismic fragilities of the deteriorated bridge are illustrated in Figure 4.6.1, Figure 4.6.2 and Figure 4.6.3.

Table 4.6.1 System fragilities for different hazard condition

System fragility	Slight		Moderate	
	Median (g)	Dispersion	Median (g)	Dispersion
With higher discharge rate scour	0.47	0.50	0.77	0.52
With lower discharge rate scour	0.46	0.53	0.76	0.55
Without scour or deterioration	0.48	0.49	0.76	0.50
With higher discharge rate scour, NBI=6	0.46	0.51	0.72	0.52
With lower discharge rate scour, NBI=6	0.44	0.58	0.69	0.65
Without scour or deterioration, NBI=6	0.45	0.49	0.69	0.50
With higher discharge rate scour, NBI=5	0.43	0.52	0.65	0.53
With lower discharge rate scour, NBI=5	0.44	0.54	0.67	0.55
Without scour or deterioration, NBI=5	0.44	0.51	0.67	0.52
With higher discharge rate scour, NBI=4	0.38	0.55	0.55	0.56
With lower discharge rate scour, NBI=4	0.40	0.56	0.59	0.57
Without scour or deterioration, NBI=4	0.43	0.54	0.64	0.54
With higher discharge rate scour, NBI=3	0.36	0.56	0.50	0.57
With lower discharge rate scour, NBI=3	0.38	0.60	0.54	0.61
Without scour or deterioration, NBI=3	0.38	0.56	0.55	0.56

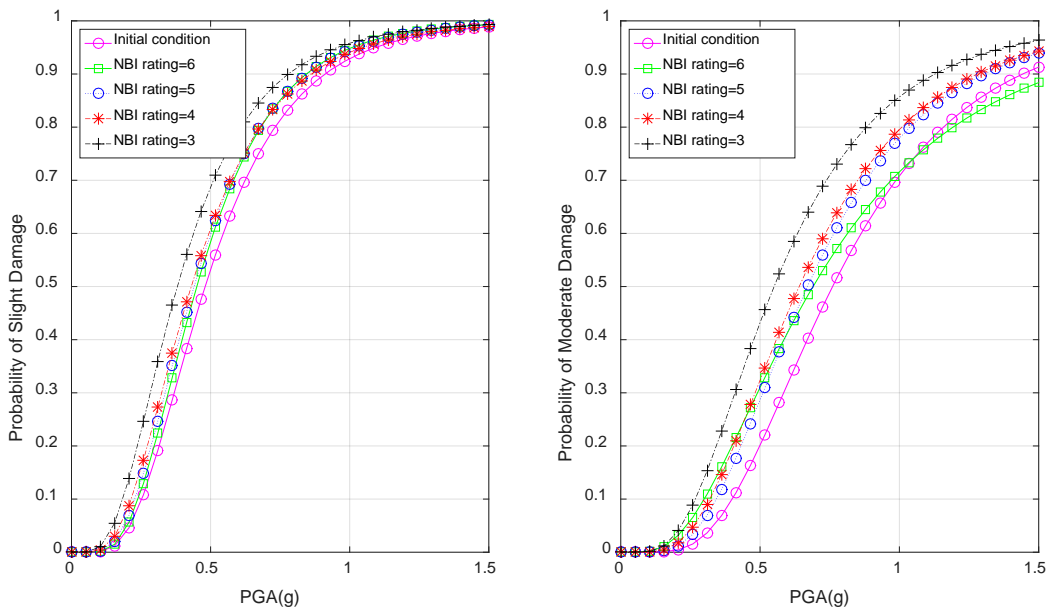


Figure 4.6.1 System seismic fragility of deteriorating bridge subjected to seismic hazard

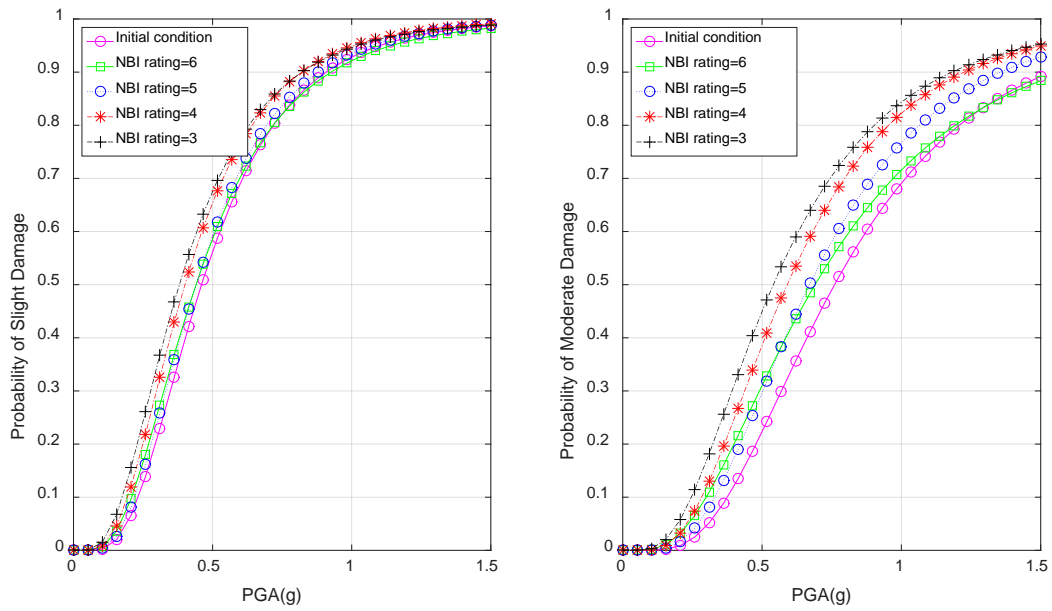


Figure 4.6.2 System seismic fragility of deteriorating bridge subjected to seismic and scour hazard (Lower discharge rate)

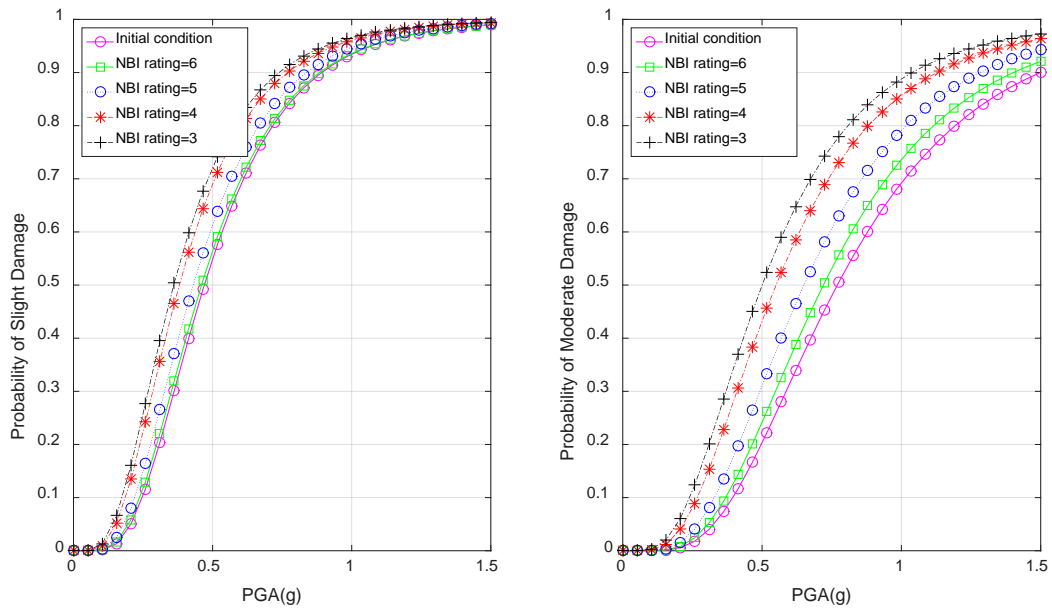


Figure 4.6.3 System seismic fragility of deteriorating bridge subjected to seismic and scour hazard (Higher discharge rate)

These tables and figures show that bridge deterioration clearly has a negative impact on column fragility. Since the system fragility is tantamount to the column fragility for the three hazard conditions considered, the bridge becomes more fragile under earthquake with increasing deterioration.

As discussed previously, serious deterioration leads to the development of P-Delta effects in the bridge column. In this section, we use the system fragility to show this P-Delta effect. For a slight damage state, the system fragilities of three hazard condition are plotted in Figure 4.6.4, under a given deterioration condition defined by NBI rating equals to 4, and initial conditions respectively. In addition, the system fragilities of moderate damage state are plotted in Figure 4.6.5.

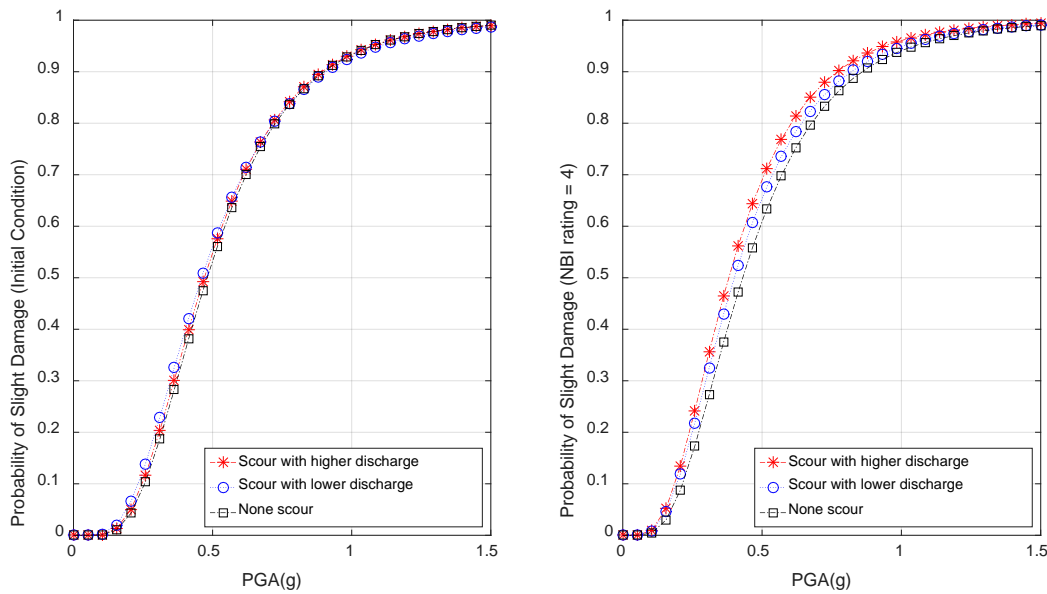


Figure. 4.6.4. System fragilities of the bridge that under initial condition and NBI rating=4 for slight damage state

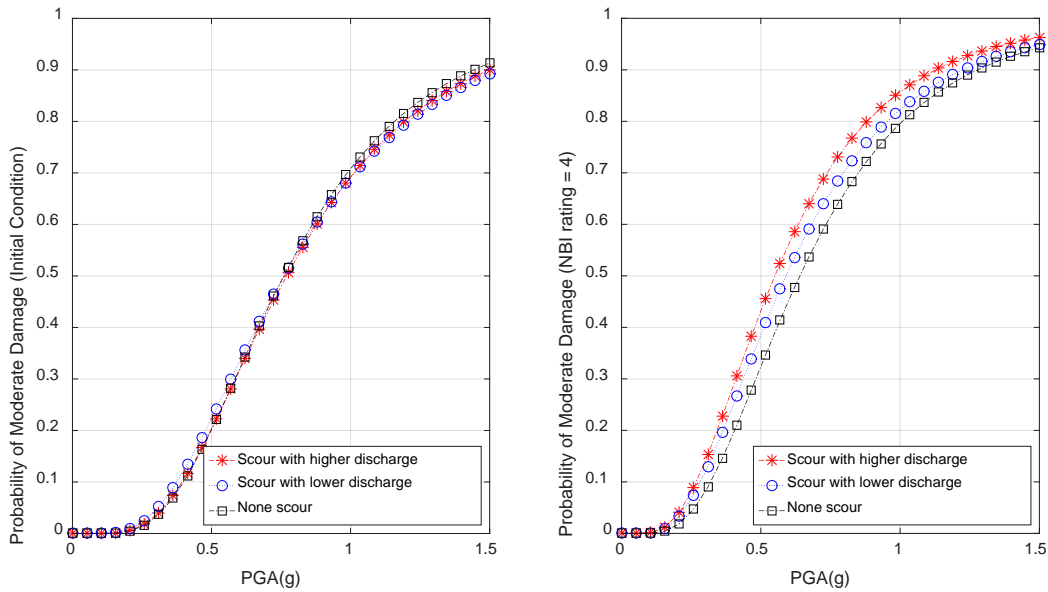


Figure. 4.6.5. System fragilities of the bridge that under initial condition and NBI rating=4 for moderate damage state

Assuming that NBI = 4, the P-Delta effect has a more pronounced effect on the fragility of the bridge that is subjected to scour; Figure 4.6.4 and Figure 4.6.5 show that the seismic fragility of a seriously deteriorating bridge does not benefit from scour. Besides, according to the results in table 4.6.1, the level of P-Delta effect depends both on the scour and deterioration level: a bridge that suffers more serious deterioration and is subjected to a scour with higher discharge rate is more likely to develop significant P-Delta effects in its columns.

4.7 Service life prediction of bridges under competing hazards

Based on the system fragilities that are shown in Table 4.6.1, a service life prediction of the bridge under competing hazards can be made by combing the bridge system fragility with elapsed time.

Adopting the results of the time dependent Markov Transition Probability Matrix MTM, for any given year in the service life of the bridge, the time-dependent probability of failure can be derived by the total probability theorem:

$$P_f^T(x) = P(NBI = 9|T_i)P_f(x|NBI = 9) + \dots + P(NBI = 3|T_i)P_f(x|NBI = 3) \quad (4.7.1)$$

in which, $P_f^T(x)$ is time-dependent probability of failure for a given PGA x ; $P_f(x|NBI = 9...3)$ is the probability of failure for a given PGA x and a deterioration condition, which can be calculated by Table 4.6.1.

In this study, the seismic hazard data of San Francisco, CA, which is known as a high seismic risk area, and that of Charleston, SC, which is known as a moderate seismic risk area, are adopted to give the numerical results of Eqn. (4.7.1). The time-dependent failure rate, $h(t)$, of the deteriorating bridge sited in San Francisco and Charleston subjected to seismic hazard and various conditions of scour hazards are shown through Figure 4.7.1 and Figure 4.7.2. The time-dependent failure rate, $h(t)$, is calculated based on the slight damage state. The conditional failure rates for San Francisco and Charleston differ by an order of magnitude.

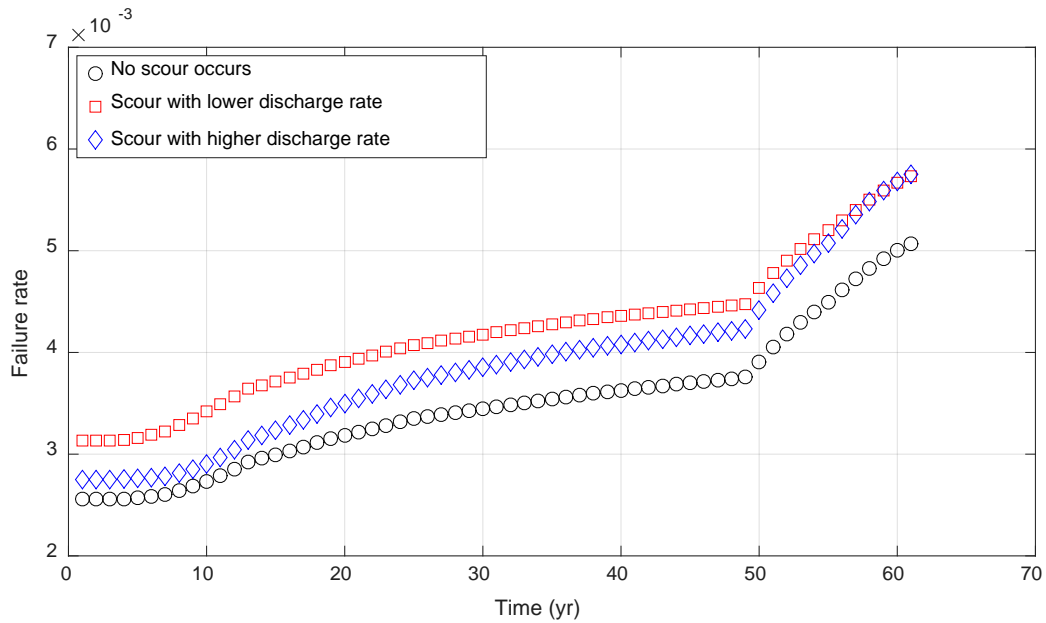


Figure 4.7.1 Time-dependent failure rate of deteriorating bridge (San Francisco)

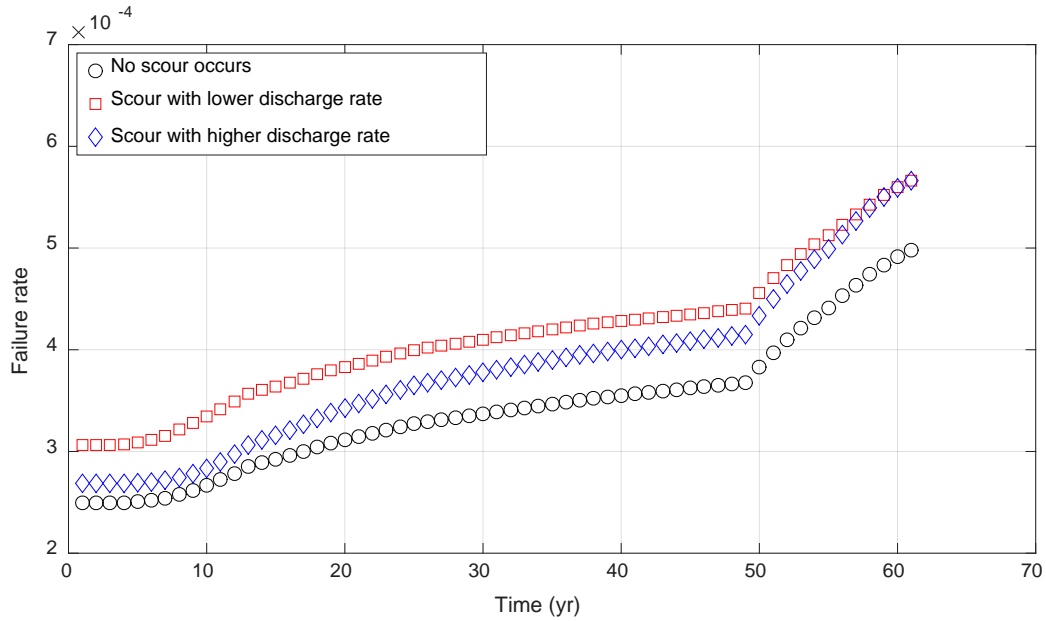


Figure 4.7.2 Time-dependent failure rate of deteriorating bridge (Charleston)

All hazard situations show an increasing failure rate, which is typical of the “wear out period” of mechanical and electrical equipment as well as aging civil infrastructure (Sobanjo et al. 2010). After fifty years, the conditional failure rate increase sharply, which is due to the serious nature of deterioration late in the life of the structure. For a bridge subjected to scour, this increase of failure rate is especially significant, since the P-Delta effect may occur when the bridge is seriously deteriorated.

For a process with an increasing time-dependent failure rate, the Weibull distribution often is used to model the uncertainty characteristics of the deterioration process. As discussed in Chapter 3.4, the cumulative conditional failure function $H(t)$ is derived from the Weibull probability distribution. Based on the data of failure rate, a regression analysis is conducted to calculate the parameters of $H(t)$. Because there is an abrupt change of failure rate at fiftieth year, a piecewise function of $H(t)$ would be a better way to fit the data. For a deteriorating bridge subjected earthquake and scour, the parameters of $H(t)$ are shown in Table 4.7.1, Table 4.7.2 and Table 4.7.3.

Table 4.7.1 Conditional failure rate function (No scour occurs)

Time(yr.)	Slight damage state		Moderate damage state	
	$H(t)$	R^2	$H(t)$	R^2
1-50	$\left(\frac{t}{237.7}\right)^{1.177}$	0.9887	$\left(\frac{t}{496.9}\right)^{1.208}$	0.9735
51-61	$\left(\frac{t}{146.7}\right)^{2.254}$	0.9945	$\left(\frac{t}{198.8}\right)^{2.464}$	0.9942

Table 4.7.2 Conditional failure rate function (Scour with lower discharge rate)

Time(yr.)	Slight damage state		Moderate damage state	
	$H(t)$	R^2	$H(t)$	R^2
1-50	$\left(\frac{t}{209.4}\right)^{1.143}$	0.9750	$\left(\frac{t}{388.4}\right)^{1.231}$	0.9917
51-61	$\left(\frac{t}{145}\right)^{2.014}$	0.9960	$\left(\frac{t}{196.4}\right)^{2.241}$	0.9978

Table 4.7.3 Conditional failure rate function (Scour with higher discharge)

Time(yr.)	Slight damage state		Moderate damage state	
	$H(t)$	R^2	$H(t)$	R^2
1-50	$\left(\frac{t}{210.9}\right)^{1.209}$	0.9795	$\left(\frac{t}{387.9}\right)^{1.291}$	0.9736
51-61	$\left(\frac{t}{137.8}\right)^{2.287}$	0.9939	$\left(\frac{t}{169.1}\right)^{2.703}$	0.9930

As mentioned in Section 3.4, the parameter β in $H(t)$ indicates different failure rates. For the existing bridges considered in this study, the failure rate curve should consist primarily of the wear out phase. The range of β value implies a same conclusion. Substituting the results in Table 4.7.1, Table

4.7.2 and Table 4.7.3 into the survivor function defined in Chapter 3.4, the probability of survival of the bridge can be calculated, as shown in Figure 4.7.3.

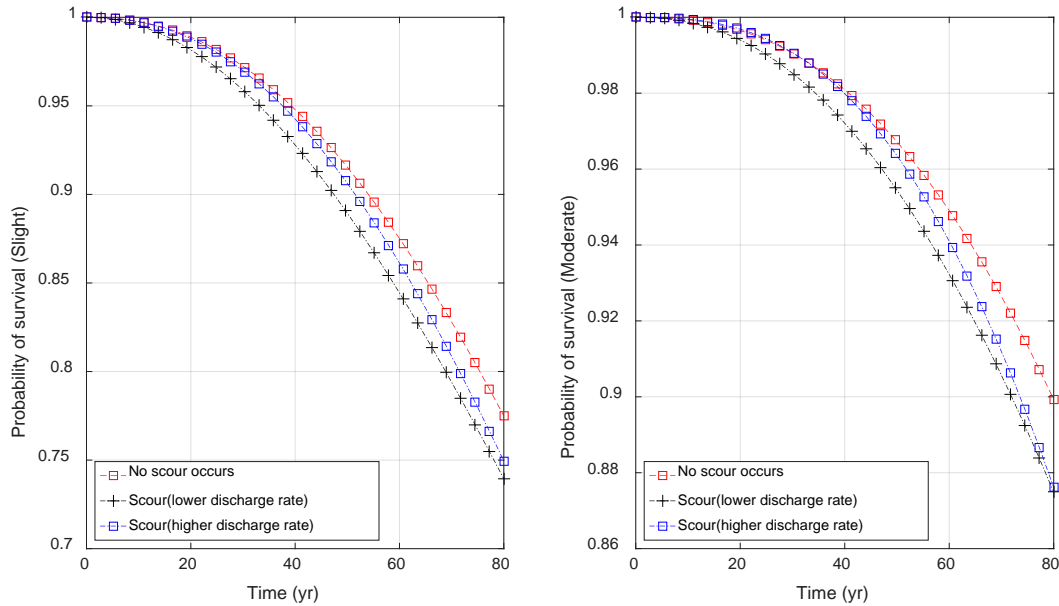


Figure 4.7.3 Survivor function of bridge service life

From Figure 4.7.3, it is easy to tell that at the beginning of its service life, bridge subjected scour have a higher probability of survival. However, as time elapses, the interaction of bridge deterioration and scour aggravate the failure of bridge. Eventually, for both slight and moderate damage states, the bridge under scour is less likely to survive to the end of its service life.

4.8 Closure

This study has investigated a multi-span simply supported reinforced concrete bridge, subjected to the four hazard conditions: earthquake, earthquake and bridge scour, earthquake and bridge deterioration, and earthquake, bridge scour and deterioration. In each hazard condition, the component and overall bridge fragilities are derived to show the bridge safety.

For the bridge that is only subjected to seismic hazard, the bridge column is the most fragile component, and the responses of the other components are highly correlated. As a result, the fragility of

bridge is dominated by that of the bridge column. The results of the study imply that improvement of column moment capacity would probably lead to a higher level of safety of that bridge under earthquake.

When considering bridge scour, the bridge fragility tends to decrease because the scour causes the lengthening of the natural period of vibration, which make the bridge more flexible. However, some component fragilities increase as scour occurs, especially for bridge bearing. In this case, system fragility would not be a good approach to estimate the bridge seismic fragility if the bridge is modeled as a series system, because the failure of each component would cause system failure. When designing a bridge that might fail under a bridge scour, bridge bearing should be a key component to be considered, and other consequences that caused by lengthening of natural variation period should be considered properly as well.

For the deteriorating bridge under earthquake, the impacts of bridge deterioration are concentrated on bridge column, and for other components, the impact is negligible. The column becomes much more vulnerable under bridge deterioration. Unlike bridge scour, bridge deterioration always has a negative impact on bridge performance. Bridge deterioration is an evitable process that begins from the first day of bridge service life. A good way to reduce the negative influence of deterioration would be conduct maintenance and repair behaviors properly and routinely. For the reason that the reinforcement contributes to the capacity of the column significantly, extra attention have be paid to deterioration of reinforcement.

A service life survivor function is plotted to present the safety of bridge subjected to scour, deterioration and earthquake. Although seismic fragility may benefit from bridge scour, the long term influence of scour is still negative. When the bridge has deteriorated significantly, scour will increase any P-Delta effect bridge column that might be present. Obviously, when designing a bridge against multi-hazard, it would underestimate the real hazard level if the bridge is designed to against each hazard independently.

Chapter 5

Conclusions and recommendations for further study

Reliability assessment of deteriorating reinforced concrete bridge that subjected to earthquake and foundation scour is presented in this study, the main research findings and recommendations for further study are summarized in this chapter.

5.1 Summary of major research findings

Analytical models of bridge scour and deterioration are presented in this study. For the two analytical models of scour depth, the major research findings are summarized as following:

- Two equations of scour depth are compared in this study. The first is given by introducing a model factor to the deterministic equation (FHWA 2001), while the second is a best-fit model derived from a deterministic equation obtained from laboratory data. According to the test results, for the best-fit model, the influence of discharge rate on scour depth is negligible. It would be unreasonable in practice.
- Rather than modelling the bridge deterioration as resulting from corrosion of reinforcement, as in previous studies, the bridge deterioration is modeled in this study as an integer stochastic process by adopting the data from NBI ratings, and a relationship is built up between NBI rating and bridge resistance. As a result, bridge resistance becomes as a stochastic process, which makes it possible to evaluate the reliability of bridge during its service life.

The main objective of this study is to assess the reliability of deteriorating reinforced concrete bridges that are subjected to multiple hazards, specifically deterioration, scour and earthquake. For a multi-span simply support reinforced concrete bridge, this study shows that:

- The bridge column is the most vulnerable component under earthquake.

- For a bridge subjected to earthquake and scour, the seismic response of the bridge column decreases when scour occurs, but the seismic responses of other bridge components increase.
- For a deteriorating bridge subjected to earthquake, the bridge column is the most negatively affected by deterioration, and the effects of deterioration on other components are negligible.
- For a deteriorating bridge subjected to earthquake and scour, under same deterioration condition, a bridge that is exposed to scour resulting from a higher discharge rate tends to be more vulnerable, due to the P-Delta effect of bridge column.

5.2 Recommendations for further study

In this study, we adopted the NBI rating data to model bridge deterioration by assuming that there is a linear relationship between NBI rating and residual resistance. However, a better estimate of effect of deterioration could be made if a more accurate relationship between NBI rating and residual resistance could be found. In addition, a more accurate estimate of bridge vulnerability would be obtained if the impact of deterioration on bridge bearings and stiffness of the bridge abutment were to be considered.

This study revealed two types of interaction of multi-hazards for bridge seismic fragility; the first interaction leads a positive impact on structural performance, while the second leads to a negative impact. Similar interactions are likely in other combinations of multiple hazards. Both of the consequences show that multiple hazards cannot be considered simply as the superposition of the effects of single hazards. For multi-hazard design, it is important to consider the interaction of multiple hazards based on a thorough assessment of how those hazards, individually and in combination, impact the vulnerability of the bridge structure.

References

- [1] *AASHTO-LRFD bridge design specifications. (2012)*, American Association of State Highway and Transportation Officials, Washington, D.C
- [2] ACI Committee, American Concrete Institute, and International Organization for Standardization. "Building code requirements for structural concrete (ACI 318-14) and commentary." American Concrete Institute, 2014.
- [3] Alipour, Azadeh, Behrouz Shafei, and Masanobu Shinozuka. "Reliability-based calibration of load and resistance factors for design of RC bridges under multiple extreme events: Scour and earthquake." *Journal of Bridge Engineering* 18.5 (2012): 362-371.
- [4] American Society of Civil Engineers. *Minimum design loads for buildings and other structures*. Vol. 7. Amer Society of Civil Engineers, 2009.
- [5] Ayyub, Bilal M., and Kwan-Ling Lai. "Structural reliability assessment using Latin hypercube sampling." *Structural Safety and Reliability*. ASCE, 1989.
- [6] Ang, Alfredo H-S., and Wilson H. Tang. *Probability concepts in engineering planning and design*. 1984.
- [7] Angelakos, Dino, Evan C. Bentz, and Michael P. Collins. "Effect of concrete strength and minimum stirrups on shear strength of large members." *ACI Structural Journal* 98.3 (2001).
- [8] Barker, Richard M., and Jay A. Puckett. *Design of highway bridges: An LRFD approach*. John Wiley & sons, 2013.
- [9] Beyer, Katrin, and Julian J. Bommer. "Selection and scaling of real accelerograms for bi-directional loading: a review of current practice and code provisions." *Journal of Earthquake Engineering* 11.S1 (2007): 13-45.
- [10] Bolukbasi, Melik, Jamshid Mohammadi, and David Arditi. "Estimating the future condition of highway bridge components using national bridge inventory data." *Practice Periodical on Structural Design and Construction* 9.1 (2004): 16-25.
- [11] Caltrans (1999). *Caltrans Seismic Design Criteria*. California Department of Transportation,

Sacramento, CA, first edition.

- [12] Cesare, Mark A., et al. "Modeling bridge deterioration with Markov chains." *Journal of Transportation Engineering* 118.6 (1992): 820-833.
- [13] Chee, Raymond Kin Weng. "Live-bed scour at bridge piers." *Publication of: Auckland University, New Zealand* 290 (1982).
- [14] Chiew, Yee Meng. *Local scour at bridge piers*. Diss. ResearchSpace@ Auckland, 1984.
- [15] Choi, Eunsoo. "Seismic analysis and retrofit of mid-America bridges." (2002).
- [16] Cornell, C. Allin, et al. "Probabilistic basis for 2000 SAC federal emergency management agency steel moment frame guidelines." *Journal of Structural Engineering* 128.4 (2002): 526-533.
- [17] Crosti, Chiara, Dat Duthinh, and Emil Simiu. "Risk consistency and synergy in multihazard design." *Journal of Structural Engineering* 137.8 (2010): 844-849.
- [18] Duthinh, Dat, and Emil Simiu. "Safety of structures in strong winds and earthquakes: multihazard considerations." *Journal of structural engineering* 136.3 (2009): 330-333.
- [19] Ellingwood, Bruce R. "Risk-informed condition assessment of civil infrastructure: state of practice and research issues." *Structure and infrastructure engineering* 1.1 (2005): 7-18.
- [20] Enright, Michael P., and Dan M. Frangopol. "Service-life prediction of deteriorating concrete bridges." *Journal of Structural engineering* 124.3 (1998): 309-317.
- [21] Estes, Allen C., and Dan M. Frangopol. "Bridge lifetime system reliability under multiple limit states." *Journal of Bridge Engineering* 6.6 (2001): 523-528.
- [22] FHWA (US Federal Highway Administration). "Load and Resistance Factor Design (LRFD) for Highway Bridge Substructures." (2001).
- [23] FHWA, US. "Department of Transportation." *Highway Safety Improvement Program* (2009).
- [24] Gazetas, George. "Seismic response of end-bearing single piles." *International Journal of Soil Dynamics and Earthquake Engineering* 3.2 (1984): 82-93.
- [25] Ghosn, Michel, Fred Moses, and Jian Wang. Design of highway bridges for extreme events. No. 489. Transportation Research Board, 2003.

- [26] Ghosh, Jayadipta, and Jamie E. Padgett. "Aging considerations in the development of time-dependent seismic fragility curves." *Journal of Structural Engineering* 136.12 (2010): 1497-1511.
- [27] Harrison, Lawrence J., and Johnny L. Morris. "Bridge scour vulnerability assessment." *Stream Stability and Scour at Highway Bridges@ sCompendium of Stream Stability and Scour Papers Presented at Conferences Sponsored by the Water Resources Engineering (Hydraulics) Division of the American Society of Civil Engineers*. ASCE, 1991.
- [28] Johnson, Peggy A., and Bilal M. Ayyub. "Assessing time-variant bridge reliability due to pier scour." *Journal of Hydraulic Engineering* 118.6 (1992): 887-903.
- [29] Johnson, Peggy A. "Comparison of pier-scour equations using field data." *Journal of Hydraulic Engineering* 121.8 (1995): 626-629.
- [30] Johnson, Peggy A. "Uncertainty of hydraulic parameters." *Journal of Hydraulic Engineering* 122.2 (1996): 112-114.
- [31] Johnson, Peggy A., and Daniel A. Dock. "Probabilistic bridge scour estimates." *Journal of Hydraulic Engineering* 124.7 (1998): 750-754.
- [32] Johnson, Peggy A., and Sue L. Niezgod. "Risk-based method for selecting bridge scour countermeasures." *Journal of hydraulic engineering* 130.2 (2004): 121-128.
- [33] Landers, Mark N., David S. Mueller, and Gary R. Martin. *Bridge-scour data management system user's manual*. US Geological Survey, 1996.
- [34] Makris, N., et al. "Prediction of observed bridge response with soil-pile-structure interaction." *Journal of Structural Engineering* 120.10 (1994): 2992-3011.
- [35] Ma, Y. and Deng, N. (2000). "Deep Foundations." *Bridge Engineering Handbook*, W.-F. Chen and L. Duan, eds., CRC Press
- [36] McCalmont, D. "A Markovian model of bridge deterioration." *Bachelor of Science in Engineering thesis* (1990).
- [37] Melville, Bruce W. "Live-bed scour at bridge piers." *Journal of Hydraulic Engineering* 110.9 (1984): 1234-1247.

- [38] Mori, Yasuhiro, and Bruce R. Ellingwood. "Reliability-based service-life assessment of aging concrete structures." *Journal of Structural Engineering* 119.5 (1993): 1600-1621.
- [39] Nielson, Bryant G. "Analytical fragility curves for highway bridges in moderate seismic zones." (2005).
- [40] Nielson, Bryant G., and Reginald DesRoches. "Seismic fragility methodology for highway bridges using a component level approach." *Earthquake Engineering & Structural Dynamics* 36.6 (2007): 823-839.
- [41] Nowak, Andrzej S. "Calibration of LRFD bridge code." *Journal of Structural Engineering* 121.8 (1995): 1245-1251.
- [42] Nowak, A., and K. R. Collins. 2000. *Reliability of Structures*. McGraw-Hill Companies, Inc., New York, NY.
- [43] O'Connor, Jennifer M., and Bruce Ellingwood. "Reliability of nonlinear structures with seismic loading." *Journal of Structural Engineering* 113.5 (1987): 1011-1028.
- [44] Padgett, Jamie Ellen, and Reginald DesRoches. "Sensitivity of seismic response and fragility to parameter uncertainty." *Journal of Structural Engineering* (2007).
- [45] Padgett, Jamie E., Bryant G. Nielson, and Reginald DesRoches. "Selection of optimal intensity measures in probabilistic seismic demand models of highway bridge portfolios." *Earthquake Engineering & Structural Dynamics* 37.5 (2008): 711-725.
- [46] PEER. NGA Strong Motion Database. (<http://peer.berkeley.edu>)
- [47] Richardson, Everett V., Daryl B. Simons, and Pierre Y. Julien. *Highways in the River Environment: Participant Notebook*. Federal Highway Administration, 1990.
- [48] Robert B. Abernethy. *The new Weibull handbook*. RB Abernethy, 1996.
- [49] Stewart, Mark G., and Dimitri V. Val. "Multiple limit states and expected failure costs for deteriorating reinforced concrete bridges." *Journal of Bridge Engineering* 8.6 (2003): 405-415.
- [50] Shirole, A. M., and R. C. Holt. "Planning for a comprehensive bridge safety assurance program." *Transportation Research Record* 1290 (1991).

- [51] Sobanjo, John, Primus Mtenga, and Michelle Rambo-Roddenberry. "Reliability-based modeling of bridge deterioration hazards." *Journal of Bridge Engineering* (2010).
- [52] Tavares, Danusa H., Jamie E. Padgett, and Patrick Paultre. "Fragility curves of typical as-built highway bridges in eastern Canada." *Engineering Structures* 40 (2012): 107-118.
- [53] U.S. Geological Survey, 2012, Surface Water for USA: Peak Streamflow, accessed [June 10, 2014], at URL [<http://nwis.waterdata.usgs.gov/usa/nwis/peak>].
- [54] Wang, Zhenghua, Leonardo Dueñas-Osorio, and Jamie E. Padgett. "Influence of scour effects on the seismic response of reinforced concrete bridges." *Engineering Structures* 76 (2014): 202-214.
- [55] Jiang, Yi. "The development of performance prediction and optimization models for bridge management systems." (1990).
- [56] Zakeri, Behzad, Jamie E. Padgett, and Gholamreza Ghodrati Amiri. "Fragility analysis of skewed single-frame concrete box-girder bridges." *Journal of Performance of Constructed Facilities* 28.3 (2013): 571-582.

Appendix A – Description of finite element model of bridge

A.1 Analytical models of major bridge components

This Appendix is devoted to a presentation of bridge component models and their analytical SAP 2000 models that are used in this study. The bridge model is adopted from the study of Nielson (2005).

A.1.1 Superstructure

The superstructure of a bridge is the portion of the bridge that located above the bearings. In this study, the concrete deck element is expected to remain linearly elastic under seismic loading, and it is modeled as a shell element in SAP 2000. The modulus of elasticity of the concrete is assumed as 2.78×10^4 Mpa, and a typical value of weight per volume for concrete is adopted as 24 KN/m^3 .

A.1.2 Elastomeric bearing

A bridge bearing is a mechanical system that permits movement or transfers loads from the superstructure of the bridge to the substructure or support system of bridge. They are typical responsible for transmitting both vertical and horizontal loads to substructure (Nielson 2005).

There are various types of bearing in bridge design, the type of bearing that adopted in this study is elastomeric bearings, which have been a very common bearing used on concrete girder and slab type bridges. As mentioned previously, expansion type and fixed type of elastomeric bearings are utilized by AASHTO Type I and AASHTO Type III girders respectively. The differences between fixed bearings and expansion bearings are the size and shape of the holes for the steel holes. A typical elastomeric pad for fixed and expansion types elastomeric bearings are shown in Figure A.1.

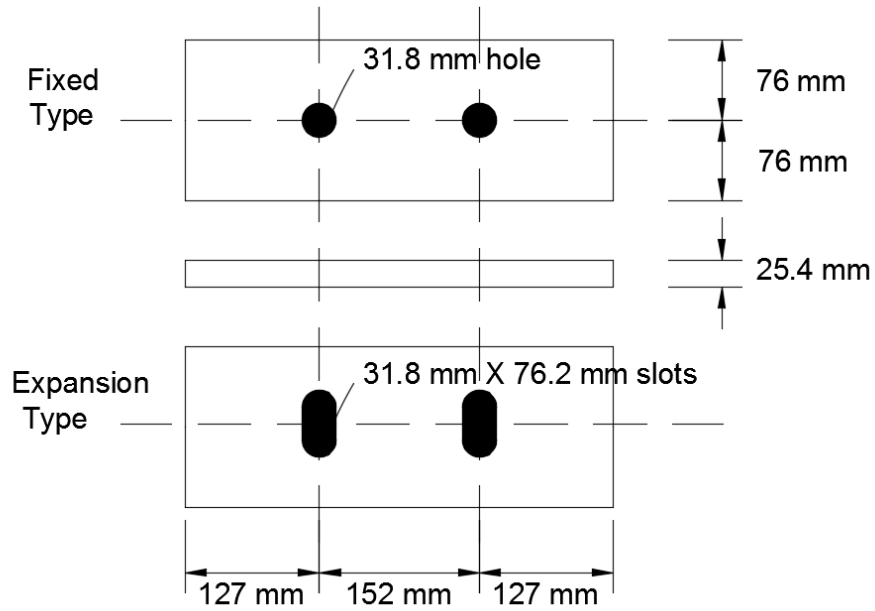


Figure A.1 Typical elastomeric pad for fixed and expansion types elastomeric bearings

The behavior of elastomeric is composed by the contributions of elastomeric pad and steel dowels. The behavior of elastomeric pad is characterized by sliding. The initial stiffness, k_e can be calculated by Eqn. (C.1) (Choi 2002),

$$k_e = \frac{GA}{h_r} \quad (C.1)$$

in which, G is the shear modulus of the elastomer, which is modeled as an uniform distribution in the range of 0.66 Mpa and 2.07 Mpa (Nielson 2005); A is the area of the elastomeric bearing; h_r is the thickness of the elastomeric pad.

The yield force of elastomeric pad is assumed as the ultimate force of it under its maximum movement.

The steel dowels are used to prevent excessive movement between the girders and the pier which they bear. The behavior of steel dowel is models using a multi-linear link element in Sap 2000, the values of parameters for steel dowel are adopted form the study of Nielson (2005). The analytical model for elastomeric bearing with fixed dowels are shown in Figure A.2.

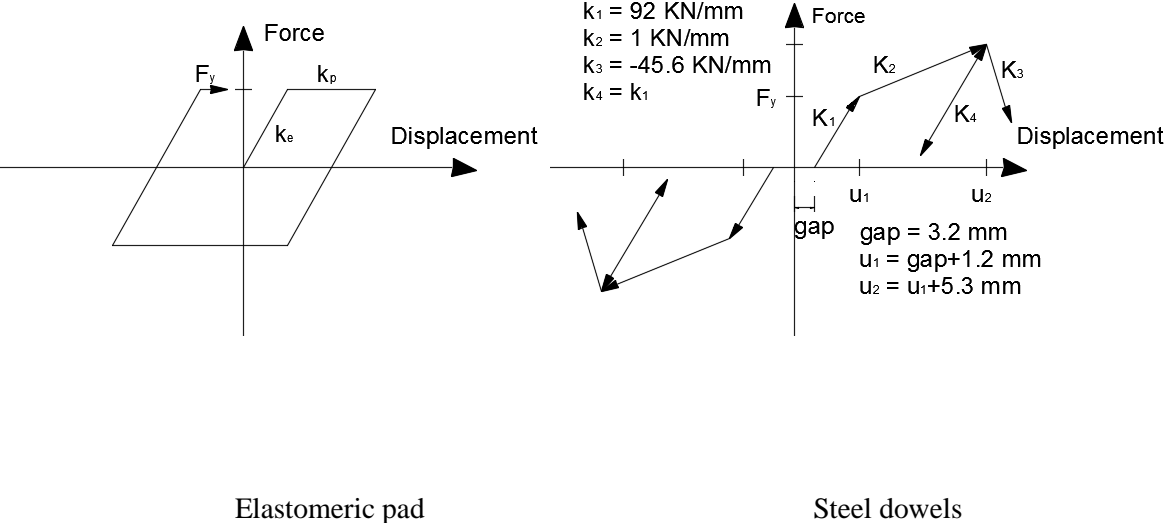


Figure A.2. Analytical model of elastomeric bearing with fixed dowels (Nielson 2005)

It is should be noted that the behaviors of elastomeric bearing with fixed dowels in both longitudinal and transverse directions are identical. For elastomeric bearing with expansion, the analytical model in longitudinal direction is shown in Figure A.3. The behavior of elastomeric bearing with expansion dowels is same with that of elastomeric bearing with fixed dowels.

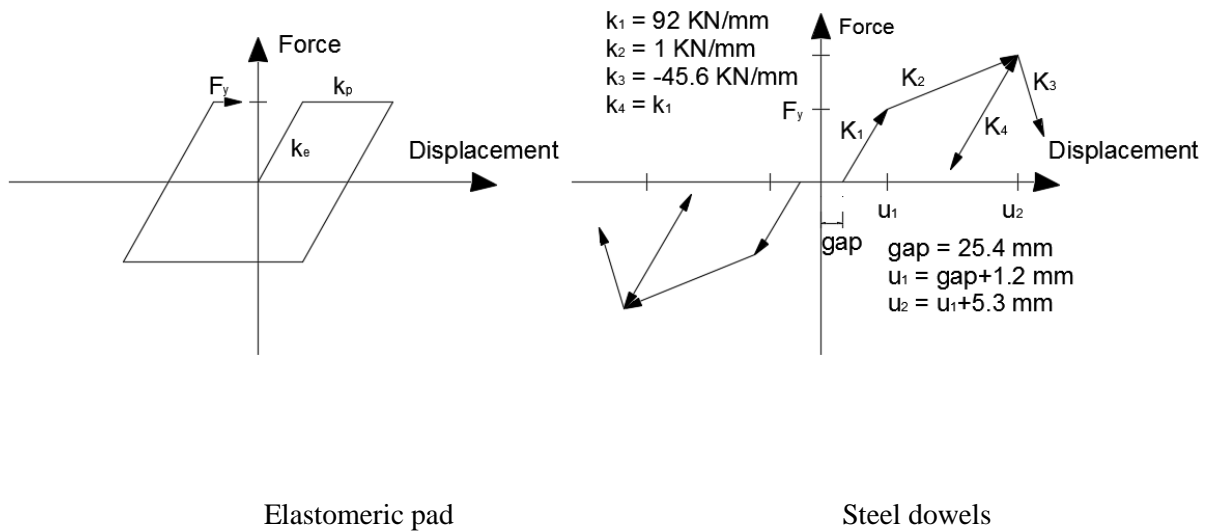


Figure A.3. Analytical model of elastomeric bearing with expansion dowels in longitudinal direction (Nielson 2005)

A.1.3 Abutment

Abutment is a vital component of bridges, it provides vertical support of the bridge superstructure at bridge both ends and connect the bridge with the roadway approaches. In bridge design, there are various type abutments, such as gravity abutment and U-shape abutment. As stated in Chapter 4, the type of bridge abutment adopted in this study is of pile-bent girder seat type abutment. Its layout is shown in Figure A.4 (a) (Nielson 2005).

Bridge abutment primarily resists vertical loads but also take horizontal loads. Horizontal loads, can occur as a result of traffic due to acceleration and braking, besides seismic load place a great demand on lateral support of bridge abutment. In this study, the horizontal restraint of abutment is modeled in both longitudinal and transverse direction. In addition, the longitudinal behavior of abutment is defined as a combination of two behaviors in passive and active directions. The piles of abutment provide stiffness for bridge in active direction, and both of soil behind abutment and the piles of abutment provide stiffness for bridge in passive direction. The definition of longitudinal abutment behavior is shown in Figure A.4 (b).

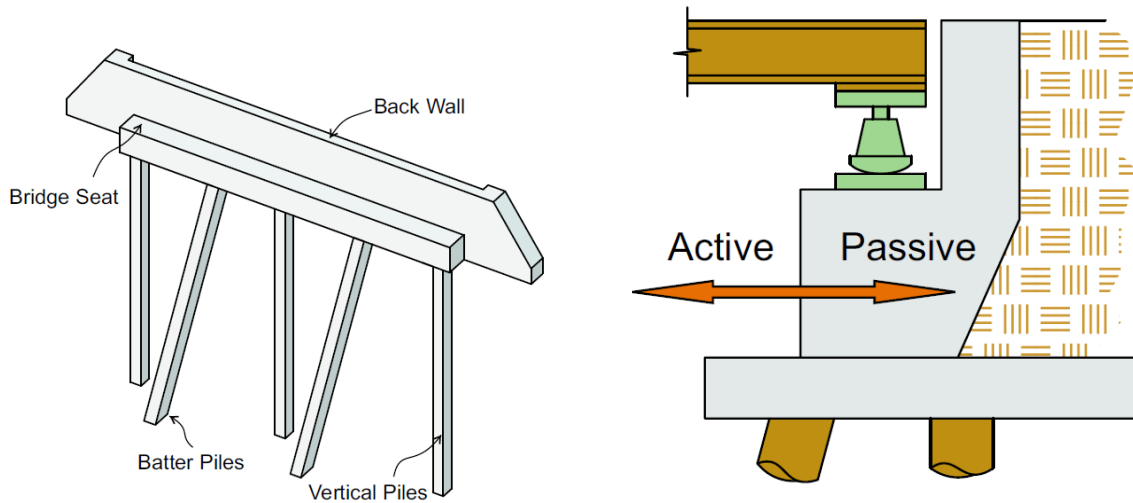


Figure A.4 (a) Layout of pile-bent girder seat type abutment (b) Definition of longitudinal abutment behavior (Nielson 2005)

According to previous studies, a possible range of passive resistance of soil is 11.5 KN/mm/m to 11.5 KN/mm/m (Caltrans 1999), and the stiffness provided by abutment pile has bounds of 3.5 KN/mm/pile and 10.5 KN/mm/pile (Nielson 2005). Both of passive and active stiffness are uniformly distributed, and link elements are adopted to model the stiffness in the two direction in Sap 2000. The analytical models of abutment are shown in Figure A.5.

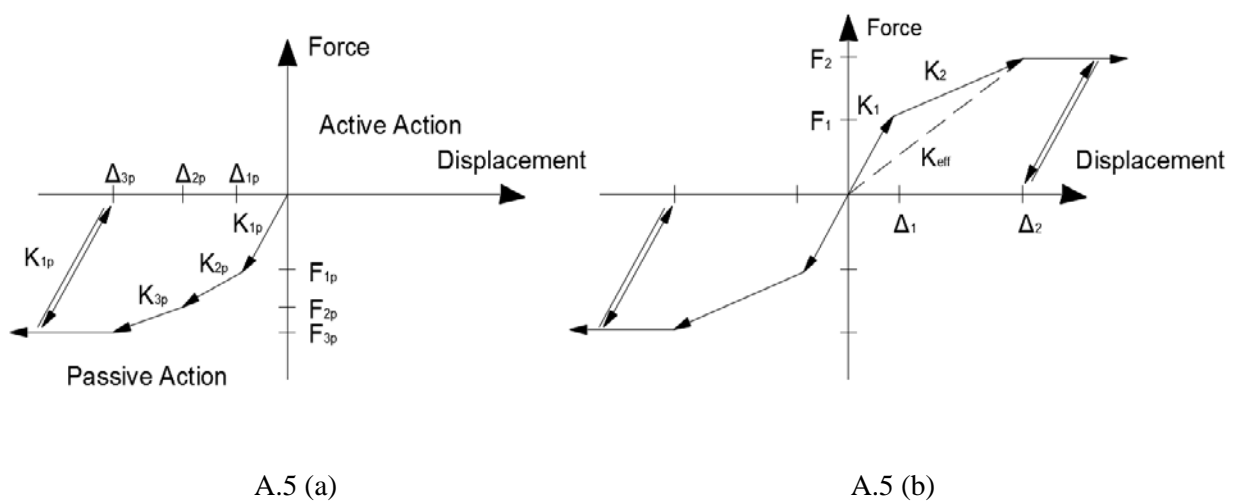


Figure A.5 Analytical Model of abutment (a) Soil contribution (b) Pile contribution

Abutment stiffness in longitudinal direction is modeled as two parallel link elements in Sap 2000, and in transverse direction the abutment stiffness is only contributed by the piles of abutment. The values for the parameters in Figure A.5 are shown in Table A.1.

Table A-1. Model Prosperities of Abutment (Nielson 2005)

Properties	Notations	Values
Soil Behavior (Passive action)		
Initial Stiffness	K_{1p}	11.5-28.8 KN/mm/m
Displacement 1 at top	Δ_{1p} / h^*	$0.1(\Delta_{3p} / h)$
Second Stiffness	K_{2p}	40% K_{1p}
Displacement 2 at top	Δ_{2p} / h	$0.35(\Delta_{3p} / h)$
Third Stiffness	K_{3p}	20% K_{1p}
Displacement 3 at top	Δ_{3p} / h	8.0%
Pile Behavior (Dual Action)		
Effective stiffness	K_{eff}	3.5-10.5 KN/mm/pile \times # of piles
Initial Stiffness	K_1	$2.333 K_{eff}$
Displacement 1 at top	Δ_1 / h	7.62 mm
Second Stiffness	K_2	$0.428 K_{eff}$
Displacement 2 at top	Δ_2 / h	25.4 mm

* h is the height of back wall of abutment, and the height is assumed as 2.4m in this study.

A.1.4 Foundation

Bridge foundation is a bridge component which transfers all inertial forces to the ground. The analytical Model of foundation is shown in Figure A.6. (a), the calculations of K_R and K_H are introduced in Chapter 3.3.2. The configuration of bridge footing is shown in Figure A.6. (b).

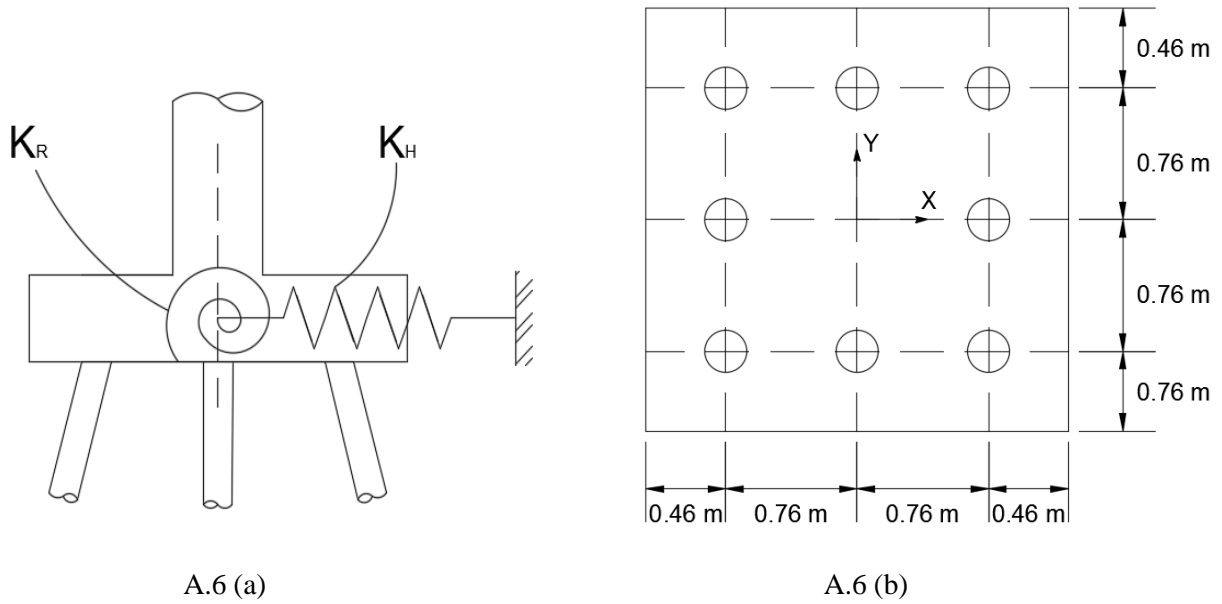


Figure A.6. (a) Analytical Model of foundation (b) Configuration of bridge footings

A.2 Seismic response

According to SAP 2000 analysis, the fundamental period of the bridge is approximately 0.58 seconds with the predominant motion being in longitudinal direction. The anticipating mass ratio in this direction is 43%. The second mode is a transverse mode with a period 0.53 seconds, the anticipating mass ratio in transverse direction is 57%.

The displacements of bridge deck in the middle span under earthquake records of Gulf of California, which has PGA equals to 0.125g in longitudinal direction and 0.066g in transverse direction, are shown in figure A.7.

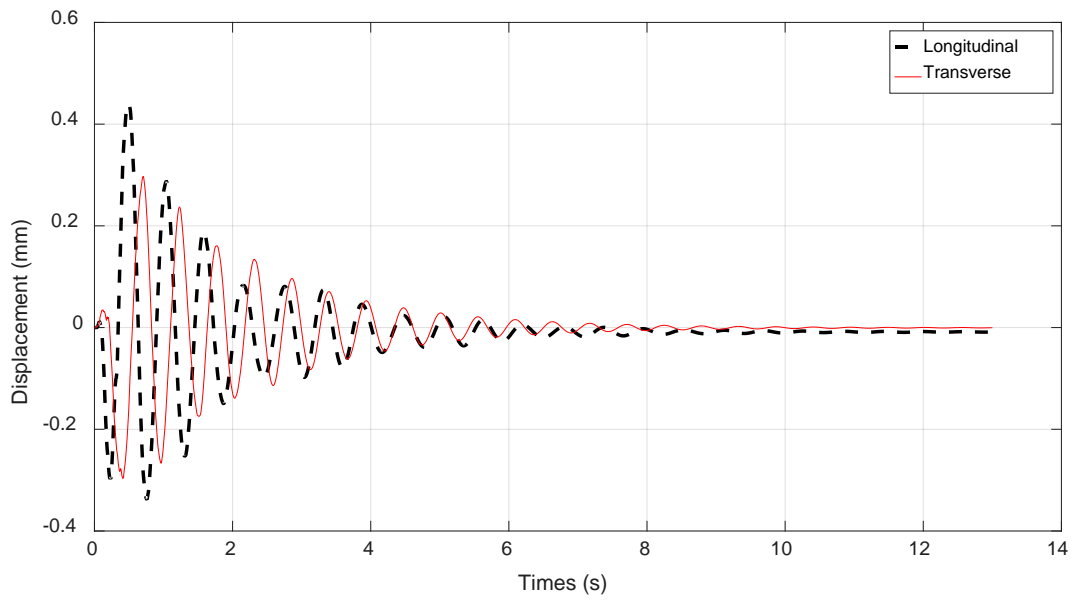


Figure A.7 Deck displacement time histories

Appendix B – Data of natural hazards

B.1 Scour

The two annual peak discharge rate records are achieved for Colorado River and Rio Grande from USGS website (<http://nwis.waterdata.usgs.gov/usa/nwis/peak>). The two flows are recorded from 1951 to 2014, and there are 64 data for each flow. The records are shown in Table B-1.

Table B-1 Annual peak discharge rate

Colorado River		Rio Grande	
Date	Annual peak discharge rate (cms)	Date	Annual peak discharge rate (cms)
6/23/1951	8552	5/28/1951	1119
6/9/1952	14725	6/12/1952	1997
6/15/1953	10562	5/28/1953	1178
5/23/1954	3285	5/22/1954	926
6/10/1955	4842	6/9/1955	1223
6/4/1956	8184	6/2/1956	969
6/9/1957	16084	7/27/1957	2016
5/31/1958	12743	5/25/1958	2011
6/11/1959	6570	6/8/1959	937
6/5/1960	6994	6/4/1960	1391
5/31/1961	5465	5/29/1961	1206
5/14/1962	11468	5/13/1962	1348
5/20/1963	3200	5/19/1963	898
5/27/1964	7731	5/25/1964	1334
6/20/1965	10307	6/21/1965	1759
5/11/1966	4078	5/8/1966	1260
5/27/1967	5494	5/23/1967	889
6/7/1968	7532	6/2/1968	1640
6/26/1969	5777	5/23/1969	1365
5/24/1970	9345	9/6/1970	2090
6/19/1971	6286	6/14/1971	898
6/9/1972	5210	5/31/1972	997
6/16/1973	9911	6/12/1973	1807
5/11/1974	6456	5/12/1974	867
6/9/1975	7447	6/15/1975	1798
6/7/1976	4078	6/6/1976	1450
6/10/1977	1439	6/2/1977	490
6/17/1978	7872	6/11/1978	1249
5/30/1979	10194	5/30/1979	2274

5/24/1980	9090	6/10/1980	2195
6/9/1981	3426	6/8/1981	1003
6/20/1982	5465	6/13/1982	1172
6/27/1983	17585	6/12/1983	1640
5/27/1984	19765	5/27/1984	2039
5/5/1985	11129	6/9/1985	2526
6/8/1986	9571	6/7/1986	2158
5/18/1987	6371	6/16/1987	2121
5/19/1988	4361	6/7/1988	974
5/31/1989	2823	5/30/1989	1031
6/12/1990	3568	6/5/1990	1566
6/16/1991	5607	5/21/1991	1348
5/28/1992	4672	5/21/1992	889
5/28/1993	12545	5/27/1993	1501
5/19/1994	3851	5/31/1994	1303
6/19/1995	13960	6/18/1995	2098
5/20/1996	8240	5/17/1996	1065
6/10/1997	10619	6/2/1997	2107
5/22/1998	7391	5/22/1998	1348
6/1/1999	5069	6/10/1999	1509
5/31/2000	5069	5/24/2000	1059
5/18/2001	3738	5/21/2001	1759
9/12/2002	1563	5/20/2002	195
6/3/2003	7391	5/23/2003	1071
5/12/2004	2676	5/21/2004	1260
5/25/2005	8778	5/22/2005	2144
5/24/2006	6145	5/25/2006	1076
5/23/2007	4163	6/6/2007	1467
6/4/2008	11214	5/21/2008	1804
5/26/2009	8212	5/8/2009	1711
6/9/2010	8580	5/29/2010	1538
6/9/2011	13507	6/7/2011	1257
10/7/2011	1688	5/23/2012	869
5/19/2013	3710	5/18/2013	952
6/3/2014	10761	5/30/2014	1597

B.2 Bridge deterioration

Table B-2 Transition probability for superstructure condition (concrete) (Yi 1990)

Age(year)	T_{99}	T_{88}	T_{77}	T_{66}	T_{55}	T_{44}
0-6	0.700	0.780	0.940	0.910	0.581	0.436
7-12	0.600	0.640	0.940	0.910	0.580	0.430
13-18	0.580	0.600	0.940	0.910	0.580	0.430
19-24	0.560	0.600	0.960	0.950	0.750	0.589
25-30	0.550	0.580	0.970	0.960	0.800	0.640
31-36	0.540	0.570	0.980	0.970	0.870	0.780
37-42	0.530	0.560	0.980	0.980	0.950	0.880
43-48	0.520	0.540	0.980	0.980	0.950	0.900
49-54	0.500	0.520	0.940	0.910	0.862	0.800
55-60	0.450	0.490	0.850	0.800	0.700	0.650

Table B-3 Transition probability for superstructure condition (steel) (Yi 1990)

Age(year)	T_{99}	T_{88}	T_{77}	T_{66}	T_{55}	T_{44}
0-6	0.654	0.710	0.900	0.750	0.750	0.700
7-12	0.600	0.680	0.850	0.750	0.750	0.700
13-18	0.600	0.680	0.920	0.800	0.800	0.750
19-24	0.600	0.680	0.950	0.870	0.870	0.850
25-30	0.580	0.660	0.980	0.940	0.940	0.900
31-36	0.580	0.660	0.980	0.940	0.940	0.900
37-42	0.560	0.640	0.980	0.950	0.950	0.910
43-48	0.560	0.640	0.950	0.900	0.900	0.850
49-54	0.540	0.620	0.800	0.780	0.780	0.760
55-60	0.520	0.600	0.650	0.600	0.600	0.560

Table B-4 Transition probability for substructure condition (concrete) (Yi 1990)

Age(year)	T_{99}	T_{88}	T_{77}	T_{66}	T_{55}	T_{44}
0-6	0.704	0.741	0.850	0.800	0.700	0.650
7-12	0.600	0.710	0.940	0.800	0.700	0.650
13-18	0.550	0.640	0.940	0.936	0.700	0.650
19-24	0.550	0.640	0.950	0.950	0.800	0.750
25-30	0.540	0.610	0.970	0.970	0.910	0.860
31-36	0.530	0.600	0.985	0.985	0.970	0.970
37-42	0.520	0.580	0.985	0.985	0.970	0.970
43-48	0.500	0.550	0.985	0.985	0.970	0.970
49-54	0.480	0.530	0.944	0.950	0.840	0.840
55-60	0.450	0.500	0.800	0.800	0.700	0.600

Table B-5 Transition probability for substructure condition (steel) (Yi 1990)

Age(year)	T_{99}	T_{88}	T_{77}	T_{66}	T_{55}	T_{44}
0-6	0.670	0.700	0.900	0.900	0.786	0.685
7-12	0.650	0.700	0.848	0.859	0.750	0.699
13-18	0.650	0.700	0.920	0.920	0.900	0.900
19-24	0.650	0.700	0.950	0.950	0.920	0.920
25-30	0.620	0.647	0.980	0.980	0.950	0.950
31-36	0.620	0.640	0.980	0.980	0.950	0.950
37-42	0.600	0.640	0.980	0.980	0.970	0.960
43-48	0.600	0.620	0.980	0.980	0.970	0.960
49-54	0.560	0.580	0.850	0.860	0.600	0.560
55-60	0.560	0.600	0.650	0.660	0.450	0.400

Appendix C – Component PSDMs and fragilities

C.1 Component PSDMs

In this study, the four deterioration conditions are considered, which include when NBI rating equals to 6, 5, 4 and 3. The PSDMs of deteriorating bridge subjected to earthquake and both earthquake and scour are shown through Table C-1 to Table C-12.

Table C-1. Probability seismic demand models for eight component responses (Scour with higher discharge rate, when NBI rating=6)

Response	PSDM	R^2	$\beta_{D PGA}$
$\ln(\mu_\phi)$	$\ln(3.30) + 1.658 \ln(PGA)$	0.6972	0.73
$\ln(fx_L)$	$\ln(28.28) + 1.513 \ln(PGA)$	0.6816	0.69
$\ln(fx_T)$	$\ln(23.03) + 1.474 \ln(PGA)$	0.6601	0.71
$\ln(ex_L)$	$\ln(57.34) + 1.756 \ln(PGA)$	0.6639	0.84
$\ln(ex_T)$	$\ln(22.85) + 1.472 \ln(PGA)$	0.6590	0.71
$\ln(ab_p)$	$\ln(16.49) + 1.784 \ln(PGA)$	0.7075	0.77
$\ln(ab_A)$	$\ln(20.37) + 1.876 \ln(PGA)$	0.7449	0.74
$\ln(ab_T)$	$\ln(17.32) + 1.677 \ln(PGA)$	0.6914	0.75

Table C-2. Probability seismic demand models for eight component responses (Scour with lower discharge rate, when NBI rating=6)

Response	PSDM	R²	$\beta_{D PGA}$
$\ln(\mu_\phi)$	$\ln(3.62) + 1.649 \ln(PGA)$	0.5457	1.03
$\ln(fx_L)$	$\ln(28.13) + 1.484 \ln(PGA)$	0.7174	0.64
$\ln(fx_T)$	$\ln(19.28) + 1.394 \ln(PGA)$	0.6574	0.73
$\ln(ex_L)$	$\ln(54.49) + 1.700 \ln(PGA)$	0.6798	0.80
$\ln(ex_T)$	$\ln(22.49) + 1.480 \ln(PGA)$	0.6771	0.70
$\ln(ab_p)$	$\ln(17.48) + 1.800 \ln(PGA)$	0.7198	0.77
$\ln(ab_A)$	$\ln(21.33) + 1.882 \ln(PGA)$	0.7437	0.76
$\ln(ab_T)$	$\ln(19.22) + 1.720 \ln(PGA)$	0.7187	0.74

Table C-3. Probability seismic demand models for eight component responses (Without Scour or deterioration, when NBI rating=6)

Response	PSDM	R²	$\beta_{D PGA}$
$\ln(\mu_\phi)$	$\ln(3.65) + 1.639 \ln(PGA)$	0.7332	0.68
$\ln(fx_L)$	$\ln(21.71) + 1.344 \ln(PGA)$	0.6909	0.62
$\ln(fx_T)$	$\ln(15.23) + 1.164 \ln(PGA)$	0.6240	0.75
$\ln(ex_L)$	$\ln(44.30) + 1.614 \ln(PGA)$	0.7112	0.70
$\ln(ex_T)$	$\ln(23.81) + 1.468 \ln(PGA)$	0.6313	0.77
$\ln(ab_p)$	$\ln(18.95) + 1.833 \ln(PGA)$	0.7506	0.72
$\ln(ab_A)$	$\ln(21.82) + 1.893 \ln(PGA)$	0.7698	0.71
$\ln(ab_T)$	$\ln(16.83) + 1.628 \ln(PGA)$	0.6726	0.78

Table C-4. Probability seismic demand models for eight component responses (Scour with higher discharge rate, when NBI rating=5)

Response	PSDM	R²	$\beta_{D PGA}$
$\ln(\mu_\phi)$	$\ln(4.01) + 1.674 \ln(\text{PGA})$	0.6974	0.74
$\ln(fx_L)$	$\ln(28.28) + 1.513 \ln(\text{PGA})$	0.6816	0.69
$\ln(fx_T)$	$\ln(23.03) + 1.474 \ln(\text{PGA})$	0.6601	0.71
$\ln(ex_L)$	$\ln(57.34) + 1.756 \ln(\text{PGA})$	0.6639	0.84
$\ln(ex_T)$	$\ln(22.85) + 1.472 \ln(\text{PGA})$	0.6590	0.71
$\ln(ab_p)$	$\ln(16.49) + 1.784 \ln(\text{PGA})$	0.7075	0.77
$\ln(ab_A)$	$\ln(20.37) + 1.876 \ln(\text{PGA})$	0.7449	0.74
$\ln(ab_T)$	$\ln(17.32) + 1.677 \ln(\text{PGA})$	0.6914	0.75

Table C-5. Probability seismic demand models for eight component responses (Scour with lower discharge rate, when NBI rating=5)

Response	PSDM	R²	$\beta_{D PGA}$
$\ln(\mu_\phi)$	$\ln(3.75) + 1.569 \ln(\text{PGA})$	0.6781	0.73
$\ln(fx_L)$	$\ln(26.64) + 1.442 \ln(\text{PGA})$	0.6923	0.64
$\ln(fx_T)$	$\ln(22.53) + 1.481 \ln(\text{PGA})$	0.6565	0.72
$\ln(ex_L)$	$\ln(48.09) + 1.643 \ln(\text{PGA})$	0.6516	0.81
$\ln(ex_T)$	$\ln(22.99) + 1.491 \ln(\text{PGA})$	0.6614	0.72
$\ln(ab_p)$	$\ln(16.18) + 1.765 \ln(\text{PGA})$	0.6962	0.78
$\ln(ab_A)$	$\ln(19.99) + 1.853 \ln(\text{PGA})$	0.7223	0.77
$\ln(ab_T)$	$\ln(17.41) + 1.675 \ln(\text{PGA})$	0.6794	0.76

Table C-6. Probability seismic demand models for eight component responses (Without Scour or deterioration, when NBI rating=5)

Response	PSDM	R²	$\beta_{D PGA}$
$\ln(\mu_\phi)$	$\ln(3.79) + 1.580 \ln(\text{PGA})$	0.7080	0.68
$\ln(fx_L)$	$\ln(20.70) + 1.322 \ln(\text{PGA})$	0.6665	0.63
$\ln(fx_T)$	$\ln(17.01) + 1.225 \ln(\text{PGA})$	0.7017	0.67
$\ln(ex_L)$	$\ln(41.64) + 1.585 \ln(\text{PGA})$	0.6847	0.72
$\ln(ex_T)$	$\ln(25.08) + 1.492 \ln(\text{PGA})$	0.6198	0.78
$\ln(ab_p)$	$\ln(17.86) + 1.807 \ln(\text{PGA})$	0.7299	0.74
$\ln(ab_A)$	$\ln(20.21) + 1.858 \ln(\text{PGA})$	0.7497	0.72
$\ln(ab_T)$	$\ln(15.85) + 1.601 \ln(\text{PGA})$	0.6472	0.80

Table C-7. Probability seismic demand models for eight component responses (Scour with higher discharge rate, when NBI rating=4)

Response	PSDM	R²	$\beta_{D PGA}$
$\ln(\mu_\phi)$	$\ln(5.50) + 1.647 \ln(\text{PGA})$	0.6808	0.79
$\ln(fx_L)$	$\ln(28.28) + 1.513 \ln(\text{PGA})$	0.6816	0.69
$\ln(fx_T)$	$\ln(23.03) + 1.474 \ln(\text{PGA})$	0.6601	0.71
$\ln(ex_L)$	$\ln(57.34) + 1.756 \ln(\text{PGA})$	0.6639	0.84
$\ln(ex_T)$	$\ln(22.85) + 1.472 \ln(\text{PGA})$	0.6590	0.71
$\ln(ab_p)$	$\ln(16.49) + 1.784 \ln(\text{PGA})$	0.7075	0.77
$\ln(ab_A)$	$\ln(20.37) + 1.876 \ln(\text{PGA})$	0.7449	0.74
$\ln(ab_T)$	$\ln(17.32) + 1.677 \ln(\text{PGA})$	0.6914	0.75

Table C-8. Probability seismic demand models for eight component responses (Scour with lower discharge rate, when NBI rating=4)

Response	PSDM	R²	$\beta_{D PGA}$
$\ln(\mu_\phi)$	$\ln(4.60) + 1.577 \ln(\text{PGA})$	0.6589	0.76
$\ln(fx_L)$	$\ln(26.64) + 1.442 \ln(\text{PGA})$	0.6923	0.64
$\ln(fx_T)$	$\ln(22.53) + 1.481 \ln(\text{PGA})$	0.6565	0.72
$\ln(ex_L)$	$\ln(48.09) + 1.643 \ln(\text{PGA})$	0.6516	0.81
$\ln(ex_T)$	$\ln(22.99) + 1.491 \ln(\text{PGA})$	0.6614	0.72
$\ln(ab_p)$	$\ln(16.18) + 1.765 \ln(\text{PGA})$	0.6962	0.78
$\ln(ab_A)$	$\ln(19.99) + 1.853 \ln(\text{PGA})$	0.7223	0.77
$\ln(ab_T)$	$\ln(17.41) + 1.675 \ln(\text{PGA})$	0.6794	0.76

Table C-9. Probability seismic demand models for eight component responses (Without Scour or deterioration, when NBI rating=4)

Response	PSDM	R²	$\beta_{D PGA}$
$\ln(\mu_\phi)$	$\ln(3.97) + 1.532 \ln(\text{PGA})$	0.7058	0.67
$\ln(fx_L)$	$\ln(19.14) + 1.290 \ln(\text{PGA})$	0.6524	0.63
$\ln(fx_T)$	$\ln(18.28) + 1.267 \ln(\text{PGA})$	0.6774	0.71
$\ln(ex_L)$	$\ln(37.15) + 1.536 \ln(\text{PGA})$	0.6195	0.78
$\ln(ex_T)$	$\ln(26.29) + 1.511 \ln(\text{PGA})$	0.6176	0.80
$\ln(ab_p)$	$\ln(15.85) + 1.757 \ln(\text{PGA})$	0.7203	0.74
$\ln(ab_A)$	$\ln(17.57) + 1.801 \ln(\text{PGA})$	0.7430	0.71
$\ln(ab_T)$	$\ln(16.40) + 1.615 \ln(\text{PGA})$	0.6424	0.81

Table C-10. Probability seismic demand models for eight component responses (Scour with higher discharge rate, when NBI rating=3)

Response	PSDM	R²	$\beta_{D PGA}$
$\ln(\mu_\phi)$	$\ln(6.95) + 1.727 \ln(\text{PGA})$	0.6556	0.85
$\ln(fx_L)$	$\ln(28.25) + 1.512 \ln(\text{PGA})$	0.6723	0.71
$\ln(fx_T)$	$\ln(22.76) + 1.469 \ln(\text{PGA})$	0.6493	0.73
$\ln(ex_L)$	$\ln(58.73) + 1.766 \ln(\text{PGA})$	0.6573	0.85
$\ln(ex_T)$	$\ln(22.83) + 1.472 \ln(\text{PGA})$	0.6495	0.73
$\ln(ab_p)$	$\ln(16.93) + 1.795 \ln(\text{PGA})$	0.7017	0.79
$\ln(ab_A)$	$\ln(20.72) + 1.883 \ln(\text{PGA})$	0.7385	0.75
$\ln(ab_T)$	$\ln(14.67) + 1.609 \ln(\text{PGA})$	0.6842	0.74

Table C-11. Probability seismic demand models for eight component responses (Scour with lower discharge rate, when NBI rating=3)

Response	PSDM	R²	$\beta_{D PGA}$
$\ln(\mu_\phi)$	$\ln(5.34) + 1.549 \ln(\text{PGA})$	0.6336	0.81
$\ln(fx_L)$	$\ln(24.24) + 1.425 \ln(\text{PGA})$	0.6839	0.66
$\ln(fx_T)$	$\ln(21.39) + 1.467 \ln(\text{PGA})$	0.6476	0.74
$\ln(ex_L)$	$\ln(43.29) + 1.615 \ln(\text{PGA})$	0.6588	0.80
$\ln(ex_T)$	$\ln(21.52) + 1.470 \ln(\text{PGA})$	0.6500	0.74
$\ln(ab_p)$	$\ln(14.66) + 1.737 \ln(\text{PGA})$	0.6970	0.79
$\ln(ab_A)$	$\ln(18.41) + 1.831 \ln(\text{PGA})$	0.7231	0.78
$\ln(ab_T)$	$\ln(14.38) + 1.604 \ln(\text{PGA})$	0.6846	0.75

Table C-12. Probability seismic demand models for eight component responses (Without Scour or deterioration, when NBI rating=3)

Response	PSDM	R²	$\beta_{D PGA}$
$\ln(\mu_\phi)$	$\ln(5.24) + 1.546 \ln(\text{PGA})$	0.6539	0.72
$\ln(fx_L)$	$\ln(21.39) + 1.341 \ln(\text{PGA})$	0.6449	0.64
$\ln(fx_T)$	$\ln(17.94) + 1.216 \ln(\text{PGA})$	0.6074	0.80
$\ln(ex_L)$	$\ln(39.77) + 1.570 \ln(\text{PGA})$	0.6581	0.73
$\ln(ex_T)$	$\ln(34.23) + 1.623 \ln(\text{PGA})$	0.6410	0.79
$\ln(ab_p)$	$\ln(18.50) + 1.828 \ln(\text{PGA})$	0.7159	0.74
$\ln(ab_A)$	$\ln(19.57) + 1.850 \ln(\text{PGA})$	0.7312	0.73
$\ln(ab_T)$	$\ln(23.62) + 1.782 \ln(\text{PGA})$	0.6898	0.77

C.2 Bridge component fragilities

Table C-13. Parameters for bridge component fragilities (Scour with higher discharge rate, when NBI rating=6)

Component	Slight		Moderate	
	Median (g)	Dispersion	Median (g)	Dispersion
Column	0.57	0.57	0.76	0.54
Fxd Bearing-long	1.01	0.60	2.37	0.58
Fxd Bearing-trans	1.16	0.72	2.54	0.67
Exp Bearing-long	0.68	0.59	1.41	0.57
Exp Bearing-trans	1.17	0.72	2.56	0.67
Abut-passive	1.57	0.50	3.39	0.50
Abut-active	0.68	0.54	1.39	0.62
Abut-trans	0.71	0.61	1.60	0.70

Table C-14. Parameters for bridge component fragilities (Scour with lower discharge rate, when NBI rating =6)

Component	Slight		Moderate	
	Median (g)	Dispersion	Median (g)	Dispersion
Column	0.53	0.72	0.72	0.70
Fxd Bearing-long	1.02	0.59	2.42	0.57
Fxd Bearing-trans	1.33	0.77	3.04	0.72
Exp Bearing-long	0.69	0.59	1.46	0.57
Exp Bearing-trans	1.18	0.71	2.57	0.66
Abut-passive	1.52	0.50	3.25	0.50
Abut-active	0.66	0.55	1.36	0.63
Abut-trans	0.68	0.59	1.48	0.68

Table C-15. Parameters for bridge component fragilities (Without scour or deterioration, when NBI rating = 6)

Component	Slight		Moderate	
	Median (g)	Dispersion	Median (g)	Dispersion
Column	0.53	0.55	0.71	0.52
Fxd Bearing-long	1.24	0.64	3.21	0.62
Fxd Bearing-trans	1.73	0.94	4.64	0.87
Exp Bearing-long	0.77	0.57	1.70	0.55
Exp Bearing-trans	1.14	0.75	2.49	0.70
Abut-passive	1.44	0.47	3.05	0.47
Abut-active	0.66	0.53	1.34	0.61
Abut-trans	0.72	0.64	1.65	0.73

Table C-16. Parameters for bridge component fragilities (Scour with higher discharge rate, when NBI rating = 5)

Component	Slight		Moderate	
	Median (g)	Dispersion	Median (g)	Dispersion
Column	0.51	0.57	0.68	0.54
Fxd Bearing-long	1.01	0.60	2.37	0.58
Fxd Bearing-trans	1.16	0.72	2.54	0.67
Exp Bearing-long	0.68	0.59	1.41	0.57
Exp Bearing-trans	1.17	0.72	2.56	0.67
Abut-passive	1.57	0.50	3.39	0.50
Abut-active	0.68	0.54	1.39	0.62
Abut-trans	0.71	0.61	1.60	0.70

Table C-17. Parameters for bridge component fragilities (Scour with lower discharge rate, when NBI rating =5)

Component	Slight		Moderate	
	Median (g)	Dispersion	Median (g)	Dispersion
Column	0.51	0.60	0.69	0.57
Fxd Bearing-long	1.06	0.61	2.57	0.59
Fxd Bearing-trans	1.18	0.72	2.56	0.67
Exp Bearing-long	0.73	0.61	1.60	0.60
Exp Bearing-trans	1.16	0.72	2.51	0.66
Abut-passive	1.60	0.51	3.48	0.51
Abut-active	0.68	0.56	1.41	0.64
Abut-trans	0.71	0.62	1.59	0.70

Table C-18. Parameters for bridge component fragilities (Without scour or deterioration, when NBI rating =5)

Component	Slight		Moderate	
	Median (g)	Dispersion	Median (g)	Dispersion
Column	0.51	0.57	0.69	0.54
Fxd Bearing-long	1.29	0.66	3.40	0.63
Fxd Bearing-trans	1.54	0.85	3.93	0.78
Exp Bearing-long	0.79	0.59	1.79	0.57
Exp Bearing-trans	1.10	0.74	2.37	0.69
Abut-passive	1.50	0.48	3.20	0.48
Abut-active	0.68	0.54	1.40	0.62
Abut-trans	0.74	0.66	1.72	0.75

Table C-19. Parameters for bridge component fragilities (Scour with higher discharge rate, when NBI rating =4)

Component	Slight		Moderate	
	Median (g)	Dispersion	Median (g)	Dispersion
Column	0.41	0.60	0.56	0.57
Fxd Bearing-long	1.01	0.60	2.37	0.58
Fxd Bearing-trans	1.16	0.72	2.54	0.67
Exp Bearing-long	0.68	0.59	1.41	0.57
Exp Bearing-trans	1.17	0.72	2.56	0.67
Abut-passive	1.57	0.50	3.39	0.50
Abut-active	0.68	0.54	1.39	0.62
Abut-trans	0.71	0.61	1.60	0.70

Table C-20. Parameters for bridge component fragilities (Scour with lower discharge rate, when NBI rating =4)

Component	Slight		Moderate	
	Median (g)	Dispersion	Median (g)	Dispersion
Column	0.45	0.61	0.61	0.58
Fxd Bearing-long	1.06	0.61	2.57	0.59
Fxd Bearing-trans	1.18	0.72	2.56	0.67
Exp Bearing-long	0.73	0.61	1.60	0.60
Exp Bearing-trans	1.16	0.72	2.51	0.66
Abut-passive	1.60	0.51	3.48	0.51
Abut-active	0.68	0.56	1.41	0.64
Abut-trans	0.71	0.62	1.59	0.70

Table C-21. Parameters for bridge component fragilities (Without scour or deterioration, when NBI rating =4)

Component	Slight		Moderate	
	Median (g)	Dispersion	Median (g)	Dispersion
Column	0.48	0.58	0.66	0.55
Fxd Bearing-long	1.38	0.67	3.72	0.65
Fxd Bearing-trans	1.43	0.84	3.55	0.78
Exp Bearing-long	0.85	0.64	1.96	0.62
Exp Bearing-trans	1.06	0.74	2.27	0.69
Abut-passive	1.62	0.50	3.54	0.50
Abut-active	0.72	0.55	1.53	0.64
Abut-trans	0.73	0.66	1.68	0.75

Appendix D – Results of sensitivity analysis

The results of sensitivity analysis that under GM-1 are shown through Table D-1 to table D-7.

Table D-1 Seismic response of bridge components (Steel strength)

Component	Response	
	Lower	Upper
Concrete Column μ_ϕ	0.033785	0.024256
Elastomeric Bearing Fixed-Long(mm)	0.452388	0.452387
Elastomeric Bearing Fixed-Tran(mm)	0.262706	0.262706
Elastomeric Bearing Expan-Long(mm)	0.518744	0.518743
Elastomeric Bearing Expan-Tran(mm)	0.265783	0.265783
Abutment-Passive(mm)	0.11238	0.11238
Abutment-Active(mm)	0.133518	0.133518
Abutment-Tran(mm)	0.076317	0.076317

Table D-2 Seismic response of bridge components (Concrete strength)

Component	Response	
	Lower	Upper
Concrete Column μ_ϕ	0.029101	0.028287
Elastomeric Bearing Fixed-Long(mm)	0.452387	0.452388
Elastomeric Bearing Fixed-Tran(mm)	0.262706	0.262706
Elastomeric Bearing Expan-Long(mm)	0.518743	0.518744
Elastomeric Bearing Expan-Tran(mm)	0.265783	0.265783
Abutment-Passive(mm)	0.11238	0.11238
Abutment-Active(mm)	0.133518	0.133518
Abutment-Tran(mm)	0.076317	0.076317

Table D-3 Seismic response of bridge components (Bearing shear modulus)

Component	Response	
	Lower	Upper
Concrete Column μ_ϕ	0.027162	0.029485
Elastomeric Bearing Fixed-Long(mm)	0.470257	0.481292
Elastomeric Bearing Fixed-Tran(mm)	0.278435	0.264581
Elastomeric Bearing Expan-Long(mm)	0.552893	0.519517
Elastomeric Bearing Expan-Tran(mm)	0.278435	0.271861
Abutment-Passive(mm)	0.115583	0.108948
Abutment-Active(mm)	0.127204	0.138363
Abutment-Tran(mm)	0.077637	0.073741

Table D-4 Seismic response of bridge components (Passive stiffness of abutment)

Component	Response	
	Lower	Upper
Concrete Column μ_ϕ	0.028545	0.028611
Elastomeric Bearing Fixed-Long(mm)	0.452387	0.452909
Elastomeric Bearing Fixed-Tran(mm)	0.262706	0.262613
Elastomeric Bearing Expan-Long(mm)	0.518743	0.519323
Elastomeric Bearing Expan-Tran(mm)	0.265783	0.265641
Abutment-Passive(mm)	0.11238	0.11118
Abutment-Active(mm)	0.133518	0.14737
Abutment-Tran(mm)	0.076317	0.076388

Table D-5 Seismic response of bridge components (Active stiffness of abutments)

Component	Response	
	Lower	Upper
Concrete Column μ_ϕ	0.028523	0.028578
Elastomeric Bearing Fixed-Long(mm)	0.545229	0.498492
Elastomeric Bearing Fixed-Tran(mm)	0.258734	0.285731
Elastomeric Bearing Expan-Long(mm)	0.523209	0.520563
Elastomeric Bearing Expan-Tran(mm)	0.265118	0.282955
Abutment-Passive(mm)	0.147035	0.104251
Abutment-Active(mm)	0.182809	0.136572
Abutment-Tran(mm)	0.109755	0.072528

Table D-6 Seismic response of bridge components (Deck mass)

Component	Response	
	Lower	Upper
Concrete Column μ_ϕ	0.02978	0.028501
Elastomeric Bearing Fixed-Long(mm)	0.488169	0.448619
Elastomeric Bearing Fixed-Tran(mm)	0.270641	0.269206
Elastomeric Bearing Expan-Long(mm)	0.53561	0.526263
Elastomeric Bearing Expan-Tran(mm)	0.27749	0.268703
Abutment-Passive(mm)	0.110338	0.114246
Abutment-Active(mm)	0.133935	0.132853
Abutment-Tran(mm)	0.073323	0.078694

Table D-7 Seismic response of bridge components (Damping ratio)

Component	Response	
	Lower	Upper
Concrete Column μ_ϕ	0.031092	0.025471
Elastomeric Bearing Fixed-Long(mm)	0.535009	0.41326
Elastomeric Bearing Fixed-Tran(mm)	0.333904	0.249683
Elastomeric Bearing Expan-Long(mm)	0.57887	0.487518
Elastomeric Bearing Expan-Tran(mm)	0.342327	0.249347
Abutment-Passive(mm)	0.129899	0.09971
Abutment-Active(mm)	0.159359	0.114279
Abutment-Tran(mm)	0.08913	0.066462

The results of sensitivity analysis that under GM-2 are shown through Table D-8 to table D-14.

Table D-8 Seismic response of bridge components (Steel strength)

Component	Response	
	Lower	Upper
Concrete Column μ_ϕ	0.568571	0.408208
Elastomeric Bearing Fixed-Long(mm)	4.292281	4.292281
Elastomeric Bearing Fixed-Tran(mm)	3.527453	3.527453
Elastomeric Bearing Expan-Long(mm)	6.681357	6.681357
Elastomeric Bearing Expan-Tran(mm)	3.548986	3.548986
Abutment-Passive(mm)	2.17866	2.17866
Abutment-Active(mm)	2.790979	2.790979
Abutment-Tran(mm)	1.748436	1.748436

Table D-9 Seismic response of bridge components (Concrete strength)

Component	Response	
	Lower	Upper
Concrete Column μ_ϕ	0.485927	0.475792
Elastomeric Bearing Fixed-Long(mm)	4.292281	4.292281
Elastomeric Bearing Fixed-Tran(mm)	3.527453	3.527453
Elastomeric Bearing Expan-Long(mm)	6.681357	6.681357
Elastomeric Bearing Expan-Tran(mm)	3.548986	3.548986
Abutment-Passive(mm)	2.17866	2.17866
Abutment-Active(mm)	2.790979	2.790979
Abutment-Tran(mm)	1.748436	1.748436

Table D-10 Seismic response of bridge components (Bearing shear modulus)

Component	Response	
	Lower	Upper
Concrete Column μ_ϕ	0.483346	0.474188
Elastomeric Bearing Fixed-Long(mm)	4.342485	4.30848
Elastomeric Bearing Fixed-Tran(mm)	3.543093	3.623206
Elastomeric Bearing Expan-Long(mm)	6.970257	6.376575
Elastomeric Bearing Expan-Tran(mm)	3.498826	3.63073
Abutment-Passive(mm)	2.230859	2.096136
Abutment-Active(mm)	2.785103	2.798906
Abutment-Tran(mm)	1.744863	1.738762

Table D-11 Seismic response of bridge components (Passive stiffness of abutment)

Component	Response	
	Lower	Upper
Concrete Column μ_ϕ	0.480564	0.480772
Elastomeric Bearing Fixed-Long(mm)	4.292281	4.653717
Elastomeric Bearing Fixed-Tran(mm)	3.527453	3.549996
Elastomeric Bearing Expan-Long(mm)	4.292281	6.691564
Elastomeric Bearing Expan-Tran(mm)	3.527453	3.56908
Abutment-Passive(mm)	2.17866	2.060069
Abutment-Active(mm)	2.790979	2.804673
Abutment-Tran(mm)	1.748436	1.750011

Table D-12 Seismic response of bridge components (Active stiffness of abutments)

Component	Response	
	Lower	Upper
Concrete Column μ_ϕ	0.463412	0.474561
Elastomeric Bearing Fixed-Long(mm)	4.158255	4.527987
Elastomeric Bearing Fixed-Tran(mm)	3.468108	3.454013
Elastomeric Bearing Expan-Long(mm)	6.120552	6.623963
Elastomeric Bearing Expan-Tran(mm)	3.407342	3.468032
Abutment-Passive(mm)	2.644831	1.35597
Abutment-Active(mm)	4.6522	2.363053
Abutment-Tran(mm)	1.670955	1.318705

Table D-13 Seismic response of bridge components (Deck mass)

Component	Response	
	Lower	Upper
Concrete Column μ_ϕ	0.470567	0.490411
Elastomeric Bearing Fixed-Long(mm)	4.636024	4.350073
Elastomeric Bearing Fixed-Tran(mm)	3.706676	3.462397
Elastomeric Bearing Expan-Long(mm)	6.474917	6.711353
Elastomeric Bearing Expan-Tran(mm)	3.707131	3.416391
Abutment-Passive(mm)	2.229811	2.220225
Abutment-Active(mm)	2.790818	2.792305
Abutment-Tran(mm)	1.725878	1.751342

Table D-14 Seismic response of bridge components (Damping ratio)

Component	Response	
	Lower	Upper
Concrete Column μ_ϕ	0.534895	0.454219
Elastomeric Bearing Fixed-Long(mm)	5.024969	4.358317
Elastomeric Bearing Fixed-Tran(mm)	3.806102	3.376975
Elastomeric Bearing Expan-Long(mm)	8.148085	6.28359
Elastomeric Bearing Expan-Tran(mm)	3.906509	3.354399
Abutment-Passive(mm)	3.222699	1.854128
Abutment-Active(mm)	3.207449	2.689499
Abutment-Tran(mm)	2.145521	1.586209